UNIVERSITÀ DEGLI STUDI DI NAPOLI "FEDERICO II"

FACOLTÀ DI INGEGNERIA

DIPARTIMENTO DI INGEGNERIA DEI MATERIALI E DELLA PRODUZIONE


RESEARCH DOCTORATE IN

INGEGNERIA DEI MATERIALI E DELLE STRUTTURE

XXIII CYCLE

# Evaluation of Material Mechanical Properties Influence on Single Cell Mechanics

COORDINATOR

CH.MO PROF G. MENSITIERI

TUTOR

CH.MO PROF. P.A. NETTI

COTUTOR

PH.D. S. FUSCO

PH. D. STUDENT

ING. VALERIA PANZETTA

**Abstract**

Mechanobiology research has shown that mechanical signals influence a wide spectrum of cellular events, including cell proliferation, differentiation, gene expression, protein production and their alterations.

The objective of this projects is to elucidate the role of two mechanical factors, matrix stiffness and externally applied forces, in the organization and contractile activity of the cytoskeleton and distribution of intracellular forces. Indeed, localized concentration of cytoskeletal tensions at focal adhesions, the structures that link cells to their surrounding extracellular matrix, is the major mediator of mechanical signaling.

Therefore, in the first phase of project we have studied how matrix stiffness in coordination with surface functionalization can regulate shape and the structural organization of integrated system constituted by actin network and integrin-mediated adhesion of fibroblasts. Then, we have investigated if there is a direct correlation between ECM stiffness and intracellular mechanics, measuring mechanical properties by particle tracking technique. A mechanical model has been developed to support experimental results and explain the relation that exists between matrix rigidity, focal adhesion sites dimension, cytoskeleton structure and intracellular mechanics.

In the second part of project, we have focused attention on how integration of externally applied mechanical forces from focal adhesions over the entire cell body affects fibroblast responses to its mechanical environments both in 2D and in 3D matrix.

In conclusion, we have observed that both matrix stiffness and external mechanical stress represent important stimuli to enhance cell stiffness and contractility of fibroblasts through cytoskeleton structuration, indicating that mechanics plays a critical role in cell biology. This consideration provides a solid foundation and rationale for use of mechanics to improve human health by designing appropriate equipment/instruments, exercise protocols, and rehabilitation regimens.

**Sommario**

La ricerca nel campo della "Mechanobiology" ha dimostrato che gli stimoli meccanici influenzano un ampio spettro di attività cellulari, quali la proliferazione, la differenziazione cellulare, l'espressione genica, la produzione di proteine e le alterazioni di queste stesse attività.
L'obiettivo di questo progetto è chiarire il ruolo di due fattori meccanici, la rigidezza della matrice e le forze esercitate dall'esterno sulla cellula, nell'organizzazione e nell'attività contrattile del citoscheletro e nella distribuzione delle forze intracellulari. Infatti, la concentrazione localizzata di stress da parte del citoscheletro in corrispondenza dei siti di adesione focale, le strutture che legano le cellule alla matrice extracellulare che le circonda, è il principale mediatore del processo di signaling meccanico.

Quindi, nella prima parte del progetto abbiamo studiato come la rigidezza della matrice assieme alla funzionalizzazione superficiale possa regolare la forma e l'organizzazione strutturale del sistema integrato costituito dal network di actina e dai siti di adesioni mediati dalle integrine nei fibroblasti. Quindi, abbiamo investigato sulla possibile esistenza di una diretta correlazione tra rigidezza della matrice e meccanica intracellulare, attraverso la misurazione delle proprietà meccaniche delle cellule attraverso la tecnica del particle tracking. È stato sviluppato un modello meccanico per supportare i risultati sperimentali e spiegare la relazione che esiste tra rigidezza della matrice, dimensione dei siti di adesione focale, struttura del citoscheletro e meccanica intracellulare.

Nella seconda parte del progetto, abbiamo focalizzato l'attenzione sul modo in cui l'integrazione delle forze meccaniche applicate dall'esterno dai siti di adesione all'intero corpo della cellula influenzi le risposte dei fbroblasti al suo ambiente meccanico in contesti 2D e 3D.

In conclusione, abbiamo osservato che sia la rigidezza della matrice che gli stress meccanici esterni rappresentano stimoli importanti che aumentano le proprietà meccaniche e la contrattilità dei fibroblasti attraverso la strutturazione del citoscheletro, indicando che la meccanica gioca un ruolo importante nella biologia cellulare. Questa considerazione fornisce un'indicazione solida e razionale per l'uso della meccanica al fine di migliorare lo stato di salute di organi e strutture attraverso la progettazione di adeguati dispositivi/strumenti, protocolli e piani di riabilitazione.

**Table of contents**

# Chapter 1

# Mechanics rules Cell Biology

## 1.1 Introduction

It's not easy to provide a concise definition of cell, the basic unit of life, that describes in a comprehensive way how this living structure, by its specialized activities (growth, differentiation, translocation, adhesion, signal transductions, and gene expression), guarantees the correct development and an adequate functioning of tissues and organs.

Surely, basing on idea of Maturama [1], the father of autopoiesis' concept, the cell can be seen as "organized (defined as a unity) as a network of processes of production (transformation and destruction) of components that produces the components", that "through their interactions and transformations continuously regenerate and realize the network of processes (relations) that produce them; and they constitute the system as a concrete unity in the space in which the components exist by specifying the topological domain of its realization as such a network". In this sense, living cells are cognitive systems, that are self-creating processes that define their own identity by conserving their structure while exchanging energy and information with the environment, with which they share a structural coupling. The coupling between the unity structure and its environment leads naturally to concept of adaptation that refers to collection of state's changes that allow cell to maintain its internal structural organization. So, the cell is a mechanical machine, endowed with autonomy and a necessary structural congruence with the surrounding environment.

Then, an accurate description of cell form and functional organization is fundamental to understand how these unities integrate them within a higher order architectural system and coordinate themselves in a single functional unit.

From this point of view, the structural and mechanical perspective to describe living cells is necessary in order to understand the process of cell and tissue organization: coherent, tangible and constructable system of structural engineering represents the basis for biological architecture; the structural integrity depends predominantly on tensile forces, positional information and pattern-generating informative forces, while the stability of form and shape is guaranteed by an equilibration between many interdependent structural elements [2]. The concept of stability has not

to be confused with those of staticity: in biological systems change is the only constant; solely the continual renewal of molecular components of cell structures preserves the complexity of biological structures. It's the ability of cells to respond dynamically to external stimuli, activating specifically biological processes, to represent the main distinction between classical engineering structures and living systems. Indeed, the modulation of cell shape is controlled by a dynamic equilibrium of structural forces that provide informative instructions for the regulation of cell growth, differentiation and advancing remodeling [3].

Considering that living organisms are cellular structures hierarchically organized [4], to understand and predict physiological and pathological events at the tissue and organ levels, it's mandatory to characterize quantitatively, in terms of magnitude and direction, the forces acting at cell level. The mechanobiology constitutes the link between disciplines that study molecular, cellular and tissue level phenomena and generates new knowledge and understanding in the biomedical sciences research.

## 1.2. Mechanobiology

Biological systems are complex structure constituted by a large number of elements that interact in a simple way to produce complicate behaviors. In the last years, the interest in the regulation of growth and size of biological systems has focused on the details of intracellular signaling mechanisms, but it's necessary to highlight that the control of size and shape of multicellular tissues, organs and bodies must be regulated from extracellular environment, through mechanisms that somehow obtain and integrate information at a scale that is relevant to the dimensions of the object being regulated. Understanding how the machinery of life controls and regulates the phenomena of growth and pattern formation is important to transfer design principles of Nature in a "engineering-centered approach" aimed at reproduction of biological systems and to create new technologies that could potentially transform biomedical sciences [5]. Indeed, from a tissue engineer's perspective, in order to grow tissue grafts ex vivo or induce tissue formation in situ, for a huge range of tissues, from skin to heart, it's better mimic early development rather than adult tissue repair. It's fundamental to take into account that a multitude of cellular, biochemical and biophysical mechanisms participate in the development of a functioning organ. To rerun the necessary environment for tissue formation, it's fundamental to

know how regulatory factors are orchestrated in space and time and how cells respond to external and internal signals and stressors. The differentiation of cellular function depends on the microenvironment in which the cells reside. As early said, the cells are active protagonists and can modify their niches by secreting or degrading the ECM, secreting cytokines and communicating with other cells and matrix by molecular and physical signals. Dissolution, diffusion and immobilization are the forms by which biochemical and molecular signals are transmitted to the cells through specific spatial and temporal profiles. Hormones, cytokines, chemokines and growth factors bind their cell surface receptors and elicit the production of chemical signals, that in their turn alter gene expression, protein synthesis and other aspects of metabolism. The molecular factors act in collaboration with biomechanical signals to regulate cell functions and tissue assembly. Strain induced signals can affect checkpoints in the cell cycle and cell proliferation and can cause cell fates to switch between growth and apoptosis. In these processes, the cytoskeleton acts as a key integrator of the extracellular molecular, mechanical and structural context during development, and can coordinate growth, size and shape at the tissue level [6]. It's interesting to consider that cell, using a structured organization, that is those of cytoskeleton, is able to convey mechanical cues across integrins and channel them through load-bearing cytoskeletal elements in the cytoplasm and nucleus. This way to transmit signals is much faster than chemical diffusion and also more focused by the sites at which stresses are concentrated, such as focal adhesions and cell-cell junctions [7].

To do this it's important to furnish a complete description of the complexity of cell that requires a broad knowledge, ranging from molecular biology to biophysics, materials science, chemical, mechanical and biomedical engineering. The discipline that studies the roles that these physical signals play in the fundamental processes of growth, development, cell differentiation and apoptosis is the *Mechanobiology*.

The control of cell functions is associated to the ability of cells to sense force and physical environment via the process of *Mechanosensing*. From the side of cells, the force sensing produces the recruitment of specific transmembrane cell surface receptors, the *integrins*, that act as mechanoreceptors, then the clustering of these receptors to distribute forces to many bonds and the force regulated strengthening of integrin-cytoskeleton linkages, which are closely associated with the actin cytoskeleton [6,8]. If the cytoskeleton is the main system implicated in the mechanosensing, it's not the only. Also the lipid-bilayer can mediate mechanosensing: forces at the cell membrane could determine its chemical reorganization; more stable lipids in curved

membranes diffuse into, whereas those seeking flat membranes diffuse out. Mechanosensing can also independent form proteins or lipids, but could be the consequence of change between signaling centers or enzymes and their substrates [9]. The conversion of these mechanical signals into biochemical responses, phenomenon known as *Mechanotransduction*, is associated with the structural reorganization of cytoskeleton and the propagation of signals from adhesion sites to nucleus via specific molecular pathways. Finally, cell alters protein expression and adjusts its function. It's interesting to observe that the force-mediated activation of adhesion sites produces a series of subsequent events also from the extracellular matrix side: tension applied to the extracellular matrix causes opening of cryptic sites, then the recruitment of matrix proteins associated to the integrins recruitment and translocation, and matrix remodeling with a following cellular response to altered matrix [8].

### 1.2.1 Cellular Mechanobiological Responses

There are numerous examples that show the ability of cells to perceive mechanical forces and transduce them into biological responses. Endothelial cells can recognize the magnitude, mode (steady or pulsatile), type (laminar or turbulent) and duration of applied shear flow, and respond accordingly, maintaining healthy endothelium or leading to vascular diseases including thrombosis and atherosclerosis [10-11]. Vascular smooth muscle cells in the arterial wall remodel when subjected to pressure induced wall stress. Fibroblast cells 'crawl' like an inchworm by pulling the cell body forward using contractile forces. Bone alters its structure to adapt to changes in mechanical environment as occurs, for example, in spaceflight. Stem cells sense the elasticity of the surrounding substrate and differentiate into different phenotypes accordingly [12]. Observations on single cells include the dysfunction of lymphocytes in near-zero gravity [13], force-dependent acceleration of axonal elongation in neurons [14-15], force-dependent changes in the transcription of cytoskeletal proteins in osteoblasts and other types of cell [16], and altered transcription in endothelial cells where disturbed flow occurs [17]. When repetitive stretching at a magnitude of 5% and a frequency of 1 Hz was applied to human tendon fibroblasts for one day, cell proliferation increased significantly. When the same conditions were applied for two days, however, cell proliferation was inhibited [18], indicating that stretching-induced proliferation of tendon fibroblasts also depends on stretching duration. In another study it has been demonstrated that multidimensional cyclic mechanical strain that mimics the physiological conditions in vivo has the potential to increase human tendon fibroblasts proliferation as well as gene expression and ECM

production in 3D scaffolds made from chitosan and hyaluronan [19]. Other studies show that cells can perceive two different forms of mechanical stimuli and respond in a differential manner relative to type I collagen mRNA expression and fibronectin and extracellular matrix protein synthesis and degradation [20]. In addition to cell proliferation and protein expression, mechanical forces can also induce the expression and production of inflammatory mediators, including COX-2, PGE2, and LTB4, in a stretching magnitude-dependent fashion [21-22]. In the presence of IL-1β, a potent inflammatory mediator present in injured tissues, 4% cyclic uniaxial stretching decreased COX-2 and MMP-1 gene expression and PGE2 production whose levels had been elevated by IL-1β treatment; in contrast, cells under 8% stretching further increased the expression levels of these genes and PGE2 production in addition to the effects of IL-1β stimulation [23]. The findings of this study indicate that mechanical loading regulates cellular inflammatory responses in a loading magnitude-dependent manner. These findings suggest that when tissues such as tendons are injured, appropriate levels of exercise could be beneficial as it may reduce the inflammatory response. On the other hand, excessive loading of injured tendons, which may worsen tissue inflammation, could be detrimental. In chondrocytes, mechanical loading has also been found to regulate cellular inflammatory response via the NF-κB signaling pathway [24].

In addition to responding to externally imposed forces, cells also exert internally generated forces on the materials to which they adhere, and some types of cells are exquisite detectors of material stiffness, changing their structure, motility and growth as they interrogate the mechanical properties of their surroundings [25].

### 1.2.2 Adhesion-dependent Cell Mechanosensitivity and Mechanotransduction

As previously said, cells use their sensory skills to explore the chemical and physical properties of an unknown environment, gathering such information at sites of ECM attachment and using them to activate specific signaling pathways within the cells [26-27].

It's well-known now that mechanosensitivity is guided by adhesion sites, that constitutes the sole cellular structures which cellular surface is physically connected to signaling and cytoskeletal proteins [27]. These structures are generated by the interaction of integrins with clustered ECM; scaffolding proteins allow the linkage between integrins and actin cytoskeleton, constituting the nascent ECM-integrin-cytoskeleton connections that develop to focal complexes [28]. The maturation of focal complexes to focal adhesions requires the force generated by myosin II and sustained forces for their stabilization and connection to stress fibers [29].

The forces that stimulate the formation, the stabilization and the maturation of focal adhesion can be generated by the cell itself through the cellular contractile machinery [30], but also from the outside. Different authors have observed that forces applied to nascent adhesions induce strengthening of the integrin-cytoskeleton connections, promoting the phenomenon of focal complex initiation and stabilization [31], also when the actomyosin system is blocked by specific inhibitors.

Riveline *et al.* have demonstrated the effects of external forces on the development of focal adhesions, observing that the application of local force to a focal complex determines the recruitment and a force-directed assembly of new proteins with a directional assembly. Under external forces, the phenomenon can also occur bypassing the requirement for ROCK–mediated myosin II [29]. Davies *et al.* have observed that under steady laminar flow focal adhesion sites and connected stress fibers remodeled in direction of flow. The alignment of focal adhesions was accompanied by coalescence of smaller sites, determining fewer, but bigger adhesions sites [32]. Also Guo and Wang have demonstrated as structural assembly and directional reorganization of actin filaments and some focal adhesion proteins can be controlled by force-induced structural shear inside the focal adhesion [33]. When cells are stretched, remodeling of adhesion sites is also accompanied by an increasing in number and size of focal adhesions [34] and by thickening and remodeling of actin stress fibers, that reorient in perpendicular direction respect to the stretch axis [34]. Very interesting is the work in which Mack *et al.* studied the mechanism by which magnitude and frequency of loading control phenomenon of focal adhesion sites remodeling, suggesting their role as mechanosensors in processes of balance of force transmission and triggering of biochemical events [35].

Also the local stiffness of extracellular matrix has a determining role in determining the adaptation of adhesions in terms of strength and size. The reduced cell spreading, the absence or reducing of stress fibers [36] and the increase of cell motility on soft matrix are associated to formation of irregular shaped and highly dynamic focal adhesions through a process that involves tyrosine phosphorylation and myosin-generated contractile forces [37-38]. Katz *et al.* have demonstrated that integrins constitute a way for cells to explore and response to the rigidity of the ECM. Not only the chemical composition, but also the physical properties of matrix are important in controlling the assembly of adhesion sites, as proved by covalent immobilization of fibronectin that inhibits cell motility [39] and in determining the strength of these structures in a matrix rigidity-dependent manner [40]. The ECM rigidity affects also the zyxin unbinding kinetics

within focal adhesions, as proved by the increase of unbinding rate constants (that implies a rapid and large scale focal adhesion disassembly) and by the reduction of traction forces that cells exert on polyacrylamide gels with increasing compliances [41].

The same results have been observed in 3D scaffolds. Tamariz and Grinnell explored the ability of cells to form cell-matrix adhesions in collagen gels of two different densities and, thus, stiffness, observing that fibroblasts in higher-density collagen gels have more adhesions containing vinculin and $\beta_1$ integrin [42]. Provenzano *et al.* observed a similar behavior in epithelial cells, that didn't' produce protrusions in lower stiffness collagen, but only cytoplasmic paxillin and vinculin, differently than on higher collagen concentration, in which cells exhibited adhesion sites [43].

Understanding the mechanisms that entail the bidirectional and reciprocal interaction between cell and its surrounding matrix the physical/structural roles of cell-ECM adhesions in affecting all facets of cell life. Indeed, the process of formation of adhesions and the regulation of their dynamics are crucial not only to guarantee the correct cell positioning into functional tissues and organs, but in particular to allow transfer of information between intra- and extra-cellular environments, that affect, in cooperation with other pathways, all biological processes, such as cell proliferation [44], cell differentiation [45-46], cell fate [47-48], embyogenesis, wound healing [49], but also tumorigenesis [50] or immune disorders[51].

### 1.2.3 Mechanobiology as a Tool to Design the Right Context for *in Vitro* Cell Culture

Currently, the goal of tissue engineering is to determine how multiple exogenous cues integrate intracellularly to regulate cell function. Indeed, solely if the cells composing the engineered tissue express the appropriate genes, the tissue specific function of the engineered tissue can be maintained.

In order to understand the phenomena of *mechanosensing* (the ability of a cell or tissue to detect the imposition of a force) and *mechanotransduction* (the ability of a cell to transduce mechanical signals in biochemical responses), it's fundamental to take into account that biochemical, but in particular mechanical signals are generated by interactions between cells and the extracellular matrix. Mechanical and biochemical signals cooperate within the functional unit composed of both the cell and the ECM in the coordination of a complex signaling hierarchy that guarantees the emergency of the correct functional phenotype. Then, the differentiation of cellular function depends profoundly on the microenvironment in which cell lives and it's well-known that cells are able to modify their boundary conditions by synthesizing or degrading the

ECM, secreting cytokines, and communicating with other cells and matrix. There are different ways to control the cellular function that consist in manipulating molecular or biomechanical signals. In the first case, the possible manipulations comprise the realization of biochemical gradients or micropatterning that defines cell-cell contact and distance or the control of the level of growth factors secreted by cells by modulating the size colony [52]. In the second one, it's necessary to consider that the cellular shape appears to be the most obvious indicator and regulator of physical effects on cell behaviors, including adhesion, spreading, migration and proliferation [53]. Indeed, the consequences of cell spreading and the cell shape are exhibited in processes of DNA synthesis and cell growth. In particular, the cell microenvironment imposes specific boundary conditions that influence cell architecture, mechanics, polarity and function. As early said, the cell volume and cell spreading are limited by the size of the microenvironment. Its structure, i.e. the positioning of adjacent cells and the location and orientation of ECM fibres, dictates the spatial distributions of cell adhesion and that of unattached cell surfaces. The biochemical composition and stiffness of the microenvironment specify the factors that can engage in cell adhesion, and thereby affect intracellular signalling pathways. These pathways subsequently dictate the assembly and dynamics of cytoskeleton networks. In addition to having a role in the conFiguretion of intra-cellular organization, the cell microenvironment also influences gene expression and cell differentiation. For example, in some types of cells, their shapes are firmly coupled to their differentiation and secretions of intrinsic substances. Cell shapes and architectures can be regulated by osmotic pressure, by micro/nanotopological features of the cell attachment substrate, by the adhesiveness and stiffness of the substrate, or by dynamic external force stimuli such as shear stress [54].

Then, we can assert than the two-way communication between ECM and cells (in particular cytoskeleton and nucleus), controlled by physical and biochemical connections, is very important in the regulation of cellular processes and gene expression. So, understanding the integrated mechanobiological responses of cells to the microenvironment is necessary in order to predict and control the behaviors of cells for therapeutic applications. In particular, understanding how to regulate the cell shape and functions, controlling the signals coming from ECM and the external forces are the primal tasks in tissue engineering as well as in development of functional biomaterials.

Then, providing insight into what, where and when a cell senses ECM cues and activates its biochemical responses is fundamental to understand how such cues can be incorporated into new, three-dimensional scaffolds to treat diseases. There are several works in literature that demonstrate the possibility to control biochemical response of cells by modulating mechanical properties of optimally designed substrates, in particular their elasticity.

### 1.3. The Ph.D. Project

We know that mechanical and chemical signals complement each other in biology. As previously said, a number of phenomena, such as cell shape and differentiated phenotype, and elastic properties cannot be explained by chemical signals alone. Mechanical and chemical signals have distinct characteristics, despite the fact that they share many intracellular molecules and processes. Chemical signals, with which we are most familiar, decay rapidly in strength with distance from their source and are usually meaningful over relatively short distances. Because they rely on diffusion or need to be carried in fluids or gases, chemically signals generally travel slowly. By contrast, mechanical signals, transmitted by tensed networks of fibers or other substances, travel rapidly over long distances, and might be terminated equally fast. Finally, mechanical signals can contain complex spatial information from multiple sources. Whereas chemical information is usually restricted to relatively simple chemical gradients.

Disruption of the normal mechanical environment can perturb cell function to the same extent as chemical stimuli. Cells and tissue have tightly controlled mechanical properties that are specific to their cell type and functions, and that are determined by their intrinsic mechanical properties and interactions with their mechanical environment. Abnormalities in cell mechanical properties or mechanical environment can result in altered cell function and disease, including malignancy, loss of altered stem cell potential and cardiac hypertrophy.

Then, for the reasons outlined all along this review chapter, the study of the role of mechanics in biology is of great importance in the scientific community. The keys to understand mechanical force-regulated cell biology are cellular mechanotransduction mechanisms by which cells "convert" mechanical force signals into biochemical signals in cells.

After this review chapter about the current knowledge about the mechanisms underlying mechanosensing and mechanotransduction processes, the thesis is organized in two more chapters written in the form of research reports and or articles and two appendixes.

Chapter 2 has focused attention on the regulation mechanisms by which fibroblasts modulate their shape and cytoskeletal organization in response to chemical functionalization and rigidity variation and on the influence that these two factors can have on intracellular mechanics of fibroblasts through processes of biridectional interaction between integrin-based adhesion complex, namely focal adhesion, and the actin cytoskeletal structure. In this sense, we are interested in understanding inside-out signaling processes, that allow to cells to sense extracellular mechanical properties and consequently adjust their tensional state.

Chapter 3 presents a possible interpretation to mechanisms of outside-in signaling, associated to cell response to external mechanical deformation, applied to the substrate to which cells are adhered.

Appendix A offers an overview of main experimental techniques available to study cell mechanics.

Appendix B offers an overview of principal models actually used to interpret single cell mechanical properties.

Only understanding the role of biochemical signals in regulation communication of the cell with the surrounding extracellular environment and in signaling through focal adhesions, we can correctly interpret their contribute into the regulation of normal developmental processes and into the pathogenesis of tissue diseases, such as cancer, hematologic disease, respiratory distress and so on and intervene to promote the first ones and control the others.

## References


[1] Maturama H. R and Varela F. J. "Autopoiesis and cognition: the realization of the living", **1928**.

[2] Ingber, D. E. "From molecular mechanotransduction to biologically inspired engineering". *Ann. Biomed. Eng*. 38, 1148-1161, **2010**.

[3] Ingber, D.E., and Jamieon, J. D. "Cells as tensegrity structures: architectural regulation of histodifferentiation by physical forces transduced over basement membrane". Pp. 13-32 in Gene Expression During Normal and Malignant Differentiation, L. C. Andersson, C. G. Gahmberg, and P. Ekblom, eds. Academic Press, Orlando, FL, **1985**.

[4] Ingber, D. E. "Cellular mechanotransduction: putting all the pieces together again". *FASEB J.* 20, 811-827, **2006**.

[5] Lander, A. D. "Pattern, growth and control". *Cell* 144, 955-969, **2011**.

[6] Ingber, D. E. "Tensegrity-based mechanosensing from macro to micro". *J. P. Bio. Mol. Bio.* 97, 163-179, **2008**.

[7] Ingber, D. E. "Tensegrity and mechanotransduction". *J. Body Mov. Ther.* 12, 198-200, **2008**.

[8] Vogel, V. and Sheetz, M. "Local force and geometry sensing regulate cell functions". *Nat Rev Mol Cell Biol* 7(4), 265-275, **2006**.

[9] Janmey, P. A., and Weitz, D. A. "Dealing with mechanics: mechanisms of force transduction in cells". *Trends Biochem. Sci.* 29, 364-370, **2004**.

[10] Davies, P. F., and S. C. Tripathi. "Mechanical stress mechanisms and the cell". An endothelial paradigm. *Circ. Res*. 72, 239-245, **1993**.

[11] Lehoux, S., Y. Castier, and A. Tedgui. "Molecular mechanisms of the vascular responses to haemodynamic forces". *J. Intern. Med*. 259, 381–392, **2006**.

[12] Engler, A. J., S. Sen, H. L. Sweeney, and D. E. Discher. "Matrix elasticity directs stem cell lineage specification". *Cell* 126, 677–689, **2006**.

[13] Cogoli, A. *et al.* "Cell sensitivity to gravity". *Science* 225, 228–230, **1984**.

[14] Heidemann, S.R. and Buxbaum, R.E. "Mechanical tension as a regulator of axonal development". *Neurotoxicology* 15, 95–107, **1994**.

[15] Smith, D.H. *et al.* "A new strategy to produce sustained growth of central nervous system axons: continuous mechanical tension". *Tissue Eng*. 7, 131–139, **2001**.

[16] Wang, J. *et al.* "Transcriptional regulation of a contractile gene by mechanical forces applied through integrins in osteoblasts". *J. Biol. Chem*. 277, 22889–22895, **2002.**

[17] Passerini, A.G. *et al.* "Coexisting proinflammatory and antioxidative endothelial transcription profiles in a disturbed flow region of the adult porcine aorta". *Proc. Natl. Acad. Sci. U. S. A*. 101, 2482–2487, **2004**

[18] Barkhausen T, van Griensven M, Zeichen J, Bosch U "Modulation of cell functions of human tendon fibroblasts by different repetitive cyclic mechanical stress patterns"**.** *Exp Toxicol Pathol*, 55(2-3), 153-158, **2003**.

[19] Sawaguchi, N. *et al.* "Effect of cyclic three-dimensional strain on cell proliferation and collagen synthesis of fibroblast-seeded chitosan-hyaloronan hybrid polymer fiber". *J. Orthop. Sci.* 15, 569-577, **2010.**

[20] He Y, Macarak EJ, Korostoff JM, Howard PS "Compression and tension: differential effects on matrix accumulation by periodontal ligament fibroblasts in vitro"**.** *Connect Tissue Res*, 45(1), 28-39, **2004**.

[21] Li Z, Yang G, Khan M, Stone D, Woo SL, Wang JH "Inflammatory response of human tendon fibroblasts to cyclic mechanical stretching"**.** *American Journal of Sports Medicine*, 32(2), 435-440, **2004**.

[22] Wang JH, Jia F, Yang G, Yang S, Campbell BH, Stone D, Woo SL "Cyclic mechanical stretching of human tendon fibroblasts increases the production of prostaglandin E2 and levels of cyclo oxygenase expression: a novel in vitro model study"**.** *Connective Tissue Research* 44(3-4):128-133, **2003**.

[23] Yang G, Im HJ, Wang JH "Repetitive mechanical stretching modulates IL-1beta induced COX-2, MMP-1 expression, and PGE2 production in human patellar tendon fibroblasts"**.** *Gene*, 363:166-172, **2005**.

[24] Agarwal S, Deschner J, Long P, Verma A, Hofman C, Evans CH, Piesco N "Role of NF-kappaB transcription factors in antiinflammatory and proinflammatory actions of mechanical signals"**.** *Arthritis Rheum*, 50(11), 3541-3548, **2004**

[25] Pelham, R.J. Jr and Wang, Y. "Cell locomotion and focal adhesions are regulated by substrate flexibility". *Proc. Natl. Acad. Sci.* U. S. A. 94, 13661–13665, **1997**
[26] Bershadsky, A. D. *et al.* "Adhesion-dependent cell mechanosensitivity". Annu. *Rev. Cell Dev. Biol.* 19, 677-695, **2003**.
[27] Geiger, B. *et al.* "Environmental sensing through focal adhesions". *Nat. Rev. Mol. Cell. Biol.* 10, 21-33, **2009**.
[28] Geiger, B. *et al. "*Transmembrane crosstalk between the extracellular matrix–cytoskeleton crosstalk". *Nat. Rev. Mol. Cell Biol.* **2, 793-805, 2001**.
[29] Riveline, D. *et al.* "Focal contact as mechanosensors: Externally Applied Local Mechanical Force Induces Growth of Focal Contacts by an Mdia1-Dependent and Rock-Independent Mechanism". *J. Cell Biol*. 6, 1175-1186, **2001**.

[30] Wolfenson, H. *et al.* "Actomyosin-generated tension controls the molecular kinetics of focal adhesions". *J. Cell. Sci.* 124, 1425-1432, **2011**.
[31] Galbraith, C.G. *et al.* "The relationship between force and focal complex development". *J. Cell Biol.* **159**, 695–705, **2002**.
[32] Davies, P.F. *et al.* "Quantitative studies of endothelial cell adhesion. Directional remodeling of focal adhesion sites in response to flow forces". *J. Clin. Invest.* 93, 2031-2038, **1994**.
[33] Guo, W. and Wang, Y. "Retrograde fluxes of focal adhesion proteins in response to cell migration and mechanical signals". *Mol. Biol. Cell* 18, 4519-4527, **2007**.
[34] Yoshigi, M. *et al.* "Mechanical force mobilizes zyxin from focal adhesions to actin filaments and regulates actin filaments". *J. Cell Biol.* 171, 209-215, **2005**.
[35] Mack, P.J. *et al.* "Force-induced focal adhesion translocation: effects of force amplitude and frequency". *Am. J. Physiol. Cell Physiol.* 287, C954-C962, **2004**.
[36] Yeung, T. *et al.* "Effects of substrate stiffness on cell morphology, cytoskeletal structure, and adhesion". *Cell Motil. Cytoskeleton* 60,24 –34, **2005**
[37] Pelhalm, R. J. and Wang, W. "Cell locomotion and focal adhesions are regulated by substrate flexibility". *Proc. Natl. Acad. Sci*. 94, 13661-13665, **1997**.
[38] Ulrich, T.A. *et al.* "The mechanical rigidity of the extracellular matrix regulates the structure, motility, and proliferation of glioma cells". *Cancer Res*. 69, 4167-4174, **2009**.
[39] Katz, B-Z. *et al.* "Physical state of the extracellular matrix regulates the structure and molecular composition of cell-matrix adhesions". *Mol. Biol. Cell*. 11, 1047-1060, **2000**.
[40] Choquet, D. *et al.* "Extracellular Matrix Rigidity Causes Strengthening of Integrin–Cytoskeleton Linkages". *Cell* 10, 39-48, **1997**.
[41] Lele, T. P. *et al.* "Mechanical Forces Alter Zyxin Unbinding Kinetics Within Focal Adhesions of Living Cells". *J. Cell. Physiol*. 207, 187-194, **2006**.
[42] Tamariz, E. and Grinnell, F. "Modulation of fibroblast morphology and adhesion during collagen matrix remodeling". *Mol. Biol. Cell* 13, 3915-3929, **2002**.
[43] Provenzano *et al.* "Matrix density-induced mechanoregulation of breast cell phenotype, signaling and gene expression through a FAK–ERK linkage". *Oncogene* **28,** 4326–4343, **2009**.
[44] Provenzano, P.P. and Keely, P.J. "Mechanical signaling through the cytoskeleton regulates cell proliferation by coordinated focal adhesion and Rho GTPase signaling". *J. Cell Sci.* 124, 1195-1205, **2011**.

[45] Thannickal, V.J. *et al.* "Myofibroblast Differentiation by Transforming Growth Factor-β1 Is Dependent on Cell Adhesion and Integrin Signaling via Focal Adhesion Kinase" *J. Biol. Chem*. 278, 12384-12389, **2003**.
[46] Du, J. *et al.* "Integrin activation and internalization on soft ECM as a mechanism of induction of stem cell differentiation by ECM elasticity". *Proc. Natl. Acad. Sci.* 108, 9466-9471, **2011**.
[47] Wozniak, M. A. *et al.* "Focal adhesion of regulation of cell behavior" *Biochem. Biophys. Acta* 1692, 103-119, **2004**.
[48] Geiger, B. and Yamada, K.M. "Molecular architecture and function of matrix adhesions" *Cold Spring Harb. Perspect. Biol*. 3, a005033, **2011**.
[49] Shultz, G.S. and Wysocki, A. "Interactions between extracellular matrix and growth factors in wound healing". *Wound Rep. Reg.* 17, 153-162, **2009**.

[50] Zhao, J. and Guan, J.L. “Signal transduction by focal adhesion kinase in cancer”. *Cancer Metastasis Rev*. 28, 35-49, **2009**.
[51] Berrier, A.L. and Yamada, K. M. “ Cell-matrix adhesion”. *J. Cell. Physiol*. 213, 565-573, **2007**.
[52] Théry, M. “Micropatterning as a tool to decipher cell morphogenesis and functions”. *J. Cell Sci*. 123, 4201-4213, **2010**.
[53] Elson, E.L. “Cellular Mechanics as an Indicator of Cytoskeletal Structure and Function”. *Annu. Rev. Biophys. Biophys. Chem.* 17, 397-430, **1988**.
[54] Freytes, D.O. *et al.* “Geometry and force control of cell function”. *J. Cell. Biochem.* 10, 1047-1058, **2009**.

# Chapter 2

# Cell Mechanics as Consequence of Focal Adhesion Adaptation to Elasticity of Extracellular Matrix

## 2.1 Introduction

Mechanosensing deals in understanding and interpreting the way in which cells use stresses generated internally to sense the mechanical properties of their microenvironment and activate specific responses associated to the extracellular stiffness. The cells probe elasticity, anchoring and pulling on their surroundings through transmembrane adhesion receptors that provide a structural connection between external cellular contacts and internal cytoskeleton [1-7]. The forces generated by the interconnected network of actin and myosin can be transferred to soft matrix, inducing wrinkles and deformation. Cell, in turn, responds re-assembling the cytoskeleton and its overall state, closing the feedback loop correlated to the substrate stiffness.

Indeed, the growth and remodeling phenomena of the functional state of living cells seem strictly associated to their capacity to respond to resistance of microenvironment, through actively cytoskeleton and adhesions adaptations and shape and internal organization changes.

Although most of research has focused on the role of biochemical agents in guiding cellular processes and determining tissue functions [8-11], it's now acknowledged the importance of mechanical properties of extracellular matrix in controlling cell-dependent responses [12-14]. Nowadays a lot of research effort focuses on understanding how biochemical and physical signals can act in a coordinated way to activate specific signaling pathways. In this context, the matrix cannot be merely consider a structural support, but its way of deformation is the way to expose cryptic sites to receptors or molecules in order to regulate cellular activities [15].

The most important effect of substrate stiffness is exhibited in the structure and dynamics of adhesion sites and therefore in cytoskeleton organization and cell spreading. Pelham and Wang have observed that 3T3 fibroblasts and rat kidney epithelial cells are able to sense the rigidity of the microenvironment that surround them and regulate the adhesion sites and motility. In

particular, the speed of fibroblasts is higher on flexible substrates than on hard substrate [16]. In other words, the tyrosine phosphorylation increases with stiffness substrate as showed by the formation of stable focal adhesions. Yeung *et al.* have demonstrated that fibroblast and endothelial cells develop a spread morphology and actin stress fibers only when are cultured on substrates with an elastic modulus greater than 2 kPa [17]. The sensitivity of living cells, in particular NIH3T3, to substrate stiffness and topography has also been investigated in terms of spreading area. Cheng *et al.* have found a decrease of 30% of cell area when cells are cultured on softer PDMS substrate instead that on unmodified PDMS substrate [18].

Furthermore, physical and, in particular, mechanical properties of cell microenvironment are of great importance in guiding differentiation processes. Early studies that have demonstrated such phenomenon have showed that mouse mammary cells have an increased differentiation when grown on soft collagen gel substrates, as opposed to tissue culture plastic [19]. It has been reported that mesenchymal stem cells can differentiate into different anchorage-dependent cell types, such as myoblasts, osteoblasts and neurons. Furthermore, Engler *et al.* have demonstrated that simply plating MSCs on polyacrylamide gels of varying stiffnesses in absence of soluble factors, it's possible to drive expression of neuronal, skeletal muscle, or osteogenic markers [20]. Similarly, it has been demonstrated that the effective stiffness of the substrate regulates the differentiation of neural stem cells. Adult neural stem cells have been grown on substrates with elastic moduli varying between 10 and 10,000 Pa. While soft substrates (10 Pa) have induced cell spreading and differentiation, cells have exhibited growth and high levels of a neuronal marker, beta-tubulin III, on substrates with a stiffness similar to those of brain tissue. In addition, softer substrates (100-500 Pa) have promoted neuronal differentiation, whereas stiffer substrates (1,000-10,000 Pa) have led to glial differentiation [21]. In other studies, it has been demonstrated that the elasticity of substrates can be used as mechanical signal to preserve the multilineage potential of human mesenchimal stem cells. These cells can be induced into adipogenic or osteogenic lineages when seeded on stiff substrates, using the appropriate induction medium [22]. Another interesting observation is that the effective moduli of substrate sensed by cells depends not only on the intrinsic elastic modulus of materials, but also on the thickness of substrate. Indeed, bone marrow hMSCs were seeded onto thin (130 μm), thick (1440 μm) collagen gel. As well as on the hard substrate, cells seeded onto thick gel have not expressed specific marker and remained at their quiescent state, while the thin gels have induced changes in morphology, actin fiber structures, proliferation and adipogenic and osteogenic differentiation [23]. However, the matrix stiffness alone

is not most effective to induce a specific differentiation, but it works in concert with soluble biochemical factors such as TGF-β to define a sole differentiation pathway [24].

The stiffness of substrate plays an important role in the correct expression of cell phenotype and then in the normal functioning of the tissue that cells make, for example the myocardium. In their study Bajaj *et al.* have cultured embryonic cardiac myocytes on laminin-coated polyacrylamide substrates with elastic moduli ranging from 1 and 50 kPa. The stiff substrates (18, 50 kPa and tissue culture dishes) have guaranteed the formation of higher percentage of aligned focal adhesions, whereas the cells seeded onto soft substrate (1 kPa) have showed only non-aligned sarcomeric fibers, because this substrate don't provide enough actomyosin-based contractions. The force of contraction of cells on tissue culture dishes is bigger than on other substrates, in according with the higher percentage and stability of focal adhesions that cells form on these dishes [25].

The increase in spreading area and traction forces that cells exert on stiff substrate is associated to a preference of cells for stiff substrate in a process that is called *durotaxis* or *mechanotaxis*. This phenomenon has been observed by Lo *et al.*, that have demonstrated the ability of 3T3 fibroblasts to sense and respond to substrate stiffness and migrate towards region of increasing stiffness [26]. Also vascular smooth muscle cells have exhibited a preferential migration toward the stiffer region of the substrate, while on a homogeneous compliance gel the movement presented the features of a random walk. Also the speed has been different in dependence on the substrate rigidity, resulting higher on soft regions than on stiff ones [27]. Adhesion, spreading and migration seem to be affected by substrate stiffness also for neutrophils, that generate bigger traction stresses on stiff regions of substrate than on soft ones [28]. The optimum stiffness value for motility depends also on the concentration of ECM proteins covalently attached to the substrate [29-30]. The same result has been observed on PDMS membrane bonded to PDMS patterned substrate, that realize mechanical gradient: the cells seem more motile on softer substrate, forming filopodia-like extensions and a preferential accumulation on stiffer regions [31]. Also in 3D collagen matrix there is over a sufficiently long time span a migration into stiff regions [32].The migratory capability of cells depends not only on the rigidity of substrate, but also on the ability of cells to deform soft substrates and communicate with other cells through these cellular traction stresses [33]. Indeed, *durotaxis* can be explained as a stabilizing mechanical phenomenon. The stable conFiguretions on stiffer substrates seems to be energetically more convenient, determining a directional movement towards stiffer regions [34].

To better understand the mechanisms through which mechanical cues and in particular substrate stiffness can affect adhesion and then migration process, it's required to investigate the relationship between cellular and substrate elasticity. Being able to how the cell "senses and translates" external mechanical cues in a biomechanical/biochemical adaptation is today very crucial in tissue engineering. In this direction, some studies have demonstrated a direct mechanical way to communicate between cells and surrounding environment. For example, it has been shown that fibroblasts adjust their intracellular stiffness by changing their cytoskeletal structure to match the stiffness of the substrate on which they are cultured [35]. Byford *et al.* have observed that the systems used in these studies do not allow to culture cells in a three-dimensional matrix, that better mimics the context in which living cells live. It's been shown that also when the cells are cultured in 3D matrix, they alter their structure increasing the elastic modulus when the collagen concentration increases. The elastic moduli of living cells were measured using the technique of atomic force microscopy (AFM), imposing the isolation of cells from 3D gels [36]. Baker *et al.* have overcame the technical limitation of AFM, investigating the intracellular microenvironment by using particle tracking microrheology technique [37-38]. They have measured the viscoelastic moduli of prostate carcinoma cells cultured both in 2D and 3D collagen gels and found contrasting results with previous commented ones, indeed the elastic modulus in three-dimensional matrices decrease with increasing collagen concentrations, whereas the intracellular mechanics has been not noticeably affected by substrate stiffness, when the cells have been cultured onto 2D substrates [39]. The same authors have observed that the transforming potential affects intracellular stiffness in a matrix-stiffness-dependent manner. The human mammary transformed-cells have exhibited a stiffening behavior in response to the increase of matrix stiffness [40].

From a different point of view, several studies indicate that substrate rigidity sensing is mediated by focal adhesions (FAs). They demonstrate that FAs are force-transducing, mechanosensory complexes, and their ability to grow in response to pulling forces requires attachment to an integrin-adhesive matrix [41]. In particular Prager-Khoutorsky *et al.*, have demonstrated as the mechanosensing machinery of focal adhesions seems to play an important role in regulating the rigidity-dependent cell polarization process. They have found that cell ability to distinguish between extracellular matrices with different stiffness and the ability to acquire a polarized morphology are strictly correlated since cells are able to take such morphology only on rigid substrate, and that the average size of focal adhesions on a fibronectin-coated 5 kPa PDMS

substrate was about twofold smaller than those formed on rigid substrates (2 MPa) of the same type.

Even if there is an increasing interest in revealing the extraordinary ability of cells to respond to a wide range of chemical and physical environmental features, it remains partially unknown the way in which the extracellular matrix rigidity regulates the alteration of cytoskeletal organization and then the intracellular mechanics. In this study, we investigate the role of matrix stiffness in determining the intracellular compliance of cells cultured on 2D matrices with and without RGD surface functionalization.

In particular, we investigate how 3T3 fibroblasts modulate their shape and their cytoskeletal organization in response to substrate rigidity variations and surface functionalization. Additionally, we examine how the combination of these two factors contributes to control intracellular mechanics of fibroblasts and the correlation between the exhibited cell mechanical properties and the integrated response of the system constituted by actin machinery and integrin-mediated adhesions that control the actin cytoskeleton organization.

We have focused our attention on 1) the existence of a direct relationship between ECM stiffness and intracellular mechanical properties; 2) the correlation between cell mechanics and other chemical-physical characteristics, particularly by ECM specifity and adhesive ligand density, which in an integrated manner have the effect of controlling cellular adhesion; 3) how the matrix rigidity alone or in association with the presence of adhesive ligands can activate the processes of biridectional interaction between integrin-based adhesion complex, namely focal adhesion, and the actin structure, that modulate the assembly of these two systems and signaling form the focal adhesions to the cytoskeleton.

In addition, we analyze the evolving mechanisms of the equivalent system formed by matrix, focal adhesion and stress fiber. We used a mathematical model to explain, analytically, how the remodeling FA and, as a consequence, the equivalent system rigidity are correlated to the substrate rigidity.

## 2.2 Materials and Methods

### 2.2.1 Polydimethylsiloxane Substrata Preparation and Mechanical Characterization

SYLGARD 184 has been purchased from Dow Corning (Midland, MI), SYLAGARD 184 consist of a 'base' and a 'curing agent'. The crosslinking prepolymer molecules are the main component of the curing agent and therefore will be referred to this component as 'crosslinker'. To prepare polydimethylsiloxane (PDMS) substrata with different elastic moduli, the silicone elastomer base and the crosslinker have been mixed thoroughly at various ratios and then transferred into tissue culture plates. After degassing under vacuum for 1 hour, the PDMS substrata were cured at 60°C overnight. The mixing ratios we have used between the crosslinker and the base are 1:10, 1:30, 1:50.

The mechanical properties of PDMS substrates have been evaluated by small-amplitude oscillatory shear experiments that have allowed measurement of the response of the samples and hence of their linear viscoelastic properties. This technique has been successfully used to determine the structure-mechanical properties relationship of materials [42-43]. The tests were performed by using a stress-controlled rheometer (Gemini, Bohlin Instruments) in a parallel plate geometry (20 mm of diameter). The instrument was preheated to 37° ± 0.01°C and maintained at constant temperature throughout the test. In a dynamic experiment, the material is subjected to a sinusoidal shear strain

$$\gamma = \gamma_0 \sin(\omega t) \tag{1}$$

where $\gamma_0$ is the shear strain amplitude, $\omega$ is the oscillation frequency (which can also be expressed as $2\pi f$, where $f$ is the frequency in hertz), and $t$ is the time. The mechanical response, expressed as shear stress, $\tau$, of viscoelastic materials, is intermediate between an ideal pure elastic solid (obeying Hooke's law) and an ideal pure viscous fluid (obeying Newton's law) and therefore is out of phase with respect to the imposed deformation, as expressed by

$$\gamma = G^{'}cos(\omega t) + G^{''}sin(\omega t) \tag{2}$$

where $G^{'}$ is the shear storage or elastic modulus and $G''$ is the shear loss or viscous modulus. $G'$ provides information about the elasticity or the energy stored in the material during deformation, whereas $G''$ describes the viscous character or the energy dissipated as heat. Dynamic strain sweep were performed at a frequency of 1 Hz with strain amplitude ranging from $1.5 \cdot 10^{-4}$ and $1.5 \cdot 10^{-1}$ %. The tests were repeated at least four times for each typology of sample.

To measure the shear modulus G, a stress-strain test was performed on the samples applying a shear deformation in the range from $10^{-3}$% to 80% at 1 Hz frequency.

### 2.2.2 Conjugation of RGD Peptides to PDMS

The conjugation of RGD peptides has been performed in two-steps method **Figure 1** by using a bifunctional photolinker, N-sulfosuccinimidyl-6-(40-azido-20-nitrophenylamino)hexanoate (sulfo-SANPAH, INBIOS S.r.l., Naples, Italy) as cross-linking agent to immobilize GRGDY peptides . In the first step, a sulfo-SANPAH solution in deionized water has been prepared in the following way: sulfo-SANPAH has been first dissolved in dymethylsulfoxide (DMSO) at concentration of 0.25 mg/mL and then diluted with deionized water to 1 mM concentration. The freshly prepared sulfo-SANPAH solution has been placed onto a PDMS sheet, followed by exposure to UV light for 30 min. The reaction has been stopped rinsing the PDMS samples extensively with deionized water and phosphate-buffered saline (PBS). During the treatment to UV light, is has been prepared the coupling solution made by a 50mM (pH 8.5) bicarbonate buffer with 0.5 mg/ml of peptides. After washing, the silicone sheets have been completely covered with GRGDY peptides solution and incubated at 4°C for 24 h. The RGD solution has been removed and the membranes have been washed with PBS three more times. Unreacted NHS groups have been blocked by treating the polymer surfaces with a 0.2 M methalonamine (Sigma-Aldrich) in carbonate buffer (50 nM, pH 8.5) at 4°C for 30 min. Then, samples have been stores dry until further use. Afterward, the substrates have been sterilized for cell attachment incubating them with antibiotic solution for 24 h at 37°C or thoroughly have been washed with ultrapure water and dried under vacuum for determination of conjugated peptides.

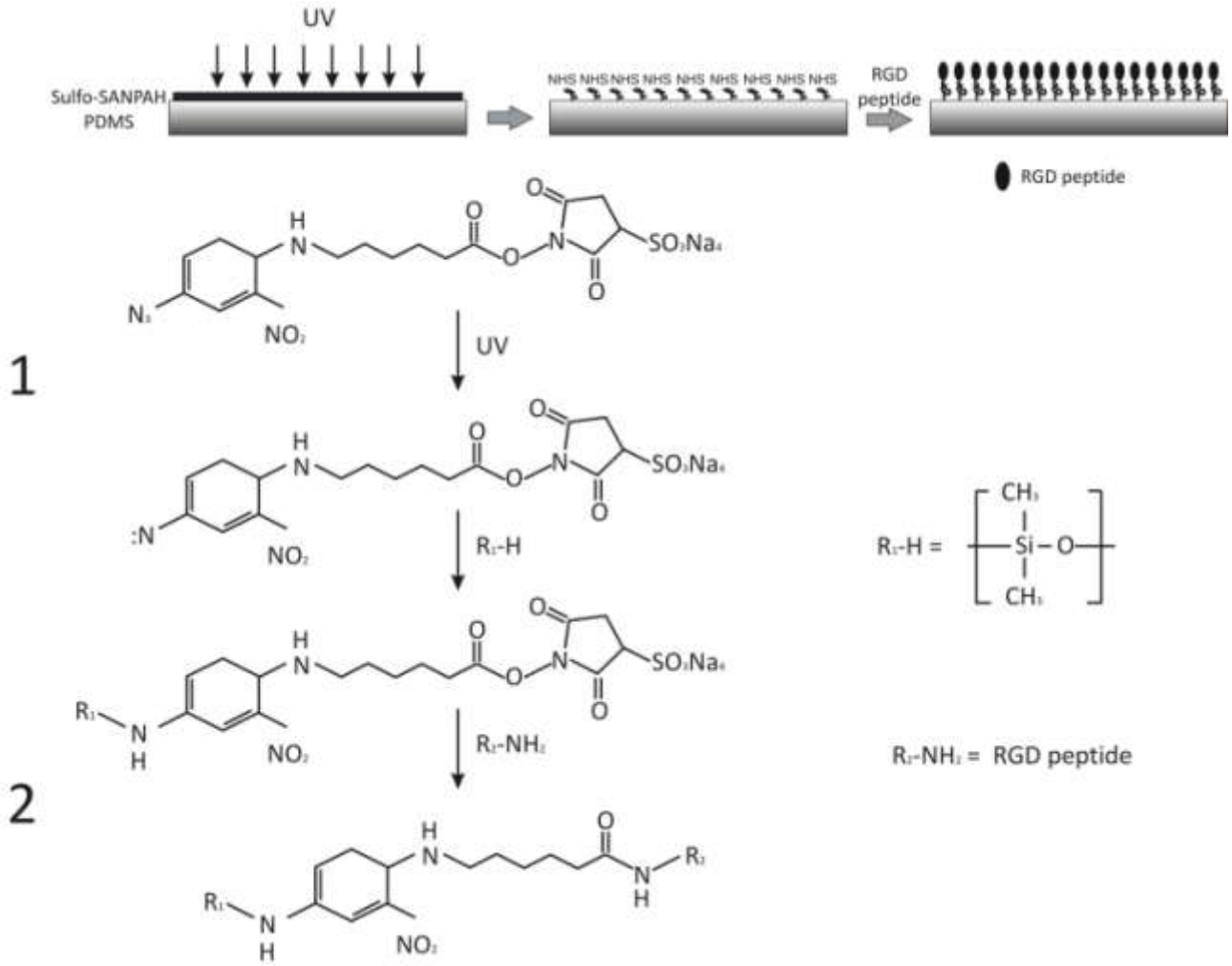


**Figure 1 | Two step method for the conjugation of the RGD peptides to PDMS surfaces:** 1 - Photochemical immobilization of functional NHS groups to PDMS surface; 2 - Linking of RGD peptide to the surface via coupling reaction with NHS.

### 2.2.3 Determination of Surface RGD Density

The density of RGD peptide on the PDMS surfaces has been determined directly on solid support by using MicroBCA assay (Sigma-Aldrich) as described from Tyllianakis *et al.* [44]. The principle both relies on the formation of a $Cu^{2+}$-protein (peptide in our case) complex under alkaline conditions, followed by reduction of the $Cu^{2+}$ to $Cu^{1+}$. The amount of reduction is proportional to protein present, that can be monitored by the purple-blue chelate complex, absorbing at 562 nm, which BCA forms in alkaline environments. This moderated purple colored complex allows a spectrophotometric determination of nanomolar quantities of functional groups in aqueous solution. The absorbance of peptide group present on surfaces has been measured at 562 nm

using a microplate reader (Victor, PE) and the evaluation of surface RGD bonds is finally carried out through standard calibration curve, obtained using RGD solutions of known concentrations.

The amount of immobilized short peptides, containing the enhancing tyrosine residue (GRGDY), has been performed by adding the MicroBCA working solution directly onto the samples in a reduced volumetric form of the assay. The determination of the nanomolar peptide concentration has been carried out by calibration curve, previously obtained at the same conditions. A nominal density has been calculated by taking into account the area of each treated sample and referred to as RGD nmol/$cm^2$. In addition, in order to finely investigate the effect of any contaminant on the assay color formation, aminolyzed substrates and pure polymer have been also tested.

### 2.2.4 Cell Culture

Experiments have been performed on mouse embryo fibroblasts NIH3T3 cells. Cell line have been cultured at 37°C in 5% CO2 in Dulbecco's modified Eagle's (DMEM) medium supplemented with 10% fetal bovine serum (FBS, BioWhatter, MD), 2 mM L-glutamine (Sigma, St. Louis, MO), 1000 U/L penicillin (Sigma, St. Louis, MO), and 100 mg/L streptomycin (Sigma, St. Louis, MO).

### 2.2.5 Particle Delivery and Particle Tracking

NIH-3T3 cells have been cultured to ~90% confluency in a 10 cm dish (Corning Incorportated) and then have been incubated with 100 nm fluorescent carboxylated nanoparticles (Invitrogen, Molecular Probes) solution (0.03% v/v) for 3 h under physiological conditions.

After incubation, cells have been detached using 0.25% Trypsin/0.53 mM EDTS, allowing to endocyted particles to free from protein motors that guide microtubule-mediated directed motion of vesicles. 40.000 cells have been added on top of each previously PDMS substrate, both with conjugated RGD peptides and without functionalization, performing subconfluent cultures. Each dish has been supplemented with 500 µl of media and subsequently incubated for 24 h at 37°C, 5% $CO_2$.

After incubation, images of NPs inside cells have been collected in real time for about 6 s by using an inverted microscope (Olympus IX70) equipped with a fluorescence mercury lamp (Olympus U-RFL–T). A 100x oil immersion objective (high numerical aperture [NA] 1.3) has been used for particle tracking, which permitted ~0.1 µm spatial resolution over a 156 µm × 125 µm field of view. To perform experiments under physiological conditions, a microscope stage incubator (Okolab) has been used to keep cells at 37°C and 5% $CO_2$, which is supplied as a 5/95% $CO_2$/air

mixture. Before supplying this gas to the cells, it is moisturized by feeding it through a closed chamber containing 5% $CO_2$satured water. The sequence of digital images has been acquired by a fast digital camera (Lambert Instruments) at a frame rate of 50 fps, forming a movie. Eight to ten cells have been analyzed for each experimental condition and an average number comprised between 30-50 particles has been tracked for each cell. Indeed, we have used a diluted particle solution (0.03 % v/v) to reduce the error in trajectory reconstruction, due to overlapping, and minimize interaction between adjacent particles. The experiments on functionalized substrates have been repeated also after 48 h, in condition of confluent cultures, in order to accounting for intercellular interactions role in controlling cytoskeletal structuring and then intracellular mechanical properties of cells.

### 2.2.6 Intracellular Rheology from Particle Tracking

The technique of particle tracking microrheology has been introduced by Tseng *et al.* [45] and allows to monitor the local viscoelastic properties of living cells with high spatio-temporal resolution, collecting and analyzing the Brownian motions of particles embedded in cytoplasm. These beads are smaller than 1 μm so that they undergo Brownian motion, as inertial forces (gravity) are negligible. Then, they are subjected to two main forces, the random force created by the thermal energy $k_BT$ that is of order of magnitude $k_BT/a$ and the counteracting frictional force proportional to the velocity of the bead and the bead's friction coefficient, that depends on the viscoelastic properties of the cytoplasm and the size of the bead.

As previously said, by using a video particle nano-tracking, the particle's displacements are tracked. To generate the point tracking trajectories, algorithm has to perform two distinct steps: first, it has to detect the points in each frame and, then , it has to link this point detection into trajectories. In ourself-developed Matlab® (Matlab 7) code, each position has been determined by intensity measurements through its centroid, and it has been compared frame by frame to produce trajectory for each particle, based on the principle that the closest positions in successive frames belong to the same particle (proximity principle). Once obtained nanoparticles trajectories, mean squared displacements (MSDs) have been calculated on

$$< \Delta r^2(\tau) >=< [x(t-\tau) - x(t)]^2 + [y(t-\tau) - y(t)]^2 > \quad (3)$$

where $< >$ means time average, $\tau$ is the time scale and $t$ the elapsed time, have been calculated from the trajectories of the centroids of the microspheres.

MSDs of microbeads can be related to shear creep compliance, $\Gamma(\tau)$, from the following relationship [46]

$$\Gamma(\tau) = \frac{3k_BT}{2\pi a} < \Delta r^2(\tau) > \quad (4)$$

The factor $3/2$ stems from the fact we track the two-dimensional projection of the three-dimensional displacements of the particle. It shares all of the same features as the MSD so that a perfectly viscous fluid will display a time scale-dependent creep compliance with a power law slope of 1, whereas a perfectly elastic solid will show a power lax slope of 0 and a viscoelastic material, such as the cytoskeleton, will have a power slope that lies between 0 and 1.

After to have calculated MSDs, local viscoelastic properties of intracellular environment can be calculated form MSDs by using the generalized Stokes-Einstein equation [47]

$$G^*(\omega) = \frac{k_BT}{\pi a i \mathfrak{F}_u\{< \Delta r^2(\tau) >\}} \quad (5)$$

where $G^*(\omega)$ is the complex shear modulus, $\omega$ is the deformation frequency and $\mathfrak{F}_u\{< \Delta r^2(\tau) >\}$ is the unilateral Fourier transform of the time-dependent MSD. The frequency-dependent elastic modulus $G'(\omega)$ and loss modulus $G''(\omega)$ are the real and the imaginary parts, respectively, of the complex modulus and obey Kramers-Kronig relationships [48].

Additionally, the translational diffusion coefficient, *D*, of a microsphere of radius *a* can be calculated from the Stokes-Einstein relationship [49-52]:

$$D = \frac{k_BT}{6\pi a\eta} \quad (6)$$

where $\eta$ is the shear viscosity of the fluid surrounding the particle and can be approximated as the product of the relaxation time (the time scale at which the viscous-to-elastic crossover occurs) and the plateau value of the elastic modulus [53]. The diffusion coefficient calculated from two-

dimensional particle trajectories can be approximated as the three-dimensional diffusion coefficient assuming that the local environment surrounding each microsphere is isotropic in three dimensions. This is a valid approximation, even in regions of the cell where long-range interactions between microspheres and the cell membrane could occur via hydrodynamic interactions, because those interactions are screened to within a mesh size of the surrounding network, which is ~50 nm. The particles embedded in regions with a thickness similar or smaller that the particle diameter have to be excluded from the analysis.

### 2.2.7 Immunofluorescence Labeling

Cells have been fixed and immunostained to quantify the focal adhesions (FAs) density and the organization of the actin cytoskeleton and in particular of bundles of actin microfilaments (stress filaments). After washing two times with phosphate-buffered saline (EuroClone), cells have been fixed in 4% paraformaldehyde in PBS for 20 min, rinsed twice with PBS and permeabilized in 0.1% Triton X 100 in PBS for 10 min. Cells have been washed three times in PBS and blocked for 15 min in 0.5% bovine serum albumin (BSA, Sigma-Aldrich) in PBS to block unspecific binding. After having washed two times, cells have been incubated for 1 h with 100 µl primary antibody, anti-vinculin, at 1:50 dilution in PBS-BSA. Then, cells have been washed for other three times with PBS-BSA and incubated for 30 min with secondary antibody, Alexa 540 anti-mouse (Sigma-Aldrich), at 1:500 dilution and Alexa 488 phalloidin at 1:200 dilution in PBS-BSA. Finally, cells have been washed three times with PBS-BSA. Images have been acquired by using a He-Ne excitation laser at the wavelength of 543 nm by using a 40x objective.

### 2.2.8 Quantification of Cell Spreading and Focal Adhesion Size on RGD-conjugated PDMS versus non functionalized PDMS

Specimens have been imaged using a Olympus IX81 inverted microscope and a 40x objective. Images of GFP-vinculin and Phalloidin-Alexa-488 have been captured from cell samples. The ventral cell area (cellular footprint), number of FAs and FA size have been quantified from fluorescent images of fluorescent cells. Fluorescent images have been captured at the ventral surface of the cells and then imported into ImageJ software (NIH, Bethesda, MD, USA) for postprocessing and analysis. Individual cells have been manually outlined and their areas have been determined. To assess the capacity of the cells to spread after attachment to the functionalized PDMS substrates, the ventral area of cells beyond that obtained by cells attached to

non functionalized PDMS substrates has been determined. Increases in ventral cell area above this level have been attributed to actin-driven formation of lamellipodia. To quantify the focal adhesion density and average size, the vinculin image has been intensity-thresholded to reduce background fluorescence, converted to binary, and extraneous objects ≤0.5 μm$^2$ have been removed. Focal adhesion area, length and width and total area per cell (focal adhesion mean number multiplied for mean focal adhesion area), have been calculated for the cell as a whole.

## 2.3 Results

### 2.3.1 Mechanical Properties of PDMS Substrates

In **Figure 2**, the Young's moduli $E$ for the three different elastomer base-crosslinker ratio values are shown. They are calculated by shear modulus $G$, in turn determined as slope of stress-strain curves, by using the following relationship

$$E = 2G(\nu + 1) \tag{7}$$

where $\nu$ is the Poisson's coefficient, supposed equal to 0.5.

The elastomer base-crosslinker ratio increase produces an increase in PDMS mechanical properties.

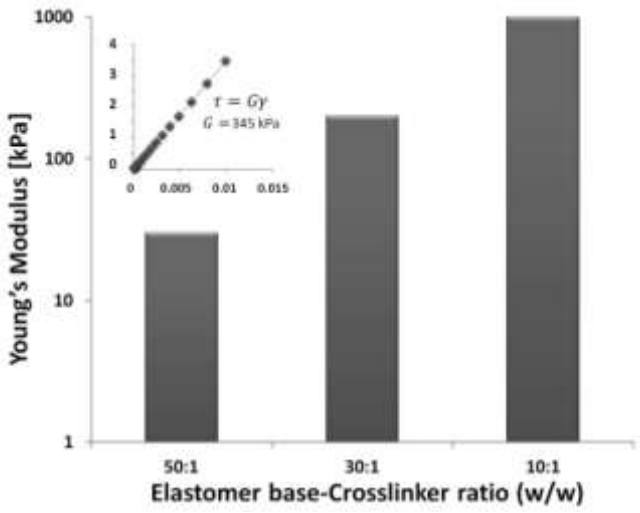


**Figure 2 | Relationship between PDMS substrate Young's modulus and elastomer base-crosslinker ratio**. As expected, increasing the amount of crosslinker in elastomer base-crosslinker mix, the elastic modulus of PDMS sample also increases. **Inset Stress-strain curves**. Shear stress versus strain at 1 Hz curve for 10:1 elastomer base-crosslinker ratio is obtained by rheometer. The Young's modulus is determined by using equation (7), in which ***G***is stress-strain curve slope.

### 2.3.2 Evaluation of RGD Peptides Density

Here, a MicroBCA assay has been used to determine the surface concentration of adhesion peptide covalently bound on PDMS substrates by comparison with the calibration curve obtained the corresponding peptide as standard. The immobilized peptide (GRGDY) is an RGD-like sequence containing at the carboxyl end the lipophilic tyrosine residue that mediates adhesion with high affinity via $\alpha_v\beta_3$ and $\alpha_{IIb}\beta_3$ integrin receptors [54] and increase the sensitivity of the assay [44]. We have found that the surface density of RGD peptides was not significantly dependent on the PDMS stiffness, if reactions on different PDMS substrates occur using the same peptide concentration **Figure 3.**

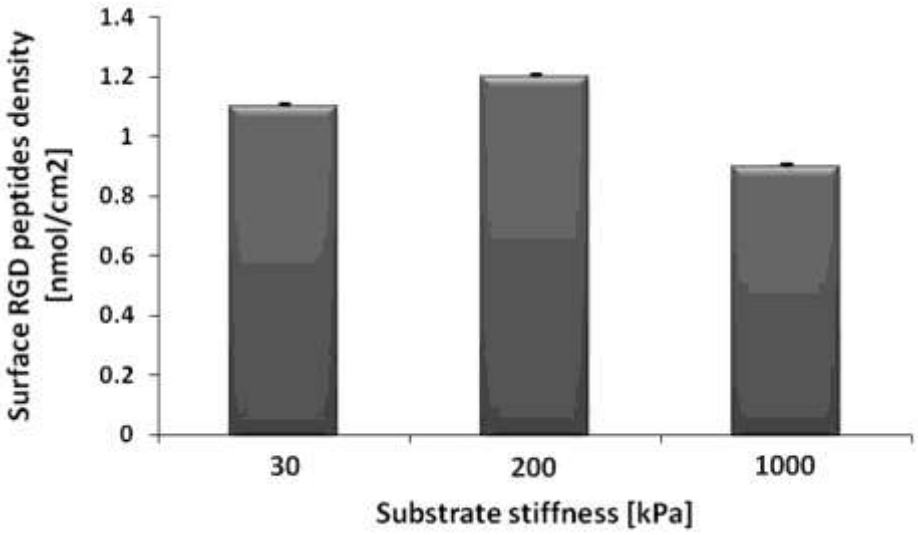


**Figure 3 | Relationship between surface RGD density and PDMS substrate stiffness.** There is not a significant dependence on matrix rigidity of RGD sequences density covalently immobilized on surfaces.

Additionally, the density of RGD peptides on PDMS surfaces was also dependent on the UV exposition time of sulfo-SANPAH (data not shown), but we have chosen a exposition of 20 minutes, because this duration for sulfo-SANPAH immobilization has revealed the best to obtain only slight differences in terms of peptides concentrations on three substrates.

### 2.3.3 RGD Functionalization of PDMS Substrates increased Cell Spreading and Focal Adhesions Dimension and Density in a stiffness-dependent Manner

When NIH3T3 have been seeded on untreated PDMS surfaces, few cells attached. On PDMS treated with sulfo-SANPAH and RGD peptide, the cells adhered well and appeared more elongated

in shape, compared with untreated PDMS surface. The morphology of NIH3T3 on RGD-conjugated PDMS have not showed apparent difference from that of NIH3T3 on standard tissue culture polystyrene (TCPS) dishes.

Furthermore, when NIH3T3 were cultured on RGD-conjugated PDMS surfaces, bundles of stress fibers and FAs have been formed, implying the strong interaction between the cells and the substrate. Close inspection of samples, indeed, did reveal that spreading area increases sensibly upon RGD-conjugated substrates and FAs in cells adhered to modified substrates appeared to be larger than the FAs in cells attached to non functionalized PDMS **Figure 4**. We therefore have quantified the effect that functionalization of substrates upon cell area and FA size in adherent cells. Mature FAs have been counted and measured using digital fluorescent images and ImageJ software as described previously only on functionalized substrates, because of the cytoplasmic vinculin high content in cells cultured on non-treated PDMS, that makes the images too noisy and difficult to process. The chemical treatment of PDMS sheets has increased cell spreading by approximately 50% in cases of hard and medium PDMS substrates. The increase on soft substrates has been more evident, due to a low adhesion on non treated sheets, that has been sensibly improved by RGD peptides conjugation **Figure 5**.

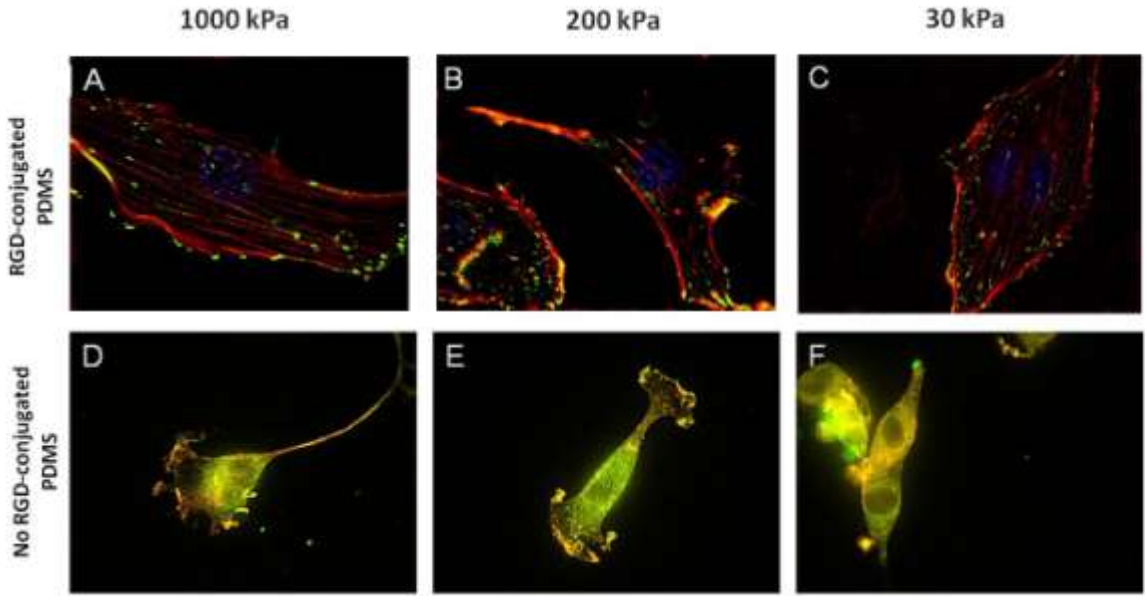


**Figure 4 | Microscopic analysis of fibroblasts on PDMS.** Cells have been plated on PDMS substrates with different rigidity, treated (**A**, **B**, **C**) or not (**D**, **E**, **F**) with RGD peptides, fixed and stained with vinculin and phalloidin. Fluorescent images of the vinculin-containing structures and actin microfilaments in ventral sections of the cells have been then captured.

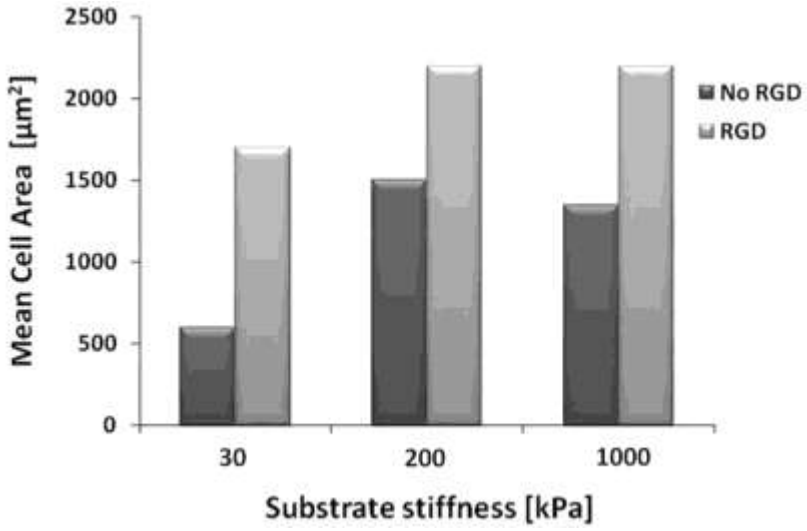


**Figure 5 | The effects of PDMS functionalization and stiffness on cell spreading.** Fixed cells plated on treated and non-treated PDMS substrates have been imaged and the cell area has been determined using ImageJ. The RGD peptide conjugation determines a sensible increase of cell area on all three PDMS substrates, that slightly increases also with matrix stiffness.

Focal adhesion area, length and total area per cell (focal adhesion mean number multiplied for mean focal adhesion area) increased sensibly with stiffness rising, while the width appeared very similar on all RGD conjugated substrates, indicating that focal adhesion growth occurs preferentially in length dimension **Table I**.

Results indicate the importance that short peptide sequences can effectively have in promoting cell adhesion, but also other cellular functions, such as proliferation and ECM protein secretion, even if they cannot replace and recapitulate all functions of adhesive proteins, such as fibronectin.

| PDMS Elastic Modulus [kPa] | Mean Area [µm²] | Total Area [µm²] | Major Axis [µm] | Minor Axis [µm] | Number per cell |
|---|---|---|---|---|---|
| 1000 | 0.932 | 141 | 1.744 | 0.592 | 155 |
| 200 | 0.886 | 103 | 1.654 | 0.551 | 133 |
| 30 | 0.698 | 94 | 1.431 | 0.547 | 130 |

**Table I | The effects of PDMS stiffness on number and size of focal adhesion.** Fixed cells plated on treated PDMS substrates have been imaged and the focal adhesion area has been determined using ImageJ. The mean area increased whereas the matrices became stiffer, such as also mean number of focal adhesions per cell and mean length, while the width underwent only to a slight increase.

### 2.3.4 Effect of Matrix Stiffness on Intracellular Microrheology

Particle tracking analyses have showed that modulation of $G_c'$ with respect to the 2D matrix environment significantly has altered the Brownian dynamics of embedded tracer beads. By extension, the intracellular compliance and the intracellular stiffness have been significantly affected as a function of matrix stiffness, with respect to the 2D matrix architecture. On functionalized substrates the magnitude of the ensemble-averaged MSD decreased ~5-fold in confluent conditions **Figure 6A** and ~3-fold in subconfluent condition **Figure 6B** as elastic modulus of substrates increased by nearly a full order of magnitude from 20 to 160 kPa. Directly proportional to the MSD the effective creep compliance decreases as the stiffness of the PDMS increases. Inversely, the apparent intracellular elastic modulus increases along with increasing substrate stiffness. Then, a positive correlation between 2D matrix stiffness and cell stiffness has been reported (**Figure 7**) both on functionalized than non-functionalized substrates. The change in intracellular elastic modulus is shown as a function of matrix stiffness in **Figure 7** at a shear rate of 1 Hz.

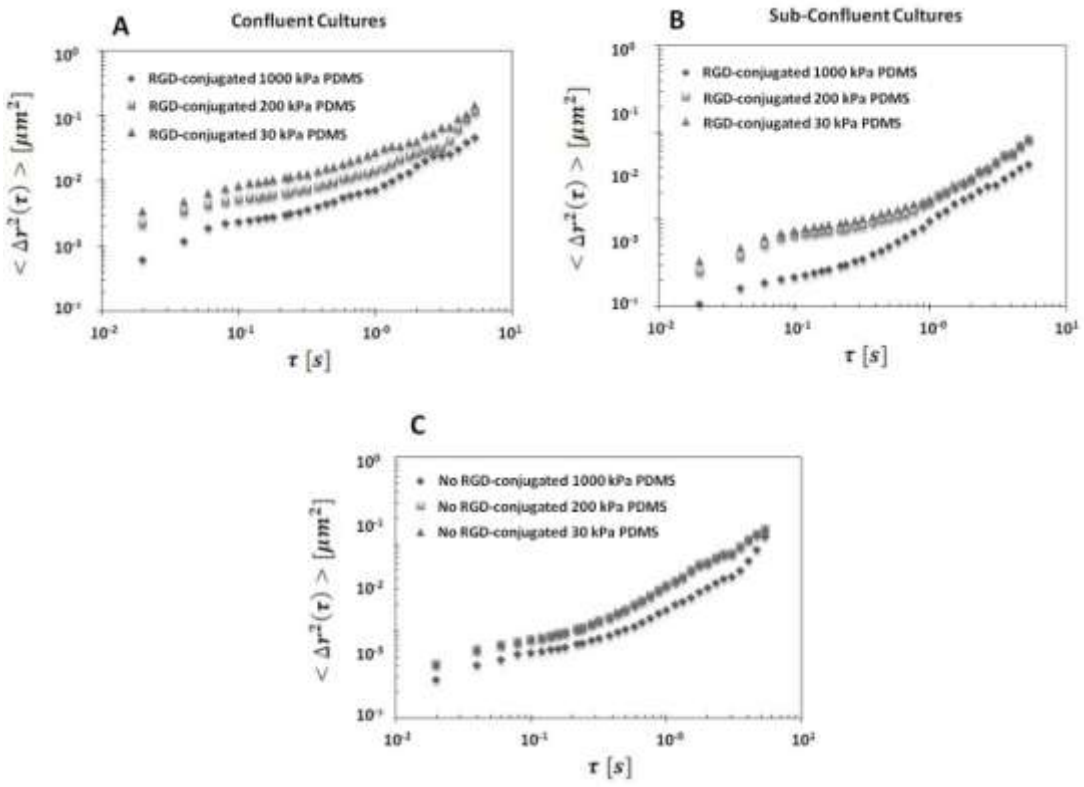


**Figure 6 | MSD of 100 nm tracer beads embedded within NIH3T3 cells attached to 2D PDMS substrates.** Increasing the matrix stiffness has yielded to a decrease in the magnitude of tracer-bead Brownian dynamics. **A** Switching from soft functionalized matrix to hard functionalized has induced a 5-fold decrease in the MSD of embedded tracer beads in cells that have been cultured in confluent condition, while **B** in case of sub-confluent culture the MSDs have been reduced of a value equal to ~3 and have been higher than in confluent cultures . **C** Also on non-functionalized substrates there is a decrease in the MSDs (2-fold), that are higher than MSD of beads embedded in cells cultured on RGD-conjugated substrates.

Furthermore, our immunofluorescent images analysis show that the content of focal adhesions, to which is associated the cell ability to sustain a more rigid cytoskeletal filament network is only weakly depending on the substrate stiffness. If it's true that RGD sequences are extremely important in promoting all steps of cell adhesion [51] (cell attachment, cell spreading, organization of an actin cytoskeleton, and formation of focal adhesions), that is the primary condition for cell to sense substrate rigidity, our study has demonstrated that, once cell adhesion has been optimized, cell is able to sense substrate rigidity and translate it in a corresponding intracellular stiffness. In case of non-functionalized substrates, instead, even if cell mechanical properties has exhibited a direct correlation with matrix rigidity, they have resulted lower than elastic moduli on RGD-conjugated substrates. Spherical, ameboidal cell morphology has been associated with relatively few and less defined actin stress fibers, yielding then a more compliant cytoskeletal filament network.

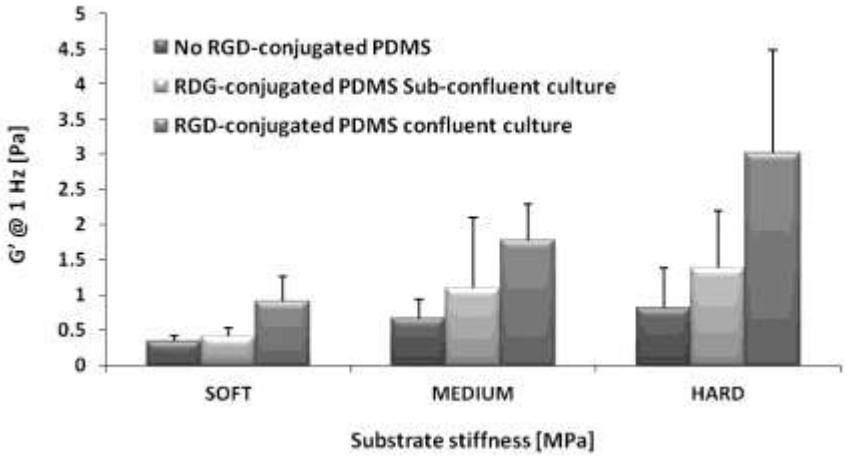


**Figure 7 | Substrate stiffness influences intracellular rheology.** Intracellular stiffness increases as matrix stiffness increases, both in case of superficial chemical treatment of substrates and in case of absence of RGD peptides on PDMS.

## 2.4 A mechanical Model of Focal Adhesion-Stress Fiber Complex Growth Process regulated from Substrate Elasticity Sensing in Adherent Cells

The role of chemical and, in particular, physical nature of extracellular matrix is crucial in controlling cell adhesion and cytoskeletal structural organization that confers to the cell its stable conFiguretion and the ability to resist and actively respond to cytoskeletal or external mechanical cues. In this interaction process with the surrounding environment, focal adhesion sites represent the structure that allows the transfer of information from inside to outside and *vice versa*. Their sensitivity to biophysical signals is accompanied and guaranteed by dynamic formation and growth processes [55]. One of the most important results of this work is that the matrix stiffness is a fundamental regulator of adhesion site remodeling, that in turn controls the cytoskeletal structuring and, then, cell stiffness.

In this section, we want to propose a mechanical model that explains the focal adhesion dynamics, when the activator of remodeling is extracellular matrix stiffness. The model is based on three fundamental assumptions, that will be better explained in the following: 1- stress at the interface between focal adhesion sites and extracellular matrix is maintained constant; 2- Focal adhesion area is a unknown function of matrix elastic modulus; 3- Stress fiber area directly depends on focal adhesion are and, indirectly on matrix elastic modulus.

We show that the model is able to predict focal adhesion growth with increasing matrix stiffness and return an analytical relationship between focal adhesion area and matrix elastic modulus, that support the experimental results.

### 2.4.1 Theoretical Model of Matrix-Focal Adhesion-Stress Fiber Complex

In our model we refer to Lazopoulos and Stamenović work [56] and consider the cytoskeleton as a planar system of elastic cables, the stress fibers, adhered to the substrate through anchorage points, the focal adhesion sites. Differently from Lazopoulos and Stamenović, we consider the possibility for the focal adhesion to deform under tension applied from the stress fiber and take into account also substrate deformation and correlated strain energy. We focus our attention on the single matrix-focal adhesion-stress fiber complex, considering that its structure governs the mechanics of all cytoskeleton, by transferring the stresses at distance through the hierarchical organization of living systems [57]. We assume the hypothesis that the tension at the interface

between adhesion protein plaque and matrices have to be maintained constant during the evolution of focal adhesion, as observed by Balaban *et al.* [58]

### 2.4.2 Stress Fiber, Focal Adhesion and Matrix Mechanical Behavior

We assume that stress fibers can be modeled as elastic cables that carry initial prestress, that is the element key of tensegrity structures, by which it's possible to explain the architecture of cytoskeletal polymeric networks, whose shape stability and rigidity are the result of a state of self-stressed equilibrium between cables under tension (actin filaments) and compression elements (microtubule) [59-60].

When a stress fiber is anchored to a complex consisted of a rigid substrate and a rigid focal adhesion, it can be represented as a strut constrained at the side of matrix-focal adhesion system, supporting the initial prestress $\sigma_0$ and the associated prestrain $\varepsilon_0$, that is generated by its contractile motors [61], acting on the other side of stress fiber.

We use the following strain energy function for stress fibers [56], indicating the stiffening behavior of contractile bundles of actin filaments

$$W(\varepsilon) = \frac{1}{2}E_{SF}^{1}\varepsilon^{2} + \frac{1}{4}E_{SF}^{2}\varepsilon^{4} \tag{8}$$

where $E_{SF}^{1} = 1.45$ MPa and $E_{SF}^{2} = 9$ MPa are the material constants, determined from the experimental stress-strain curves for stress fibers [61].

The total potential energy of stress fibers after the adhesion to the matrix can be written as

$$\Pi_{SF} = [W(\varepsilon_0 - \varepsilon') - \sigma \cdot (\varepsilon_0 - \varepsilon')]A_{SF}L_{SF} \tag{9}$$

where $\sigma$ can is the first derivative of strain energy function calculated at the deformation $\varepsilon_0 - \varepsilon'$

$$\sigma = E_{SF}^{1}(\varepsilon_0 - \varepsilon') + E_{SF}^{2}(\varepsilon_0 - \varepsilon')^{3} \tag{10}$$

and $A_{SF}L_{SF}$ is the stress fiber volume.

We assume that also the focal adhesion and the matrix can modeled as linear elastic cables, whose stress-strain behavior can be expressed in the following way

$$\sigma_{FA} = E_{FA}\varepsilon_{FA} \qquad \sigma_M = E_M\varepsilon_M \tag{11}$$

where $E_{FA}$ and $E_M$ are respectively the focal adhesion and matrix elastic moduli.

In our works, we doesn't consider the way in which the pulling force alters the chemical potential, then when we write the total potential energy associated to the focal adhesion, we consider this term as a constant that doesn't move the stability condition, but only its value. Then, the total potential energy of focal adhesion and matrix is

$$\begin{aligned} \Pi_{AF} &= \tfrac{1}{2}\mathrm{E}_{AF}\mathrm{A}_{AF}\mathrm{L}_{AF}\varepsilon_{AF}^2 - \sigma_{AF}\varepsilon_{AF}\mathrm{A}_{AF}\mathrm{L}_{AF} \\ \Pi_M &= \frac{1}{2}\mathrm{E}_M\mathrm{A}_M\mathrm{L}_M\varepsilon_M^2 - \sigma_{AF}\varepsilon_M\mathrm{A}_M\mathrm{L}_M \end{aligned} \tag{12}$$

### 2.4.3 Stability Condition

When stress fiber is anchored to matrix-focal adhesion system, the pulling force is partially distributed between the three elements that constitute the system, causing a decrease of prestrain $\varepsilon_0$ in the stress fiber to the value $\varepsilon_0 - \varepsilon$. We suppose that the reduced strain $\varepsilon_0 - \varepsilon$ remains positive to guarantee the self-stressed state of stress fiber, necessary to stabilize the entire cytoskeleton lattice. Indeed, when the strain in stress fiber vanishes, that, how we demonstrate in the following, occurs for matrix elastic moduli too low for cell adhesion, the stress fiber doesn't support any force and, from a physical point of view, its contribution is not more necessary to guarantee the system stability. Although the stress fiber is also the source of pulling force, then its break up coincides with the focal adhesion site disruption and then cell adhesion loss.

In our model we model substrate, focal adhesion and stress fiber as springs mechanically in series. The other two ends of the substrate and the stress fiber are considered fixed, then the total length $L = L_M + L_{AF} + L_{SF}$, cannot change. The deformation $\varepsilon = \frac{\Delta L}{L_M + L_{FA}}$ that substrate-focal adhesion system holds due to its compliance can be related to the stress fiber reducing strain $\varepsilon' = \frac{\Delta L}{L_{SF}}$ by the length factor $\lambda = \frac{L_{SF}}{L_M + L_{FA}}$, so that $\varepsilon = \lambda \cdot \varepsilon'$. The strain $\varepsilon$ is shared between focal

adhesion and matrix according to the following two equations $\varepsilon_{FA} = \frac{\varepsilon}{E_m[E_m{}^{-1}\phi + E_{FA}{}^{-1}(1-\phi)]}$ and $\varepsilon_{FA} = \frac{\varepsilon}{E_{FA}[E_m{}^{-1}\phi + E_{FA}{}^{-1}(1-\phi)]}$.

By considering the equation of equilibrium of the system, $\varepsilon$ can be expressed as follows

$$\varepsilon' = \frac{\varepsilon_0}{1 + \frac{E_{equ}}{E_{SF}} \frac{A_{FA}}{A_{SF}} \frac{L_{SF}}{L_M + L_{FA}}} \tag{13}$$

In the hypothesis that the stress at the matrix-focal adhesion substrate is maintained constant, we can rewrite $\varepsilon' = \frac{\sigma_{const}}{E_{equ}}$ and determine the other strain as function of $\sigma_{const}$.

The total potential of a single adhesion structure is

$$\Pi = \Pi_{SF} + \Pi_{AF} + \Pi_M \tag{14}$$

The negative terms in $\Pi_{SF}$, $\Pi_{AF}$, $\Pi_M$ indicates the works that initially protein motors make to stabilize cytoskeleton with prestress and that, after the adhesion on a deformable substrate, is distributed between on the three elastic struts.

Using the previous relation (14), it's possible to verify that total energy depends on the prestress and on the geometric and elastic properties of stress fiber, focal adhesion and matrix.

To demonstrate the dependence of stress fiber area on matrix elastic modulus, we suppose that this parameter in the expression of total potential energy is a function of matrix modulus, $A_{SF} = A_{SF}[E_M]$. Referring on experimental observations [17,35], we can hypothesize that stress fiber area increases with focal adhesion area and that the growth rate is lower for stress fibers, then we assume that the relationship between focal adhesion sites and stress is $A_{SF}[E_M] = \alpha\sqrt{A_{FA}[E_M]}$.
In search of stable configurations, we use the principle of minimum total potential energy. It asserts that a body shall deform or/and displace to a position that minimizes the total potential energy of the body, with the lost potential energy being dissipated. At equilibrium, a minimum potential energy configuration is a stable configuration. Since there can be multiple energy minima, the configuration which corresponds to the global minimum is considered the stable configuration according to the Maxwell's criterion [62]. The research of the global minimum transforms in a variational problem, that consists in determining the function $A_{FA}[E_S]$ that

extremizes the functional $U$. The extremal functions are solutions of the Euler-Lagrange equations that are obtained by setting the first variational derivates of the functional $U$ with respect the function $A_{FA}[E_S]$, $VarD[U, A_{FA}[E_S], E_S]$ , equal to zero.

We tried an unique analytical solution that can be written in the following synthetic form:

$$A_{FA}[E_M] = \frac{\left(c_1 + \frac{c_2}{E_M^6} - \frac{c_3}{E_M^5} + \frac{c_4}{E_M^4} - \frac{c_5}{E_M^3} + \frac{c_6}{E_M^2} - \frac{c_7}{E_M} + c_8 E_M^2 - c_9 E_M\right)}{c_{10} E_M^2 - c_{11} E_M + c_{12}} \quad (15)$$

where the $c_i$ are positive constants depending on $\alpha, \varepsilon_0$ $E_{SF}$, $E_{SF}^2$, $L_{SF}$, $L_{FA}$ and $L_S$ that is the thickness on which the force and, then, the deformation are transmitted.

### 2.4.4 Numerical Analyses

To obtain quantitative values of the focal adhesion area, we substitute numerical values to the model parameter. We use the values suggest by Balaban *et al.* for constant stress within the focal adhesion, $\sigma_{const} = 5.5$ kPa, for stress fiber material constant and for prestrain $\varepsilon_0 = 0.22$, while we use an elastic modulus for protein plaque equal to 2 kPa, as suggested by Nicolas and Safran [63]. For the estimate of coefficient $\alpha$ we use the maximum values of focal adhesion area (0.93 μm$^2$)and stress fiber cross-sectional area (0.28 μm$^2$) we measured in our experiments. The length of stress fiber, focal adhesion and substrate are posed equal to 10, 0.5 and 1 μm, respectively.

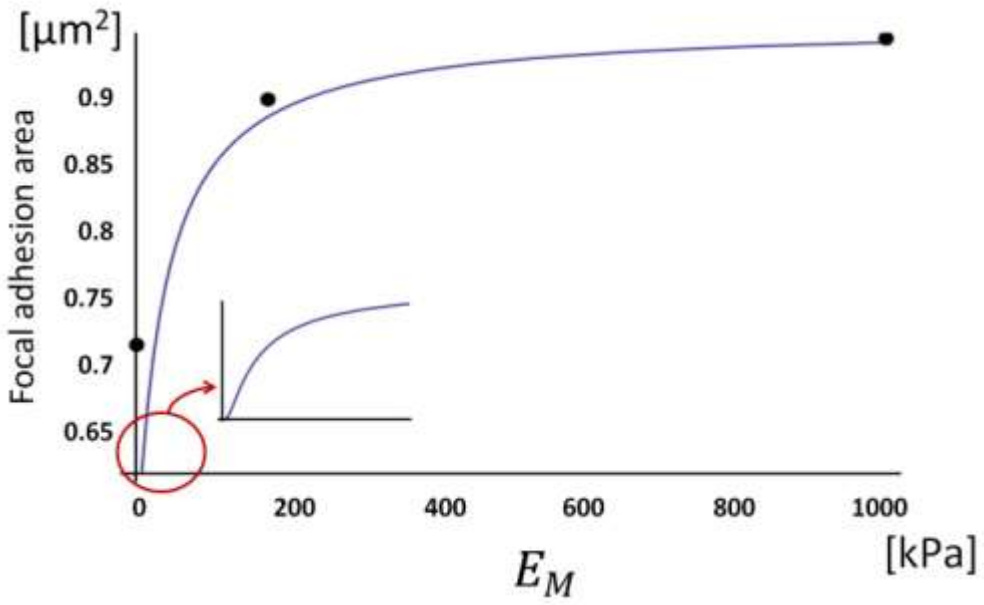


**Figure 8 | Focal Adhesion area vs matrix elastic modulus.** The solution to the variational problem is a monotonically increasing focal adhesion area function, that stabilizes to 0.95 μm$^2$ for high elastic modulus and reach a zero value for $\boldsymbol{E_S^{min}}$= 4.7 kPa, causing the collapse of the entire system constituted by focal adhesion and stress fiber.

As shown in **Figure 8**, the mathematical solution to the variational problem returns a function that increases with the matrix elastic modulus with a saturation behavior, that produces an area for infinite substrate elastic modus equal to 0.95 μm$^2$, suggesting that the stiffer substrate we used (1000 kPa) represents for cells a rigid substrate, that stabilizes focal adhesions and doesn't reduce the level of prestress internally to the stress fibers. About the adhesion areas at low moduli, we can consider that the value for which $A_{FA}[E_S]$ vanishes, such as its derivative respect to $E_S$ (indicating that the model doesn't predict negative values for area), $E_S^{min}$= 4.7 kPa, corresponds also to the vanishing of the prestress inside the stress fibers. This condition consists in stress fiber collapse, because of their ability to sustain only tensional stress state, and then of focal adhesions, that don't receive mechanical signals from the cell inside, necessary to their remodeling and stabilization. For values low than $E_S^{min}$, the model fails, because doesn't consider the possibility for stress fibers and then focal adhesions to disgregate with depolymerization processes initiation.

### 2.4.5 Energetic Considerations

Replacing the $A_{FA}[E_S]$ function in the expression of total potential energy, we obtain a $U$ vs. $E_S$ relationship **Figure 9**. We found that $U$ decreases with increasing $E_S$, indicating that the structure

assumes a more stable conFiguretion and justifying the experimentally verified preference for stiffer substrate during cell migration [16,26-27].

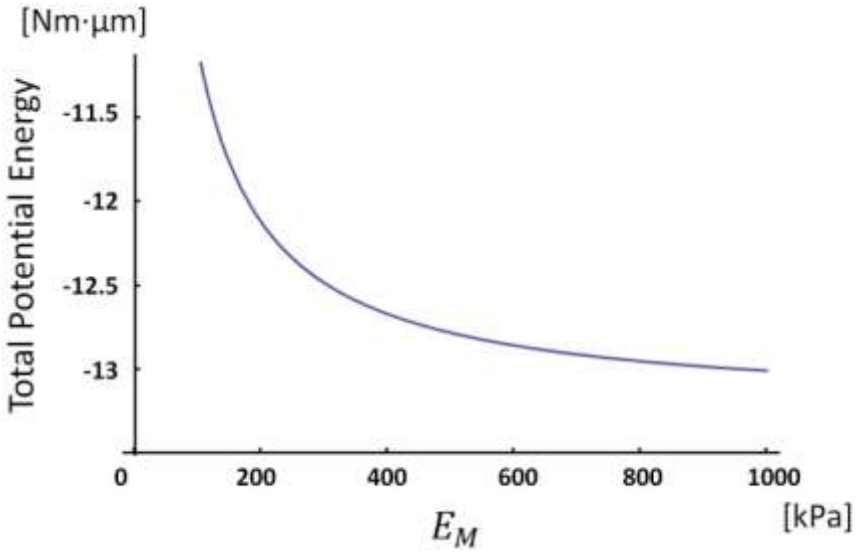


**Figure 9 | Total potential energy vs. matrix elastic modulus.** The total potential energy decrease, whereas matrix modulus increases, indicating that the equilibrium conFiguretions that structure reaches on stiffer substrate are more stable than on softer substrate.

Finally, we have determined the equivalent elastic modulus of the cytoskeletal unit (focal adhesion-stress fiber) involved in the adhesion process and in mechanosensing and mechanotransduction activities. The elastic constant of the structure equivalent to the serie constituted by the stress fiber cable and the focal adhesion cable is given by the following

$$K_{FA-SF} = \frac{K_{FA}\,K_{SF}}{K_{FA}+K_{SF}} \tag{16}$$

where $K_{FA}$ and $K_{SF}$ are the elastic constant of the focal adhesion and stress fiber, that can be written as

$$K_{FA} = \frac{E_{FA}\,A_{FA}}{L_{FA}}\,, \qquad K_{SF} = \frac{E_{SF}\,A_{SF}}{L_{SF}} \tag{17}$$

To obtain a mechanical parameter that dimensionally is an elastic modulus, we divide the elastic constant $K_{FA-SF}$ for the total length of the system, $L_{FA}+L_{SF}$.

$$E_{FA-SF} = \frac{K_{FA-SF}}{L_{FA} + L_{SF}} \tag{18}$$

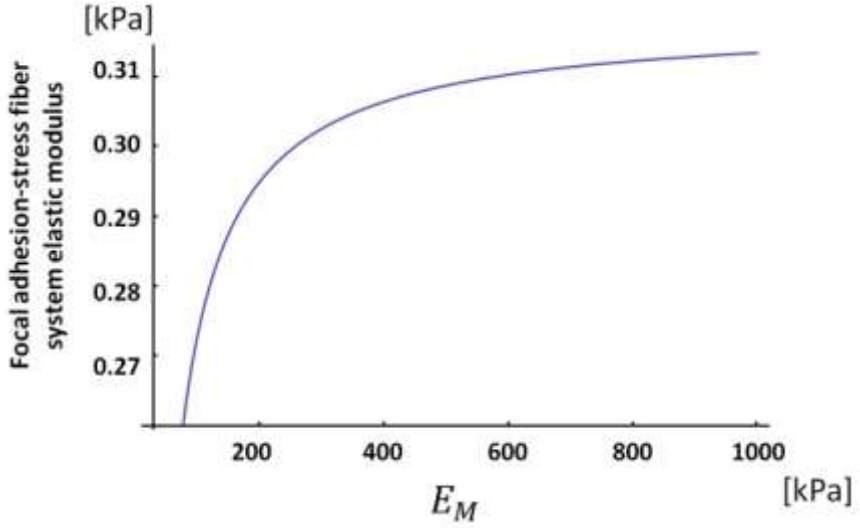


**Figure 10 | Focal adhesion-stress fiber system elastic modulus vs. matrix elastic modulus.** Also the elastic modulus of the focal adhesion-stress fiber system increases with matrix elastic modulus, in according to microrheological results, that show the existence of a positive correlation between elastic modulus of cytoskeletal structure and substrate elasticity.

Also the equivalent elastic modulus increases with stiffnness, supporting experimental results about the relationship between intracellular microrheology and substrate stiffness.

The elastic modulus determined by the mechanical model is ~0.3 kPa, that is posed in the range of living cell mechanical properties measured by atomic force microscopy, that directly probes the focal adhesion-stress fiber structure. Using on particle tracking we measure principally cytoplasmic network that is less densly structured than cortical actin structure. Although, the increase of mechanical properties measured by particle tracking technique indicates the ability of focal adhesion-stress fiber unit to transfer internally the stress, causing an overall increase of cellular resistence.

### 2.5 Discussion

Extracellular matrix provides chemical and biophysical cues to cells, that sense, process and respond to them through a set of intimately connected and interdependent set of structures, that

spans length scales from single molecules to tens of microns, including small clusters of force-sensing molecules at the cell surface, micron-sized cell-ECM focal adhesion complexes and the cytoskeleton that permeates and defines the entire cell. The preliminary and necessary cell adhesion process is guaranteed by transmembrane integrin proteins [64], that respond to external signals clustering laterally in the membrane and engaging structural and signaling proteins for focal adhesion complexes formation [65-66]. Assembled focal complexes carry out signaling functions and physically link the actin cytoskeleton to the ECM, allowing the self-assembly of higher order structural components, the stress fibers [67]. These structures are able to transmit high traction forces [68], to stabilize the cell structure, and to transduce mechanical information, promoting typical cellular activities, such as motility, cell shape changes and ECM remodeling [69].

It's well known that both physical and chemical properties of the ECM influence integrin adhesion complex assembly [70-72]. To explore the underlying biophysical mechanism of cytoskeletal structuring and elucidate the coupling between substrate stiffness and chemical treatment with ligands, we compared spreading capacity and focal adhesions number, area and size in fibroblast cells cultured on 2D PDMS matrices in response to substrate stiffness variations and chemical surface functionalization.

Soft mammalian tissues elasticity ranges from 30-100 Pa for the softest (i.e. brain), to tens of kPa in muscle tissues, reaching the higher values of MPa in tissues like cartilage and tendons [73]. In order to provide an in vitro compliant model of ECM elasticity we used as culture substrate PDMS, in which the concentration of the crosslinking agent sets the different elastic modulus, and as substrate surface coating a peptide containing the Arg-Gly-Asp (RGD) amino acid sequence which is known to promote cell adhesion [54]. First, we measured the projected area of cells on matrices with different stiffness, both with and without RGD peptide conjugation. Results show that for a fixed substrate stiffness, only cells cultured on functionalized substrate develop a spread morphology, with an increase of 300% on 30 kPa substrates and of 50% on 200 and 1000 kPa than on correspondent unmodified substrate **Figure 5**. Increase of spreading area on chemically functionalized substrates seems to be characterized by a threshold value, that induces a very similar value for cellular projected area on 200 and 1000 kPa PDMS matrices. From data in literature, a value of 2 kPa for matrices is already suitable to develop a spread morphology in fibroblasts 17, justifying the similar spreading area values on our three chemically modified substrates. Our results confirm, such as previously demonstrated [54,61,74-75], that protein density on substrate has predominant role in guiding the process of cell adhesion and spreading compared to

the role of substrate elastic modulus, at least in the stiffness range (30-1000 kPa) we examined. Indeed, adhesion and spreading represent the necessary requisite so that cells can feel the mechanical characteristic of the surrounding environment. From this point of view, the surface concentration of binding sites is an important parameter and the differences in cell area we found in RGD-coated PDMS and pure PDMS are also supported from the mechanical characterization of cell tensional state.

However, in order to dissect the molecular mechanisms through which cells sense and respond to their biophysical environment, it is critical to understand how all elements in the cytoskeleton, focal adhesions and the ECM come together in a organized fashion to allow the cell to generate and sense mechanical force. In this perspective, it's necessary to underline the importance of focal adhesions, that, with their ~156 proteins, act as bidirectional mechanosensors to transmit and transduce mechanical information between the cell exterior and the interior [76]. To discriminate the different roles that chemical surface functionalization and substrate rigidity play in promoting focal adhesion assembly after a cell binds to ECM components, we determined the amount and dimension of stable focal adhesions, measuring vinculin-containing structures by immunostaining. As shown in **Table I**, the effect of RGD-conjiugation is clearly evident not only in the increase of spreading area, but also in that of number and dimension of focal adhesion for all three different stiffness substrates. We found a positive correlation between number and size of focal adhesion and matrix elasticity, confirming previous results that indicate the development of more grown adhesive contacts [16,77]. Then, both the chemistry and rigidity of the ECM components influence the strength of the attachment and lead to structural rearrangements in the receptor/ligand complex [78]. Attachment to suitable surfaces also causes conformational changes that promote rapid clustering of adhesion receptors and recruitment of components that link the receptors to the actin network. Probably, the formin mediates the assembly of actin filaments, contributing to focal adhesion maturation and stability and to structuring of long thick actin bundles, known as stress fibers. The increase of substrate elasticity increases also stress fibers in a positive correlated way with stiffness substrate (**Table I**), indicating more force generation by cells and at the same time the possibility to direct external forces towards the adhesion receptor throughout the internal cytoskeleton [79].

The increase of tensional state caused by the rising of focal adhesions and associated stress fibers can be quantified measuring cellular mechanical properties. By using particle tracking microrheology (PTM) technique, we probe how chemical treatment and matrix stiffness affect

intracellular rheology. It's necessary clarify that even if, as demonstrated, the mechanical properties of cells are directly linked to density of focal adhesions and, then, of stress fibers, through the particle tracking technique we doesn't measure the stiffness of stress fibers, as atomic force microscopy (AFM) technique does, but the cytoplasmic regions, devoid of stress fibers but closely connected to them, are probed. The difference in structures probed explains also the difference in magnitude order of mechanical properties measured by particle tracking microrheology (~1-10 Pa [80]) and AFM (~0.1-100 kPa [81]). However, results obtained by PTM technique are indicative of the modification in the tensional state that cell adopt in correspondence of different substrate rigidity. Indeed, the cytoskeleton can be assumed as formed by an interpenetrate network in which coexist different single networks (microtubules, actin filaments as microfilaments and stress fibers) all connected to cell nucleus. The increase in the mechanical properties of one of them (i.e by the formation of new stress fibers generated from new focal adhesions) produces an overall increment in cytoskeleton mechanical response. The random spontaneous movements of the beads are monitored with high spatial and temporal resolution and transformed in mean squared displacements (MSDs) and the time lag-dependent MSDs of the beads are subsequently transformed into local values of either the frequency-dependent viscoelastic moduli. Our results suggest that RGD-conjugation and matrix stiffness significantly affect the Brownian motion of embedded tracer beads. For a fixed stiffness, the chemical treatment decreased the magnitude of the ensemble-averaged MSD ~2-fold for all three stiffness substrates. Also the increase of matrix stiffness contributes sensibly to decrease the MSDs of ~4-fold in confluent conditions, ~2-fold both in case of subconfluent conditions and in case of untreated matrices. Inversely proportional to the MSD, the apparent elastic modulus increases with functionalization and substrate stiffness. Our results confirm that the level of elasticity in the cell correlates with the local concentration of F-actin present in the cytoplasm. The assembly of actin filaments into organized structures, that is strictly associated to the existence of focal adhesions functioning as nucleation sites for stress fibers, is positively affected by chemical and mechanical properties of substrates, and consequently is the factor that influences the cellular mechanical properties. Furthermore, our results show that the cell density also influences the dependence of fibroblasts on matrix stiffness. When cells make in contact each other becoming confluent or sub confluent, signaling from cadherins in cell-cell interactions overlap signals from the cell-matrix adhesion complexes increasing the cell mechanical properties. In other words, in

case of confluence cell can regulate the tensional state sensing not only the physical properties of substrate through FA but also the tensional state of cells its proximity.

To support experimental data, we have proposed a mechanical model that describes the increase of focal adhesion area and the increase of cellular mechanical properties as stability phenomenon. We consider the cell as a planar system of elastic cables, representing the stress fiber anchored to the substrates mediated by the focal adhesion. We focus our attention on the single unit consisted of stress fiber and focal adhesion, considering that the mechanical behavior of this equivalent system can be opportunely transferred on other length scales. Differently from Nicolas and Safrani[63], we don't omit the contribution of stress fiber in determining the stable conFiguretion of the system and differently from Lazopoulos and Stamenović [34], we consider the adhesion site as an mechanical element able to deform and to which it's associated an elastic strain energy. The fundamental hypotheses of the model are i) the constant stress at adhesion sites surface [61], ii) the dependence of focal adhesion area on matrix elastic modulus $E_M$ and iii) the existence of a direct relationship between stress fiber cross-sectional area and focal adhesion area, as observed by Yeung *et al.* that demonstrate the existence of a lower bound, under which fibroblast cells don't spreading and don't develop stress fibers [17]. As consequence of these hypotheses, the total potential energy becomes a functional, whose variables are the functions class $A_{FA}[E_M]$ and the variable $E_M$. The research of the stable conFiguretion consists in determining the functions $A_{FA}[E_M]$ that extremizes the functional $\Pi$. From a practical point of view, the problem consists in resolving the Euler-Lagrange equation. We find an analytical solution to this variational problem, that is a monotonically increasing function and highly overlapping with our experimental data. For high moduli, the function stabilizes to an asymptotic value, not too different from that we found on 1000 kPa PDMS, indicating that the cell perceives this value as the elastic modulus of an infinitely rigid material. On the other hand, we determined the minimum of the function as around 4.7 kPa, corresponding to the case in which the stress inside the stress fiber vanishes and impairing its structure. Model predicts a minimum matrix modulus for cell adhesion very close to the limit value (3 KPa) for cell spreading and stress fiber development measured by Yeung *et al.* [34]. In the same way, the homogeneized elastic modulus of the focal adhesion-stress fiber unit increases with matrix stiffness, confirming the data obtained from intracellular microrheology experiments. The values of elastic modulus estimated by the model have the same magnitude order of elastic modulus measured on living cell by atomic force microscopy, that presumably is able to investigate the structure composed from focal adhesion and stress fiber.

This model, in its simplicity, reproduces very well the results obtained in experimental campaign, confirming from a theoretical point of view, the importance of the interaction between cell and matrix in controlling cellular processes, such as durotaxis, and the cell stressed state, necessary to preserve its adhesion and then viability.

## References


[1] Kessels, M. M. *et al.* "Controlling actin cytoskeletal organization and dynamics during neuronal morphogenesis". *Eur. J. Cell Biol*., *90*, 926-933, **2011**.

[2] Novack, D. V. and Faccio, R. "Osteoclast motility: putting the brakes on bone resorption". *Ageing Res. Rev*., *10* (1), 54-61, **2011**.

[3] Kirmse, R. *et al.* "Interdependency of cell adhesion, force generation and extracellular proteolysis in matrix remodeling". *J. Cell Sci*., *124*, 1857-1866, **2011**.

[4] Keely, P. J. "Mechanisms by Which the Extracellular Matrix and Integrin Signaling Act to Regulate the Switch Between Tumor Suppression and Tumor Promotion". *J. Mamm. Gland Biol.*, *16*, 205-219, **2011**.

[5] Biones, A. M. *et al.* "Role of extracellular matrix in vascular remodeling of hypertension". *Curr. Opin. Nephrol. Hypertens.*, *19*, 187-194, **2010**.

[6] Karamikos, D. *et al.* "Collagen stiffness regulates cellular contraction and matrix remodeling gene expression". *J. Biomed. Mater. Res. A*, *83*, 887-894, **2007**.

[7] Kass, L. *et al.* "Mammary epithelial cell: Influence of extracellular matrix composition and organization during development and tumorigenesis". *Int. J. Biochem. Cell BIol. 39*, 1987-1994, **2007**.

[8] Viallard, J. F. *et al.* "Molecular mechanisms controlling the cell cycle: fundamental aspects and implications for oncology". *Cancer Radiother. 5*, 109-29, **2001**.

[9] Polager ,S. and Ginsberg, D. "p53 and E2f: partners in life and death". *Nat. Rew. Cancer*, *9,* 738-748, **2010**.

[10] Swiss, V. A. and Casaccia P. "Cell-context specific role of the E2F/Rb pathway in development and disease". *Glia*, 58, 377-390, **2010**.

[11] Hallstrom, T. C. and Nevins, J. R. "Balancing the decision of cell proliferation and cell fate". *Cell Cycle*, 8, 532-535, 2008.

[12] Lin, C. Q. and Bissell, M. J. "Multi-faceted regulation of cell differentiation by extracellular matrix". *FASEB J*. 7, 737-743, **1993**.

[13] Wells, R. G. "The role of matrix stiffness in regulating cell behavior". *Hepathology,* 47, 1394-1400, **2008**.

[14] Fong-Chin, S. *et al.* "Review: Roles of microenvironment and mechanical forces in cell and tissue remodeling". *J. Med. Biol. Eng*. 31*,* 233-244, **2011**.

[15] Kim, S.-H. *et al.* "Extracellular matrix and cell signaling: the dynamic cooperation of integrin, proteoglycan and growth factor receptor". *J. Endocrinol.* 209, 139-151, **2011**.

[16] Pelham, R. J. and Wang, Y. "Cell locomotion and focal adhesions are regulated by substrate flexibility". *Proc. Natl. Acad. Sci. USA*, 94, 13661-13665, **1997**.

[17] Yoeung, T. *et al.* "Effects of substrate stiffness on cell morphology, cytoskeletal structure, and adhesion". *Cell Motil Cytoskeleton 60*, 24-33, **2005**.

[18] Cheng, C. *et al.* "Probing cell structure by controlling the mechanical environment with cell–substrate interactions". *J. Biomech*. *42*, 187-192, **2009**.

[19] Emerman, J.T. *et al.* "Substrate properties influencing ultrastructural differentiation of mammary epithelial cells in culture". *Tissue Cell*, 11, 109–119, **1979**.

[20] Engler, A. J. *et al.*, "Matrix Elasticity Directs Stem Cell Lineage Specification". *Cell* 126, 677-689, **2006**.

[21] Saha, K., *et al.*, "Substrate modulus directs neural stem cell behavior". *Biophys. J*. 95, 4426–4438, **2008a**.

[22] Winer, J.P. *et al.,* "Bone marrow-derived human mesenchymal stem cells become quiescent on soft substrates but remain responsive to chemical or mechanical stimuli". *Tissue Eng. Part A* 15, 147–154, **2009**.

[23] Leong, W. S. *et al.*, "Thickness sensing on hMSCs on collagen directs stem cell fate". *Biochem. Biophysic. Res. Comm*. 401, 287-292, **2010**.

[24] Park, J. S. *et al.*, "The effect of matrix stiffness on the differentiation of mesenchimal stem cells in response to TGF-β". *Biomaterials 32*, 3921-3939, **2011**.

[25] Bajaj, P. *et al.*, "Stiffness of substrate influences the phenotype of embryonic chicken cardiac myocytes". *J. Biomed. Mater. Res. A* 95, 1261-1269, **2010**.

[26] Lo, C. *et al.* "Cell Movement Is Guided by the Rigidity of the Substrate". *Biophys. J. 79*, 144-152, **2000**.

[27] Wong, J.Y. *et al.* "Directed movement of vascular smooth cells on gradient-compliance hydrogels". *Langmuir*, 19, 1908-1913, **2003**.

[28] Oakes, P.W. *et al.* "Neutrophil morphology and migration are affected by substrate elasticity". *Blood* 114, 1387-1395, **2009**.
[29] Peyton, S.R. and Putnam, A.J. "Extracellular matrix rigidity governs smooth muscle cell motility in a biphasic fashion". *J. Cell. Physiol.* 204, 198–209, **2005**.
[30] Stroka, K. M. and Aranda-Espinoza, M. "Neutrophils display biphasic relationship between migration and substrate stiffness". *Cell. Motil*. *Cytoskel*. 66, 328-341, **2009**.
[31] Cortese, B. *et al.* "Mechanical gradient cues for guided cell motility and control of cell behavior on uniform substrates". *Adv. Funct. Mater*. 18, 2951-2968, **2009**.
[32] Hadjipanayi, E. *et al.* "Guiding cell migration in 3D: a collagen with graded directional matrix". *Cell. Motil*. *Cytoskel*. 66, 121-128, **2009**.
[33] Reinarth-King, C. A. *et al.* "Cell-Cell Mechanical Communication through Compliant Substrates". *Biophys. J. 95*, 6044-6051, **2008**.
[34] Lazopoulos, K.A. and Stamenović, D. "Durotaxis as an elastic phenomenon". *J. Biomech*. 41, 1289-1294, **2008**.
[35] Solon, J. *et al.*, "Fibroblast adaptation and stiffness matching to soft elastic substrates". *Biophys. J*. *93*, 4453-4461, **2007**.
[36] Byfield, F. J. *et al.*, "Endothelial actin and cell stiffness is modulated by substrate stiffness in 2D and 3D". *J. Biomech*. *42*, 1114-1119, **2009**.
[37] Wirtz, D. "Particle-tracking microrheology of living cells: principles and applications". *Annu. Rev. Biophys*. 38, 301-326, **2009**.
[38] Hale, C.M *et al.* "Role of actomyosin contractility in cell microrheology". *PLos One* 4, e7054, **2009**.
[39] Baker, E. L. *et al.*, "Extracellular matrix stiffness and architecture govern intracellular rheology in cancer". *Biophys. J*. *97*, 1013-1027, **2009**.
[40] Baker, E. L. *et al.*, "Cancer cell stiffness: integrated roles of three-dimensional matrix stiffness and transforming potential". *Biophys. J. 99*, 2048-2055, **2010**.
[41] Doi, M. "Viscoelastic and rheological properties" In *Materials Science and Technology: Structure and Properties of Polymers*; Thomas, E. L., Ed.; Wiley-VCH: Weinheim, 12, 389–425, **1993**.
[42] Ferry, J. D. "Viscoelastic Properties of Polymers" *John Wiley: New York*, **1980**.
[43] Tyllianakis, E. P.*et al.* "Direct colorimetric determination of solid-supported functional groupa and ligands using bicinchronic acid" *Anal. Biochem*. *219*, 335–340, **1994**.
[44] Tseung, Y. *et al.* "Micromechanical Mapping of Live Cells by Multiple-Particle-Tracking Microrheology". *Biophys. J. 83*, 3162-3176, **2002**.
[45] Xu, J. *et al.* "Compliance of actin filament networks measured by particle-tracking microrheology and diffusing wave spectroscopy" Rheol. Acta *37*, 387–398, **1998**.
[46] Mason, T. G. *et al.* "Particle-tracking microrheology of complex fluids". *Phys. Rev. Lett*. *79*, 3282–3285, **1997**.
[47] Dasgupta, B. R. *et al.* "Microrheology of polyethylene oxide using diffusing wave spectroscopy and single scattering". *Phys. Rev. E. Stat. Nonlin. Soft. Matter Phys*. *65*, 051505, **2002**.
[48] Einstein, A. "Über die von der molekularkinetischen Theorie der Wärme geforderte Bewegung von in ruhenden Flüssigkeiten suspendierten Teilchen". *Ann. Physik 17*, 549, **1905**.
[49] Chandrasekhar, S. "Stochastic problems in physics and astronomy". *Rev. Mod. Phys*. *15*, 1–89, **1943**.
[50] Qian, H. *et al.* Single particle tracking. Analysis of diffusion and flow in two-dimensional systems. *Biophys. J. 60*, 910–921, **1991**.
[51] Berg, H. C. "Random Walks in Biology", Princeton, NJ: Princeton University Press, **1993**.
[52] Eckstein, A *et al.* "Determination of plateau moduli and entanglement molecular weights of isotactic, syndiotactic, and atactic polypropylenes synthesized with metallocene catalysts". *Macromolecules 31,* 1335–1340, **1998**.
[53] Hersel, U. *et al.* "RGD modified polymers: biomaterials for stimulated cell adhesions and beyond". *Biomaterials* 24, 4385-4415, **2003**.
[54] Geiger, B. *et al.* "Environmental sensing through focal adhesion". *Nature Rev. Mol. Cell. Biol*. 10, 21-33, **2009**.

[55] Lazopoulosa, K.A. and Stamenović, D.S "Durotaxis as an elastic stability phenomenon". *J. Biomech*. 41, 1289-1294, **2008**.
[56] Ingber D. E. "Tensegrity I. Cell structure and hierarchical systems biology". *J. Cell Sci.* 16, 1157-1173, **2003**.
[57] Balaban, N. Q. *et al.* "Force and focal adhesion assembly: a close relationship studies using elastic micropatterned substrates" *Nat. Cell Biol*. 3, 466-4472, **2001**.
[58] Ingber D. E. "Tensegrity and mechanotransduction". *J. Bodywork Movement Ther*. 12, 198-200, **2008**.
[59] Stamenović, D.S. and Ingber, D.E. "Tensegrity-guided self assembly: form molecules to living cells". *Soft Matter* 5, 1137-1145, **2008**.
[60] Deguchi, S. *et al.* "Tensile properties of single stress fibers from cultured vascular smooth cells". *J. Biomech.* 39, 2603-2610, **2006**.
[61] Gilmore, R. "Catastrophe Theory for Scientists and Engineers". New York, Wiley, 1981.
[62] Nicolas, A. and Safran, S.A. "Limitation of cell adhesion by the elasticity of the extracellular matrix". *Biophys. J*. 91, 61-73, **2006**.
[63] Hynes, R.O. "Integrins: bidirectional, allosteric signaling machines". *Cell* 110, 673–687, **2002**.
[64] Balaban, N.Q. *et al.* "Force and focal adhesion assembly: a close relationship studied using elastic micropatterned substrates". *Nat. Cell. Biol*. 3, 466–472, **2001**.
[65] Zaidel-Bar, R. *et al.* "Early molecular events in the assembly of matrix adhesions at the leading edge of migrating cells". *J. Cell. Sci.* 116, 4605-4613, **2003**.
[66] Zimerman, B. *et al.* "Early molecular events in the assembly of the focal-adhesion-stress fiber complex during fibroblast spreading". *Cell Motil & Cytoskeleton* 58, 143-159, **2004**.
[67] Kumar, S. *et al.* "Viscoelastic retraction of single living stress fibers and its impact on cell shape, cytoskeletal organization, and extracellular matrix mechanics". *Biophys. J.* 90, 3762-3773, **2006**.
[68] Beningo, K.A. *et al.* "Nascent focal adhesions are responsible for the generation of strong propulsive forces in migrating fibroblasts". J. Cell. Biol. 153, 881–888, **2001**.
[69] Berrier, A.L. and Yamada, K.M. "Cell-matrix adhesion". *J. Cell. Physiol*. 213, 565–573, **2007**.
[70] Cavalcanti-Adam, E.A. *et al.* "Cell spreading and focal adhesion dynamics are regulated by spacing of integrin ligands". *Biophys. J.* 92, 2964–2974, **2007**.
[71] Pelham, R.J. Jr and Wang, Y. "Cell locomotion and focal adhesions are regulated by substrate flexibility". *Proc. Natl. Acad. Sci.* USA 94, 13661–13665, **1997**.
[72] Levental, I. *et al.* "Soft biological materials and their impact on cell function". Soft Matter, 2, 1–9, **2006**.
[73] Hersel, U. *et al.* "RGD modified polymers: biomaterials for stimulated cell adhesion and beyond". *Biomaterials* 24, 4385-4415, **2003**.
[74] Kato, M. and Mrksich, M. "Using model substrates to study the dependence of focal adhesion formation on the affinity of integrin-ligand complexes". *Biochemistry* 43, 2699–2707, **2004**.
[75] Deeg, J.A. *et al.* "Impact of local versus global ligand density on cellular adhesion". *Nano Lett*. 11, 1469-1476, **2011**.
[76] Zaidel-Bar, R. *et al.* "Functional atlas of the integrin adhesome". *Nat. Cell. Biol.* 9, 858-867, **2007**.
[77] Engler, A. *et al.* "Substrate compliance versus ligand density in cell on gel responses". *Biophys. J.* 86, 617-628, **2004**.
[78] Johnson, C.P. *et al.* "Forced unfolding of proteins within cells". *Science*, 317, 663-666, **2007**.
[79] Wang, N. and Suo, Z. "Long-distance propagation of forces in a cell". *Biochem. Biophys. Res. Commun.* 328, 1133-1138, **2005**.
[80] Wirtz, D. "Particle-tracking microrheology of living cells: principles and applications". *Annu. Rev. Biophys*. 38, 301-326, **2009**.
[81] Kuznetsosa, T.G. *et al.* "Atomic force microscopi probing of cell elaticity". *Micron* 38, 824-833, **2007**.

# Chapter 3

# Strengthening of Fibroblasts under Uniaxial Stretching

## 3.1 Introduction

Living cells activities seem to be guided by their mechanical environment. Physical cues, such as forces, deformations and the geometry and stiffness of the ECM are critical for the control of cell form and function [1-3]. In particular, it was demonstrated that mechanical forces could affect cell orientation [4-6], migration [7-8], proliferation [9], differentiation [10-12].

Understanding how cell behavior can be influenced by mechanical stimuli represents still now an open question. We can answer this query focusing our attention on the way by which cells sense and respond to changes to the state of isometric tension, realized by cytoskeletal contractile filaments and counterbalanced by external adhesions to ECM and other cells and from inside by internal struts (microfilaments, stress fibers and microtubules) [13]. Adhesion complexes, based on integrin transmembrane proteins, able to transmit forces from inside (cytoskeleton) to outside the cell (ECM) [14], are naturally considered the best candidates for mechanosensing and mechanotransduction [15], allowing to trigger the assembly of signaling complexes and activate biochemical activities. Then, molecular connections between integrins, cytoskeletal filaments and nucleus, to which tensional forces are transmitted [16], endow a discrete path for mechanical signal transfer throughout living cells, but in particular a mechanism to provide tensional stability. Indeed, when cells are subjected to mechanical forces, they adopt a mechanoprotective and adaptative behavior to control membrane integrity, cell shape and integrity.

Several lines of evidence suggest cell ability to sense environmental mechanical stimuli and to develop preserving mechanisms mediated by recruitment of submembranous proteins that reinforce the plasma membrane [17-18] or by cytoskeletal structure assembly [19-20]. For example, Pender and McCulloch have demonstrated a rapid dynamic response to mechanical deformation that consists in an actin polymerization increase depending on the amount and timing of stretching and on the cell type. Indeed, periodontal ligament fibroblasts presented a 3-fold higher total actin amount compared to gingival fibroblasts, that is attributable to a phenotype of

periodontal fibroblasts rich in microfilament array due to their placement in a much more mechanically stressed environment [21]. Also in vascular stem cells [22] the actin polymerization and the cytoskeleton stabilization are promoted by mechanical stimuli, in particular by the increase in intravascular pressure. The reorganization of cytoskeletal structure consists also in the alignment of actin stress fibers away from the direction of stretching in response to uniaxial stretching of a substrate [23-25].

The preserving processes that cells adopt to sustain mechanical stress or strain seem to be mechanically explained through a strain-hardening mechanism. The early work in which this phenomenon was experimentally observed, was conducted by Petersen *et al.* that tried a non linear increase of force with depth indentation, depending on the position of the probe on cell surface [26]. The cell stiffening seems to depend also on the duration of exposure to stress, as recognized by Sato and coworkers, that indicated an increase in endothelial cells stiffness using a pipette aspiration technique when they were exposed to shear stress for 24 hours, but not for 6 hours [27]. This effect was interpreted as the resistance offered by cortical cytoskeletal elements to deformation, but it's throughout recognized that the internal cytoskeletal structure has an important effect on the local mechanical properties of cells. Then, the same authors have explored the contribution of cytoskeleton and in particular of stress fibers studying the effect of stiffening under shear stress using atomic force microscopy technique and observing an increase of cell stiffness also after 6 hours of exposure to shear stress, but only at its upstream side; this effect was propagated to downstream side of the cell with an exposure of 24 hours [28]. The determining role of actin cytoskeleton in regulating remodeling process and cell stiffening has been demonstrated for different cell lines, such as alveolar epithelial cells [29-30] and airway smooth muscle cells [31-32]. If the cells exhibit a typical elastic behavior, as demonstrated by Mizutani *et al.* through an immediate stress fiber hardening due to external deformation, they are able to compensate changes through a mechanism that allows to recover the stiffness to basal levels [33].

In these mechanosensory and mechanoprotective processes integrin-mediated adhesion are involved in increase the structural strength and integrity of the cortical actin network through cross-linking and bundling activities of actin-binding proteins. Ingber and coworkers observed that endothelial cells exhibited a "force-stiffening response", depending also on the substrate adhesion and then cell spreading (controlled by fibronectin (FN) coating density), when were stressed by twisting cell-bound ferromagnetic beads [34-35]. The stress-dependent increase of cytoskeletal stiffness is dependent on the structural integrity of microtubules, intermediate filaments and

microfilaments systems and can be explained by tensegrity models able to mimic this response [36]. The "reinforcement" of integrin-cytoskeleton linkages was also recognized in experiments that used optical tweezers to restrain the rearward movement toward the nucleus of cell-attached beads on lamellipodia of migrating fibroblasts. The application of force to integrin-mediated adhesions strengthened the cytoskeleton linkages, in a force- and FN density-dependent manner. Two important features of the rigidification of CSK were the rapidity and the locality of this effect – the reinforcement occurred only in correspondence of the stressed bead [37]. The idea that force sensing is mediated by cytoskeletal elements was confirmed by the F-actin accumulation and membrane rigidity increase, when collagen magnetic beads were bound to cells through some focal-adhesion-associated proteins, such as talin, vinculin, alpha-2-integrins, and stressed. The strengthened cortical actin preserves cells exposed to repeated mechanical stimuli, regulating cations permeable channel activity, that mediates the initial membrane extension [20,38], regulates development of traction forces and adhesion structures near the leading edge and stimulates cell migration [39]. Cell response to mechanical stress is characterized from different adaptive behaviors depending on the force application time: 1- a first viscoelastic creep response of adhesion sites with a complete elastic recovery of their initial position with stress remove within 0.5 sec; 2- a second adaptative strengthening behavior, that indicates a molecular reorganization and the necessity to preserve the tensional state and that can be suppressed by inhibiting contractility drugs; 3- a third adaptative stiffening behavior to prolonged stresses (>15 s) that was not affected by drugs action [40].

The force-dependent strengthening of integrin-cytoskeleton linkages is a process that involves tysosine phosphatase, as demonstrated by its inhibition due to phenylarsine oxide [36] and by decrease number of reinforced beads and increase of number of immature focal complexes in cells deficient in the SH2 domain containing protein tyrosine phosphatase 2 (Shp2) [41]. Furthermore, the transmembrane receptor-like protein tyrosine phosphatase $\alpha$, RPTP$\alpha$, acts as a transducer of early force exerted on cell-bound bead and has a critical role in process force-dependent reinforce of integrin-cytoskeletal linkages. The expression loss of RPTP$\alpha$ increases the mean squared displacement (MSD) of cell-attached beads. The re-expression of RPTP$\alpha$ reduced the MSDs and renovated the ability of cells to respond to forces, accumulating paxillin under beads that experiment stresses [42]. In the early mechanosensing, the stimulation of signaling pathways associated to tyrosine kinase and extracellular signal-regulated kinase (ERK) activities, that trigger two guanine nucleotide exchange factors (LARG and GEF-H1) [43], has to be directed in association

with the recruitment of proteins to early adhesion sites [44], to promote their reinforcement and stabilization. In particular, it was demonstrated that talin has a crucial role in reinforcement of early adhesion sites, even if tyrokine kinase activities are not blocked [45].

Not all the studies on cell mechanical behavior reveal a stiffening and viscoelastic behavior of living cells. For example, Yang and Saif explored the response of adherent cells to large stretching and un-stretching force, discovering a linear and reversible response to stretching, that they interpreted as a mechanism that nature adopt to assure the maximum efficiency to biological systems [46]. If recent literature emphasizes the importance of stiffening behavior in response to application of stress or strain, recent works show a softening and fluidization responses to stretch, that were attributed to the inability of cells to individuate their stable conFiguretion after transient stretch [47] or to an enhance of protein motors, that can explain both prestress and stiffening increase and softening due to their motion in a transverse direction to stretch [48].

Particle tracking microrheology (PTM) can be used to take a vision of the anisotropic and heterogeneous spatial distribution and time course of stiffness of a living cell under culture condition. We have reported that local stiffness is not uniform in the cytoplasm, but reflects the changes of the cytoskeleton networks in terms of the density of filamentous actin and intracellular tension acting along the stress fibers.

In the present study, to reveal the characteristics of the cell response to mechanical signals, mechanical responses of fibroblasts are measured as time laps images by the PTM technique when the cells are subjected to uniaxial deformation both via an elastic polydimethylsiloxane (PDMS) rubber substrate and an hyperelastic fibrin 3D matrix under culture conditions. Stiffness responses of cells are determined and the contribution of environmental dimensionality and matrix mechanical behavior is discussed.

## 3.2 Materials and Methods

### 3.2.1 Cell Culture

Mechanical stretching and PTM experiments were performed on mouse embryo fibroblasts NIH3T3 cells. Cell line were cultured at 37°C in 5% CO2 in a humidified incubator in Dulbecco's modified Eagle's (DMEM) medium supplemented with 10% fetal bovine serum (FBS, BioWhatter,

MD), 2 mM L-glutamine (Sigma, St. Louis, MO), 1000 U/L penicillin (Sigma, St. Louis, MO), and 100 mg/L streptomycin (Sigma, St. Louis, MO).

### 3.2.2 Stretch Device Fabrication

Polydimethylsiloxane (PDMS) chamber were fabricated by pouring a pre-polymer PDMS, purchased from Dow Corning (Midland, MI) and obtained by mixing the silicon elastomer base and the crosslinking agent at a ratio equal to 10:1, into a aluminum replying master, which was degassed under vacuum for 1 h, cured at 60°C overnight and subsequentely taken away the master **Figure 1**.

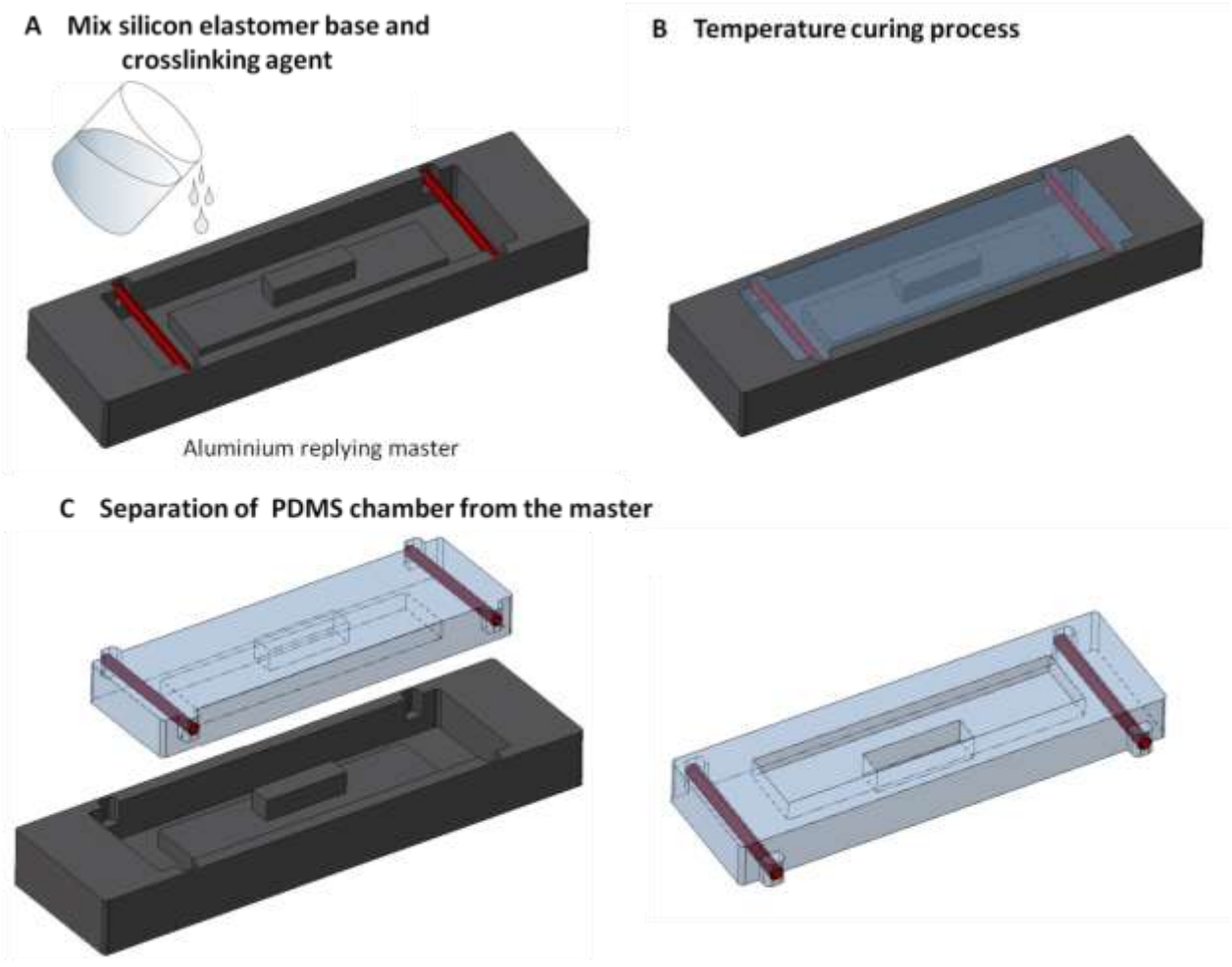


**Figure 1 | Stretch device preparation phases**. **A** the silicon elastomer base and the curing agent were mixing, then deposing in the aluminium replying master. **B** The pre-polymer PDMS was degassed under vacuum and cured at 60°C temperature overnight. **C** Then, the PDMS stretching chamber was taken away the master.

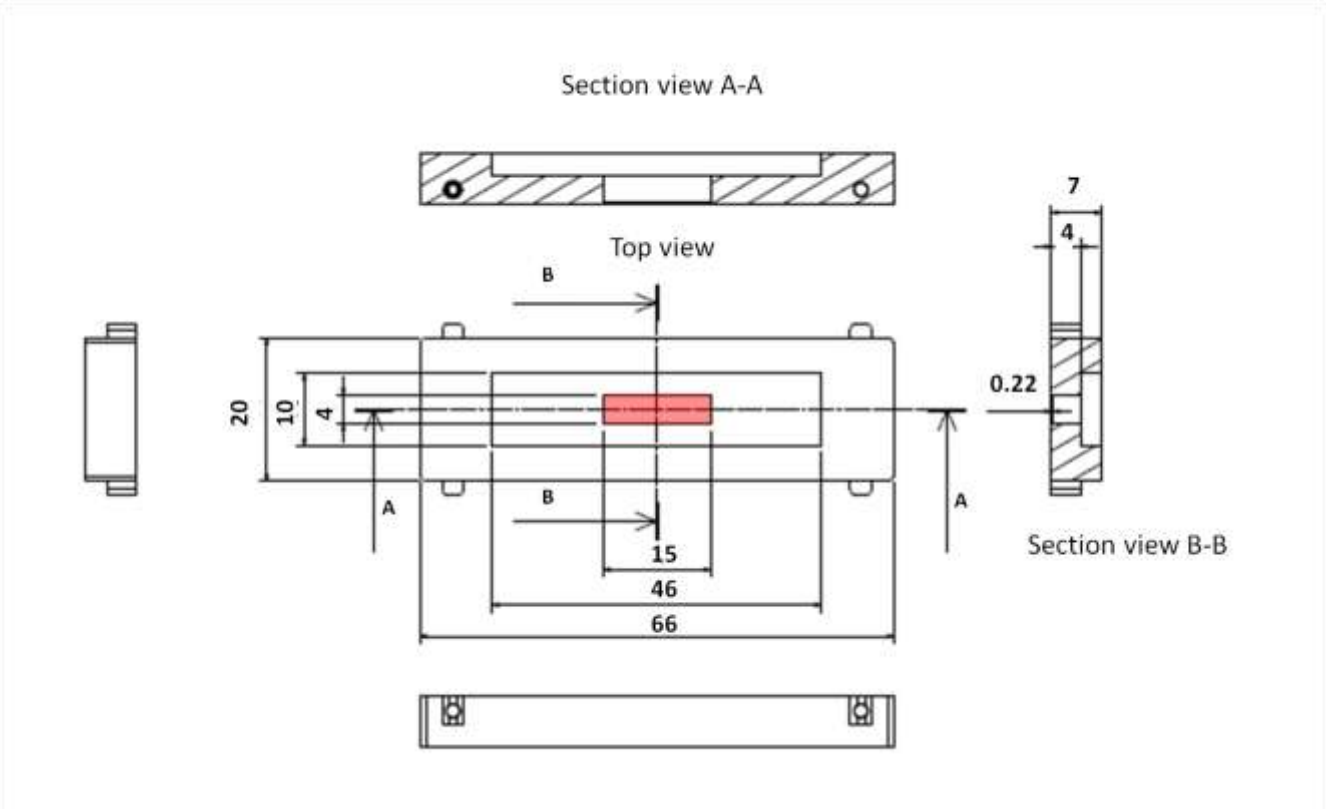


**Figure 2 | Different section views of stretching device**. In the top view, it's shown in red the window of 220 µm thickness (as shown in section view B-B) on which cells were cultured. The measure unit of dimensions is mm.

The elastic device consists of a transparent bottom, 66 × 20 mm, with a central window (the red zone in **Figure 2**), 15 × 4 mm, of 220 µm thickness and a wall of 7 mm height **Figure 2**, which is deformable up to 20% along a single direction.

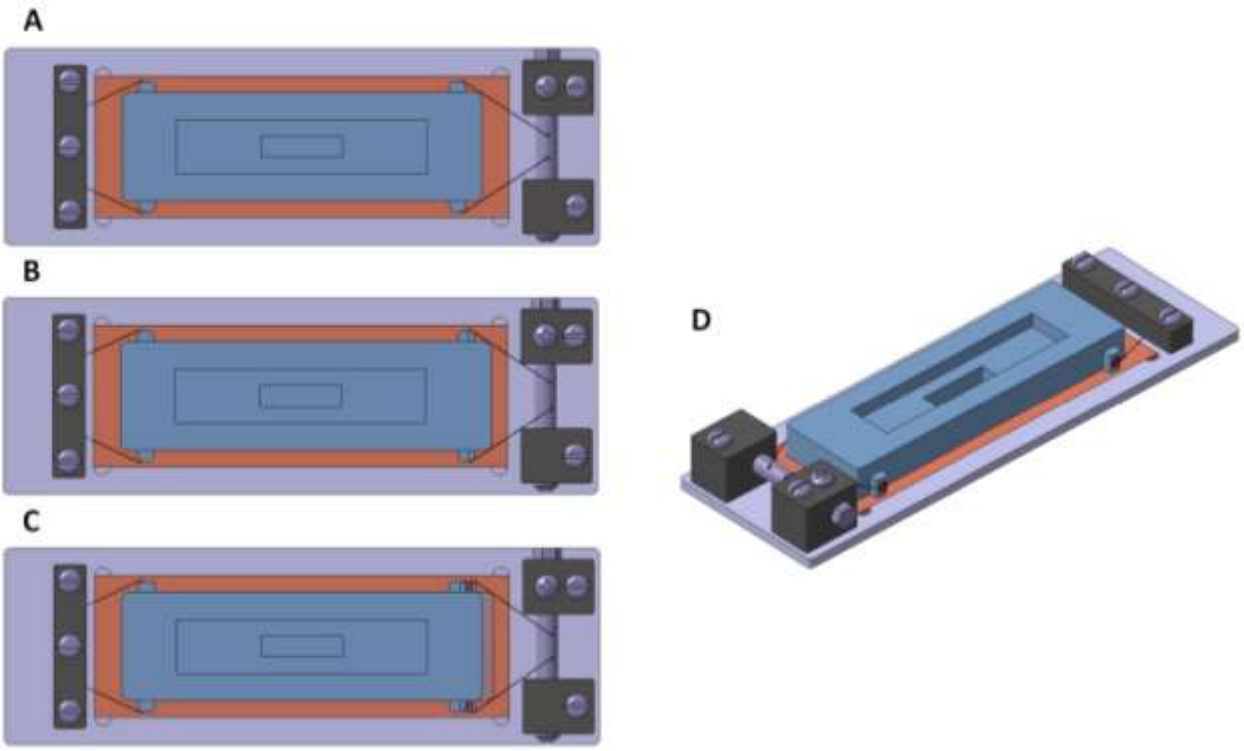


**Figure 3 | Schematic diagram of stretching system**. **A** the Stretching device is mounted on the microscope stage and fixed at its end and constrained to the opposite side, that will be moved, causing the device deformation. **B** An intermediate phase of the stretching process. The deformation is applied by rolling a iron wire attached to the unconstrained side of the chamber around a stainless steel bar. **C** After applying the prescribed deformation, the chamber was blocked and the deformation Is maintained constant during the experiment. **D** A 3D view of the stretching device mounted on the system providing deformation.

The deformation is applied by rolling a iron wire attached to the unconstrained side of the chamber around a stainless steel bar (**Figure 1**). The magnitude of deformation was calibrated from the displacement of points marked on the elastic substrate. Uniaxial deformation of the elastic substrate using the clamping device is accompanied by a small degree of subsidiary deformation in the orthogonal direction, because both sides of the elastic substrate are allowed to deform. All devices were autoclaved and then incubated with DMEM medium supplemented with 10% fetal bovine serum for 30 min to promote protein adsorption.

### 3.2.3 Particle Delivery and Particle Tracking

NIH-3T3 cells were cultured to ~90% confluency in a 10 cm dish (Corning Incorportated) and then were incubated with 100 nm fluorescent carboxylated nanoparticles (Invitrogen, Molecular Probes) solution (0.03% v/v) for 3 h under physiological conditions.

After incubation, cells were detached using 0.25% Trypsin/0.53 mM EDTS, allowing to endocyted particles to free from protein motors that guide microtubule-mediated directed motion of vesicles. 20.000 cells suspended in simple DMEM or embedded into fibrin polymer before gelation process was initiated, were added on top of thin window of PDMS chamber previously prepared. The chamber window supplemented with 200 µl of media and subsequently incubated for 24 h at 37°C, 5% $CO_2$ in a humidified incubator.

After incubation, images of NPs inside cells were collected in real time for about 6 s by using an inverted microscope (Olympus IX70) equipped with a fluorescence mercury lamp (Olympus U-RFL–T) before applying a 4% chamber elongation and after the deformation was applied, monitoring NPs displacements and , then , cell viscoelastic properties every 10 min. A 100x oil immersion objective (numerical aperture [NA] 1.3) was used for particle tracking, which permitted ~0.1 µm spatial resolution over a 156 µm × 125 µm field of view. To perform experiments under physiological conditions, a microscope stage incubator (Okolab) was used to keep cells at 37°C and 5% $CO_2$, which is supplied as a 5/95% $CO_2$/air mixture. Before supplying this gas to the cells, it is moisturized by feeding it through a closed chamber containing 5% $CO_2$satured water. The sequence of digital images were acquired by a fast digital camera (Lambert Instruments) at a frame rate of 50 Hz, forming a movie. A number comprised between 20-30 particles was tracked for each time-lapse acquired every 10 min. We used a diluted particle solution (0.03 % v/v) to reduce the error in trajectory reconstruction and to avoid overlapping and, then, effects due to interparticle forces between adjacent particles.

### 3.2.4 3D Fibrin Scaffold Preparation

Fibrin biopolymer results from the thrombin-activated cleavage of the blood-borne protein fibrinogen, and it is the major fibrillar component of blood clots. In addition to its structural role, finrin is a biochemical stimulant of the wound healing response. It is used clinically as a surgical sealant and also has been investigated as a scaffold material in tissue engineering [49]. The embedded cells can recognize, attach to and remodel the surrounding matrix, such that it becomes compacted to form a rudimentary tissue. The reason for which for which we chose fibrin is that solubilized fibrin can be cast and reconstituted into essentially molding and the cells can subsequently become homogeneously embedded in the molded matrix upon gelation, but also because is material that forms a optimal adhesion with PDMS stretching chamber, allowing the

perfect transfer of deformation from bottom elastic window to attached fibrin matrix and, then, to cells.

Three-dimensional constructs of fibrin gels were made at a 3.3 mg/ml protein content using human plasma Type III fibrinogen (Sigma) with cells at a final concentration of 1.0 $\times 10^6$ cells/ml. The lyophilized wad dissolved in warm 0.9% saline solution on a 30 mg/ml basis, filtered through a 0.2 filter and diluted in DMEM supplemented with 10% fetal bovine serum (FBS, BioWhatter, MD), 2 mM L-glutamine (Sigma, St. Louis, MO), 1000 U/L penicillin (Sigma, St. Louis, MO), and 100 mg/L streptomycin (Sigma, St. Louis, MO) to obtain a 5x fibrinogen solution. 250 U of thrombin were dissolved in 1 ml of deionized water and 9 ml of PBS (ending up with 25 U/ml solution), filtered through a 0.2 filter and diluted to 1 U/ml by adding medium containing 15 mM $Ca^{++}$. Thrombin and fibrinogen solutions were gently mixed at a ratio 1:2 and the liquid suspension was poured into a mold, in this case the stretching chamber, and exposed to 37°C temperature in order to accelerate gelation **Figure 44**.

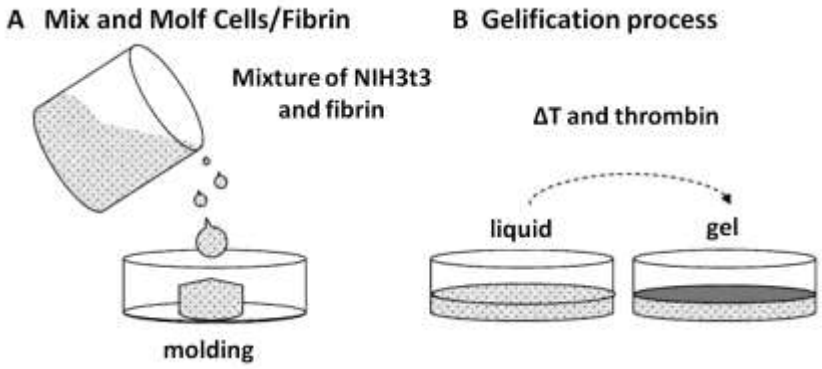


**Figure 4 | Fabrication of 3D fibrin constructs. A** solubilized fibrin is mixed with NIH3t3 and the mixture is then poured into a mold. **B** The liquid suspension is exposed to conditions that initiate gelation, such as temperature change or addition of an enzyme.

### 3.2.5 Intracellular Rheology from Particle Tracking

For the technique of particle tracking microrheology principles, see the sub-section 2.2.5 of chapter 2.

### 3.3 Results and Discussion

To determine a suitable amount of deformation that would not alter the cellular morphology and cause severe damage to the cells, we refer to Mizutani *et al.* that indicated that a large degree of deformation, greater than 15% destroyed the cells instantly. They observed that for 8% elongation or compression, the cell are not disassembled but still appear to be tensile [33].

We established to apply 4% deformation in our experiments and to determine stiffness evolution of a typical fibroblast. The particle tracking experiments were conducted every 10 minutes. As early said, the stretched cells were cultured in a 3D fibrin scaffold, but only cells that, during the adhesion process, settled on the PDMS chamber were taken into account, so that they sensed directly the prescribed deformation, but at the same time were surrounded by fibrin gel. After the elongation, the cell did not exhibit drastic changes in shape, except for those induced by the degree of elongation of the elastic substrate (**Figure 5 A and B**).

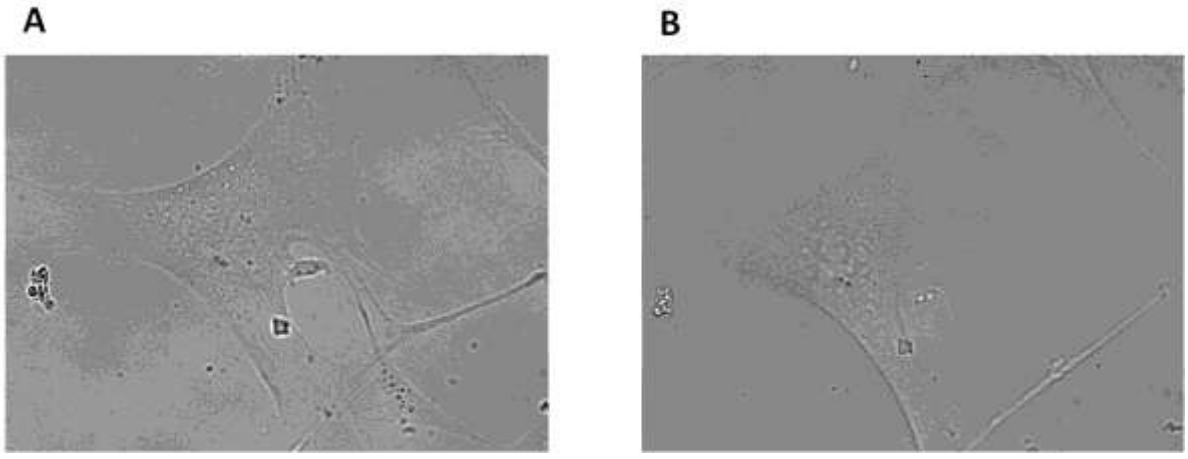


**Figure 5 | Transmission images before (A) and after (B) the application of deformation.** The cell did not show importante changes in shape, except for those inuced by the degree of elongation of the substrate.

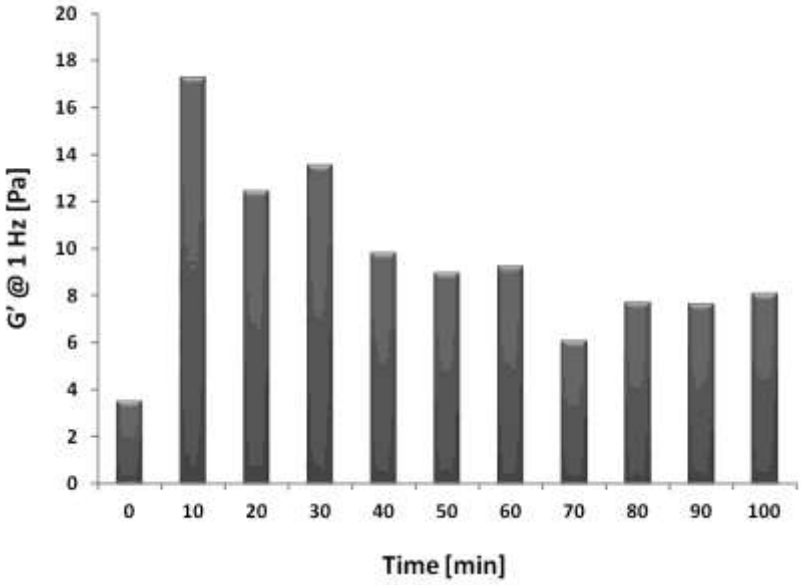


**Figure 6 | Time-dependence of intracellular stiffness of fibroblasts cultured in 3D fibrin gel**. Time 0 referred to the cell resting state. Cell stiffness increase after the elongation and decreases gradually, reaching a stable value after 1 hour.

The average degree of stiffness is plotted in **Figure 6.** The time 0 referred to the cell resting state, before applying elongation. The stiffness increases immediately after the elongation. After this rapid increase, it decreases gradually and stabilizes at a value two-fold higher than the value measured before applying deformation.

The rapid increase of the cellular stiffness induced by the elongation stimulus can be attributed to the simple elastic response of the cytoskeletal networks, consisting of filamentous actin and actin-binding proteins, such as myosin II and filamin. According to the model presented in previous chapter, the application of an external mechanical stimulus can produce cascading effects starting from rising of tensional state in stress fiber, followed by their cross sectional area increase and, then, by focal adhesion size increase, so as maintain constant the internal tensional state. As demonstrated previously, the dimension of these two structures control the mechanical properties of the focal adhesion-stress fiber complex, that mediates the transmission of forces internally, and consequently of the overall cytoskeletal structure. Indeed, Glogauer *et al.* have previously demonstrated that membrane rigidity increased 6-fold in the vicinity of collagen-coated magnetic beads that applied localized forces directly to the cortical actin of fibroblasts, for a possible change in the distribution of actin filaments, due to reconstrutction of the cell cortex and stress fibers. They also demonstrated that the calcium influx through stretch-activated channels,

and the recruitments of filamin, stabilized the actin cortex when the plasma membrane was placed under a tensile stress state for 20 minutes [37].

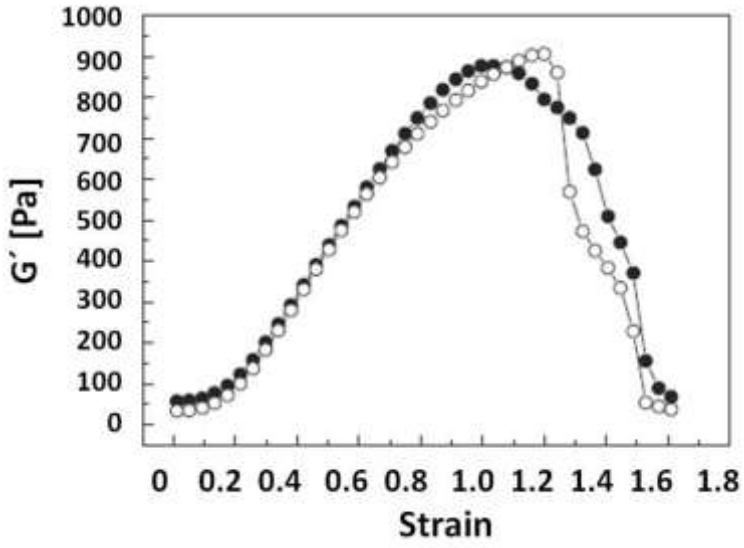


**Figure 7 | Fibrin stress-strain curve.** Filamentous biopolymer networks, such as collagen and fibrin, have larger elastic moduli compared to flexible polymer gels, and a striking increase in elastic modulus with increasing strain.

After the initial rapid change in the cellular stiffness under mechanical stress, fibroblast reduced its internal tensional state, as demonstrated by the decreasing stiffness. After about 1 h the intracellular elastic modulus stabilized to a value twofold higher that the reference value at the resting state (Figure 5). From a certain point of view, it seems that at the single cell a tensional homeostasis exists, producing the decrease of intracellular stiffness through a process of stress relaxation. As it occurs at tissue level, also at cell-matrix and cell levels experiments suggest that cells, in particular vascular cells, and sub-cellular structures such as stress fibers and focal adhesions attempt to maintain constant preferred mechanical state [50]. In this process, the role of myosin phosphorylation is determining for the coordination of the tensile force [33] and the formation o stress fibers [51]. On the other hand, the stiffness value we measured after 2 h to the elongation is twofold higher than the baseline value. We have interpreted the phenomenon through two possible mechanisms or probably as guided by both of them. The first possible explanation of the cell mechanical reinforcement is represented by cytoskeleton remodeling process associated with the dynamic reorganization of focal adhesions, that occurs in response to altered cell stretching. The ability of cells to sense and dynamically respond to stretching of the matrix is explicated by the reorientation of actin stress fibers and the activation of intracellular

signaling proteins, such as focal adhesion kinase (FAK) and the mitogen-activated proteins kinases (MAPKs) [52]. But the reorientation is not the only way the cell uses to respond external forces and reinforce its structure; indeed application of external pulling force promotes also focal adhesion growth even under condition when myosin II activity is blocked. Individual FAs behave as mechanosensors responding to the application of force by incorporating additional subunits in the direction of force [53]. Second one represents the fact that reinforcement process couldn't be a process induced by external deformation, but by stress stiffening behavior of fibrin matrix, in which cells are embedded. We know that cell mechanical properties adapt to matrix properties (Chapter 2) increasing when substrate stiffness increases. The elongation applied to the system, constituted by cells and fibrin causes the stiffening of hyper-elastic fibrin gel **Figure 7**, and could explain the increased cell elasticity after relaxation of external stress.

To separately explore the two effects, we investigated the response of cell to externally applied deformation, when fibroblasts were seeded on PDMS substrate. PDMS, differently from fibrin, have a linear mechanical behavior **Figure 8.**

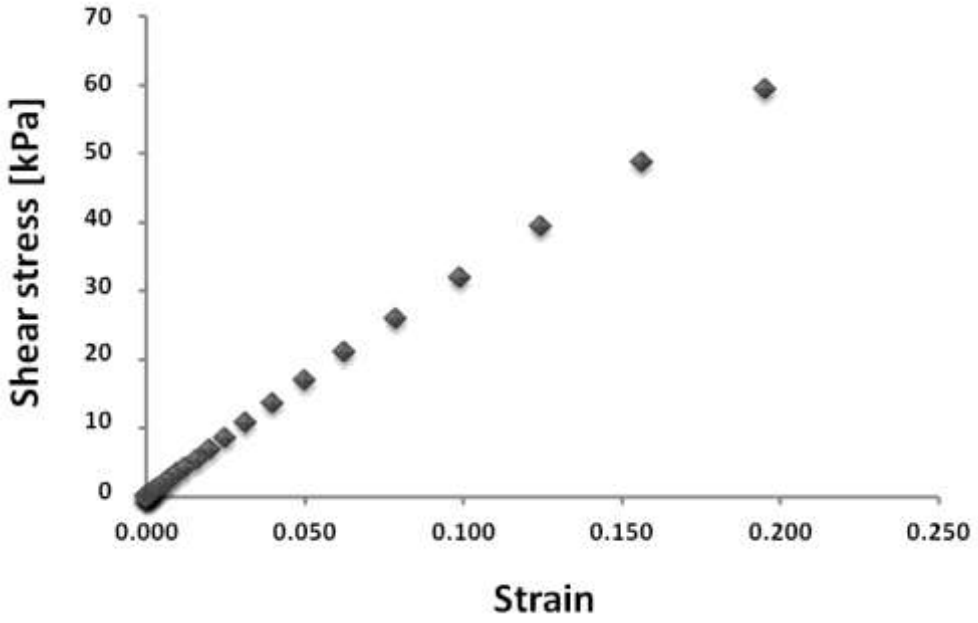


**Figure 8 | PDMS stress-strain curve**. PDMS has a linear behavior until 20% deformation.

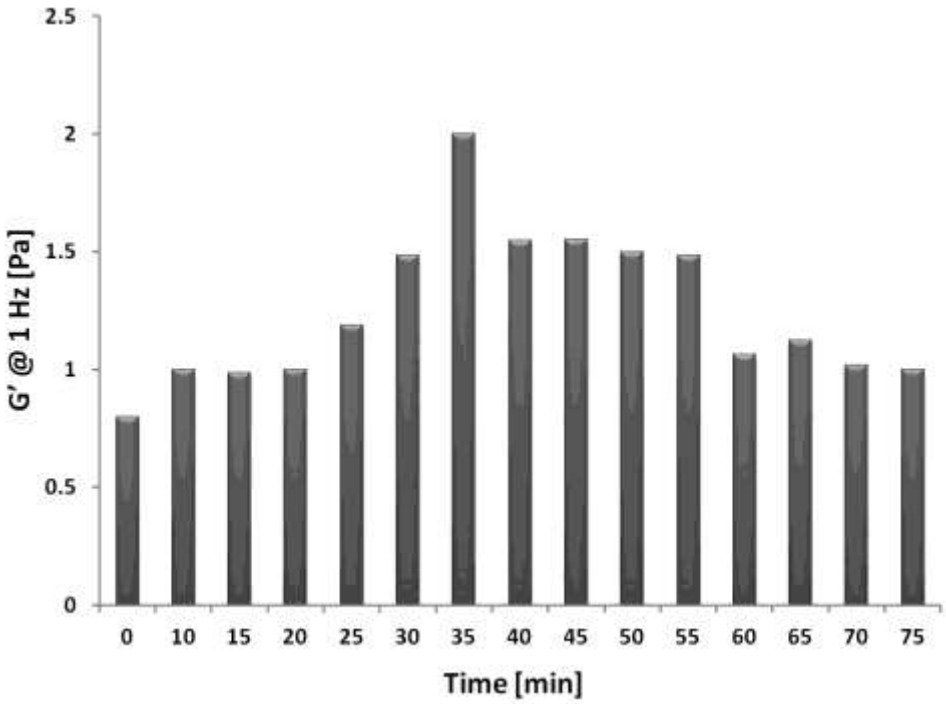


**Figure 9 |Time-dependence of intracellular stiffness of fibroblasts cultured on PDMS substrate**. Time 0 referred to the cell resting state. Cell stiffness increase after the elongation and decreases gradually, reaching a stable value after 1 hour.

As shown in **Figure 9**, the evolution of cell mechanical properties when fibroblasts were cultured directly on PDMS is different from those embedded in 3D matrix. Differences in stiffness values between fibrin and PDMS have to be attributed to the not surface functionalization of PDMS, determining a non-optimal cell adhesion. We didn't observe an instantaneous increase of cell stiffness, but the peak value was reached after 30-35 minutes, indicating a reinforcement process in response to mechanical loading that required more time. The mechanical elongation seems to improve cell spreading, promoting focal adhesion growth and providing an higher tensional state in pre-existing stress fibers, that could probably determine cross-sectional area increase, as observed by Li *et al.* [54], and consequently, size increase of focal adhesion, from which they are generated. We didn't observe the same behavior in 3D matrix, not only because the adhesion in this case was better, but also because integrins, necessary to promote new focal adhesion formation, were saturated for the attachments with all surrounding environment and the pre-existing focal adhesion growth. After reaching the maximum value, we observed a decrease of mechanical properties, with stabilization after about 1 hour at value that is 20% greater than baseline value. Then, also on PDMS substrate, stretched cells seem to be characterized by a

reinforcement process, that in this case cannot to be correlated to the mechanical behavior of matrix, but only to a cytoskeletal remodeling.

The suggested hypothesis to explain the cell reinforcement after stretching needs further investigations to be confirmed. Following the stress fiber and focal adhesion evolution during extensional experiment, could be fundamental to understand what role they play in cell response to mechanical loading. Only with the understanding of the main protagonists in the matrix-cell interactions, we shall be able to control the “network of processes” that provides the integration of cells in surrounding environment and the correct exchange of information and energy.

## References


[1] Vogel, V. and Sheetz, M. "Local force and geometry sensing regulate cell function". *Mol. Cell Biol.*, 7, 265-275, **2006**.

[2] Guilak, F. *et al.* "Control of Stem Cell Fate by Physical Interactions with the Extracellular Matrix". *Cell Stem Cell*, 5, 17-26, **2009**.

[3] DuFort, C. *et al.* "Balancing forces: architectural control of mechanotransduction". *Nat. Rev. Mol. Cell Biol*., 12, 308-319, **2011**.

[4] K. Hayakawa *et al.*" Dynamic reorientation of cultured cells and stress fibers under mechanical stress from periodic stretching". *Exp. Cell Res.*, 268,. 104–114, **2001**.

[5] Grinnell, F. and Petroll, W.M. "Cell Motility and Mechanics in Three-Dimensional Collagen Matrices". *Annu. Rev. Cell. Develop. Biol*., 26, 335-361, **2010**.

[6] Pang, Y. *et al.* "Cell Motility and Mechanics in Three-Dimensional Collagen Matrices". *Biomaterials*, 32, 3776-3783, **2011**.

[7] Shiu, Y.T. *et al.* 2004 "Rho mediates the shear-enhancement of endothelial cell migration and traction force generation" *Biophys. J.*, 86, 2558–65, **2004**.

[8] Han, Y. *et al.* **"**Cyclic Strain Promotes Migration and Proliferation of Human Periodontal Ligament Cell via PI3K Signaling Pathway". Cell. Mol. Bioeng. 3, 369-375, **2010**.

[9] Pietromaggiori, G. *et al.* "Tensile forces stimulate vascular remodeling and epidermal cell proliferation in living skin". *Ann. Surg.* 22, 3169-3178, **2001**.

[10] Sarraf, C.E. *et al.* "*In vitro* mesenchymal stem cell differentiation after mechanical stimulation". *Cell Proliferation*, 44, 99-108, **2010**.

12 Clause, K.C. *et al.* "Directed Stem Cell Differentiation: The Role of Physical Forces". *Cell. Commun. Adhes*., 17, 48-54, **2010**.

[13] Burdick, J.A. and ,Vunjak-Novakovic, G. "Engineered microenvironments for controlled stem cell differentiation". *Tissue Eng.* 15, 205-219, **2009**.

[14] Ingber, D.E. "Cellular tensegrity: defining new rules of biological design that govern the cytoskeleton". *J. Cell. Sci*., 104, 613-627, **1993**.

[15] Ingber D "Integrins as mechanochemical transducers". *Curr. Opin. Cell Biol*., 3, 841–848, **1991**.

[16] Geiger, B. *et al.* "Transmembrane extracellular matrix-cytoskeleton crasstalk". *Nat. Rev. Mol. Cell Biol*., 2, 793-805, **2001**.

[17] Wang, N. *et al.* "Mechanotransduction at a distance: mechanically coupling the extracellular matrix with the nucleus". *Nat. Rev. Mol. Cell Biol*., 10, 75-82, **2009**.

[18] McNeil, P.L. "Cellular and molecular adaptations to injurious mechanical stress". *Trends Cell Biol*., 3, 302-307, **1993**.

[19] McNeil, P.L. and Steinhardt, R.A. "Loss, restoration, and maintenance of plasma membrane integrity". *J. Cell Biol*. 137, 1-4, **1997**.

[20] Malek, A.M. and Izumo, S. "Mechanism of endothelial cell shape change and cytoskeletal remodeling in response to fluid shear stress". *J. Cell Sci*. 109, 713-726, **1996**.

[21] Glogauer, M. *et al.* "Calcium ions and tyrosine phosphorylation interact coordinately with actin to regulate cytoprotective responses to stretching". *J. Cell Sci*. 110, 11-21, **1997**.

[22] Pender, N. and McCulloch, C.A.G. "Quantitation of actin polymerization in two human fibroblast sub-types responding to mechanical stretching". *J. Cell Sci*. 100, 187-193, **1991**.

[23] Cipolla, M.J. *et al.* "Pressure-induced actin polymerization in vascular smooth muscle as a mechanism underlying myogenic behavior". *FASEB J*. 16, 72-76, **2002**.

[24] Wang, J.H. *et al.* "Contractility affects stress fiber remodeling and reorientation of endothelial cells subjected to cyclic mechanical stretching". *Ann. Biomed. Eng*. 28, 1165–1171, **2000**.

[25] Wille, J.J. *et al.* "Comparison of the effects of cyclic stretching and compression on endothelial cell morphological responses". *ASME J. Biomech. Eng*. 126, 545–551, **2004**.

[26] Stamenović , D. *et al.* "Mechanical stability determines stress fiber and focal adhesion orientation". *Cell. Mol. Bioeng*. 2, 475–485, **2009**.
[27] Petersen, N.O. *et al.* "Dependence of locally measured cellular deformability on position on the cell, temperature, and cytochalasin B". *Proc. Natl. Acad. Sci. USA* 79, 5327-5331, **1982**.
[28] Sato, M. *et al.* "Viscoelastic properties of cultured porcine aortic endothelial cells exposed to shear stress". *J. Biomechanics* 29, 461-467, **1996**.
[29] Sato, M. *et al.* "Local mechanical properties measured by atomic force microscopy for cultured bovine endothelial cells exposed to shear stress". *J. Biomechanics* 33, 127-135, **2000**.
[30] Trepat, X. *et al.* "Viscoelasticity of human alveolar epithelial cells subjected to stretch" *Am J Physiol Lung Cell Mol Physiol* 287, 1025–1034, **2004**.
[31] Trapet, X. *et al.* "Effect of stretch on structural integrity and micromechanics of alveolar epithelial cell monolayers exposed to thrombin". *Am J Physiol Lung Cell Mol Physiol* 290, 1104 –1110, **2006**.
[32] Smith, B.A. *et al.* "Probing the viscoelastic behavior of cultured airway smooth cells with atomic force microscopy: stiffening induced by contractile antagonist" *Biophysical J*. 88, 2994-3007, **2006**.
[33] Matthews, B.D. *et al.* "Cellular adaptation to mechanical stress: role of integrins, Rho, cytoskeletal tension and mechanosensitive ion channels" *J. Cell Sci*. 119, 508-518, **2006**.
[34] Mizutani, T. *et al.* "Cellular stiffness response to external deformation: tensional homeostasis in a single fibroblast" *Cell Motil. Cytoskeleton* 59, 242-248, **2004**.
[35] Wang, N. *et al.* "Mechanotransduction across the cell surface and through the cytoskeleton". *Science* 260, 1124-1127, **1993**.
[36] Wang, N. and Ingber, D.E. "Control of cytoskeletal mechanics by extracellular matrix, cell shape, and mechanical tension". *Biophys. J*. 66, 2181-2189, **1994**.
[37] Choquet, D. *et al.* "Extracellular matrix rigidity causes strengthening of integrin-cytoskeletal linkages". *Cell*, 88, 39-48, **1997**.
[38] Glogauer, M. *et al.* "The role of actin-binding protein 280 in integrin-dependent mechanoprotection". *J. Biol. Chem*. 273, 1689-1698, **1998**.
[39] Munevar, S. *et al.* "Regulation of mechanical interactions between fibroblasts and the substratum by stretch-activated $Ca^{2+}$ entry". *J. Cell Sci*. 117, 85-92, **2004**.
[40] Matthews, B.D. *et al.* "Cellular adaptation to mechanical stress: role of integrins, Rho, cytoskeletal tension and mechanosensitive ion channels". *J. Cell Sci*. 119, 508-518, **2005**.
[41] von Wichert, G. *et al.* "Force-dependent integrin-cytoskeleton linkage formation requires downregulation of focal complex dynamics by Shp2". *EMBO J.* 22, 5023-5035, **2003**.
[42] von Wichert, G. *et al.* "RTPT-$\alpha$ acts as a transducer of mechanical force on $\alpha_v/\beta_3$-integrin –cytoskeleton linkages". *J. Cell. Biol.* 161, 143-153, **2003**.
[43] Guilluy, C. *et al.* "The Rho GEFs LARG and GEF-H1 regulate the mechanical response to force on integrins". *Nat. Cell Biol.* 13,722-733, **2011**.
[44] Huang, H. *et al.* "Cell mechanics and mechanotransduction: pathways, probes, and physiology". *Am. J. Physiol. Cell Physiol*. 287, 1-11, **2004**.
[45] Giannone, G. G. *et al.* "Talin1 is critical for force-dependent reinforcement of initial integrin –cytoskeleton bonds but not tyrosine kinase activation". *J. Cell. Biol.* 163, 409-419, **2003**.
[46] Yang, S. and Saif, T. "Reversible and repeteable linear local cell force response under large stretch". *Exp. Cell Res.* 305, 42-50, **2005**.
[47] Trapet, X. *et al.* "Universal physical responses to stretch in living cells". *Nature* 447, 592–595, **2007**.
[48] Morozov, K.I. and Pismen, L.M. "Cytoskeleton fluidization versus resolidification: prestress effect". Phys. Rev. E 83, 0519201- 0519208, **2011**.
[49] Habbell, J.A. "Materials as morphogenetic guides in tissue engineering". *Curr Opin Biotechnol*. 14, 551-558, **2003**.
[50] Humprey, J. D. "Vascular adaptation and mechanical homeostasis at tissue, cellular and subcellular levels". *Cell Biochem. Biophys*. 50, 53-78, **2008**.
[51] Burridge, K., "Are stress fibres contractile?" *Nature* 294, 691–692, 1981.
[52] Hsu, H.J. *et al.* "Stretch-induced stress fiber remodeling and the activations of JNK and ERK depend on mechanical strain rate, but not FAK". *PLoS One* 30, e12470, **2010**.

[53] Riveline, D. *et al.* “Focal contacts as mechanosensors: externally applied local mechanical force induces growth of focal contacts by an mDia1-dependent and ROCK independent mechanism”. *J. Cell Biol*. 153, 1175–1186, **2001**.

# Appendix A

# Experimental Techniques to Study Cell Mechanics

## A.1 Introduction

A variety of experimental techniques have been developed for studying the mechanical properties of the cytoskeleton, such as its viscoelastic properties and its diffusion parameters. The cytoskeleton is highly heterogeneous and has an intricate yet diverse structure. Coupled with a small linear response regime and an active character (continuously remodeling and undergoing biochemical changes), the heterogeneous structure of the cytoskeleton prevents simple measurement of its rheology. The methods developed to study rheology attempt to circumvent these challenges in different and unique ways. Some monitor passive Brownian movements without directly engaging the cell mechanically, whereas others measure responses to the direct application of external force. The following sections summarize the most impactful experimental methods for studying cellular mechanical properties.

## A.2 Passive Measurement Methods

Different microrheology measurement approaches have been developed to capture and characterize the rheology of the cytoskeleton. These methods can be largely divided into two broad classes: active techniques involving the application of forces and passive techniques that examine the motion of inherent or introduced particles due to thermal fluctuations or detect forces that cells exert isotonically on flexible substrates, without any external force.

### A.2.1 Passive Microrheology

One approach to measuring the microrheology of the cytoskeleton is to monitor the displacement of a probe owing to thermal fluctuations, referred to as passive microrheology. The technique does not apply external forces, but rather monitors microscopic probes undergoing thermal fluctuations characteristic of their environment [1-7]. Micrometer-sized beads are embedded into

the cytoskeleton and monitored using either video recordings and particle tracking [8] or laser beam interferometry [9-11]. Original passive microrheology experiments utilized a method that monitored the movement of a single particle. This method was unable to account for the particle's active (nonthermal) movement or its own effects on its environment. Later, passive microrheology experiments utilized a method that calculated the cross-correlation between the individual movements of two particles [12-13]. Jonas *et al.* recently developed a new fluorescence laser-tracking microrheometer to measure cytoskeletal rheology using fluorescent microspheres as tracer particles [14-15]. This novel technique offers nanometer spatial resolution over a frequency range extending from 1 Hz to 50 kHz.

### A.2.2 Dynamic Light Scattering

For samples with a homogeneous solution of proteins or particles, the viscoelastic properties can be explored using a dynamic light-scattering experiment [16]. In this technique, a laser beam is passed through the sample, and a detector collects light scattered by the sample. Using the measured scatter, one can calculate the average mean-squared displacement of the particles. This method is not suited for the study of the cellular environment directly because of the heterogeneity of the cytoskeleton.

### A.2.3 Fluorescence Correlation Spectroscopy

Based on the principles of dynamic light scattering, a method has been developed that is suitable for use in measuring diffusion and viscoelasticity within a cell. Fluorescence correlation spectroscopy uses a laser beam focused on a small volume within the cell and photon detectors to record fluctuations in fluorescence resulting from the movement of fluorescent molecules into and out of the volume [17-18]. The method is well suited for the study of small particles.

### A.2.4 Elastic Substratum Method

The first successful attempt to measure traction forces of individual cells using artificial flexible substrata was developed by Harris *et al.* [19]. The cells were cultured on substrates made of flexible silicone sheets **Figure 2A**. These sheets were made by polymerizing silicone fluid using a flame. The stiffness of the sheets could be varied by altering crosslinking time and initial viscosity of the silicone fluid. The sheets were coated with extracellular matrix (ECM) proteins to promote cell adhesion and attachment.

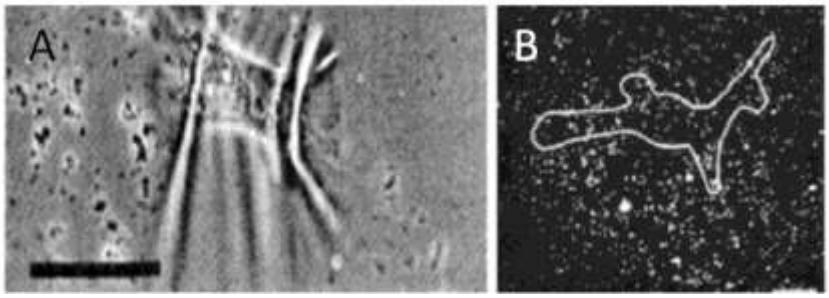


**Figure 2 | Polymer films for cell traction force microscopy. A** Wrinkling patterns produced by chicken heart fibroblasts on silicone rubber sheets. The bar is 50 µm [19]**. B** Fluorescent image of a human airway smooth muscle (HASM) cell cultured on a flexible polyacrylamide gel with embedded fluorescent beads. 20 µm bar .

As the cells exert forces on the sheets, they cause wrinkling patterns which can be visualized under a light microscope. The patterns are compared to those generated by a pulled micropipette which has been calibrated for force. Danowski uses this system to investigate the effects of microtubule inhibitors on fibroblast contractility and actin reorganization [20]. Colcemid, nocodazole and vinblastine are found to increase the contractile state of fibroblasts on the silicone sheets. This is determined by an increase in the size and number of wrinkles in the rubber sheet. The main drawback of this method is that there is not a simple way of converting the wrinkle patterns formed into a traction force map. Inaccuracy in comparing patterns, and hence measures of force, introduces significant error.

### A.2.5 Flexible Sheets with Embedded Beads

A variant of the above method involves embedding either normal latex beads or fluorescently tagged beads in the elastic substratum **Figure 2B**. The positions of the beads are tracked and the displacements over time are recorded. Cellular forces are inferred from the measured displacements. Lee *et al.* use this device to estimate the traction forces exerted by fish keratocytes [21]. They produce vector diagrams by calculating the displaced and undisplaced bead positions with respect to the centroid of a moving cell. They report traction forces ranging from a minimum of 7.5 nN to a maximum of about 20 nN. Pelham and Wang also use raw displacement data as a qualitative map of the local traction, citing the difficulty and computational intensity of deconvolving the displacements to estimate the traction forces [22]. The primary flaw in both of these methods is that neither group was able to account for the interdependence of bead displacement data due to the propagation of deformations throughout the entire sheet surface. This flaw has been addressed by other groups. Dembo *et al.* address this issue using statistical

methods [23]. They estimate traction forces by considering the problem as a superposition of elementary ‘‘delta influences.’’ They then use maximum likelihood statistical methods to find the most probable amplitude and locations of the traction forces. Using this method they report that a typical locomoting keratocyte generates a maximum traction force of ;140 nN. Munevar *et al.* use methods similar to those of Dembo *et al.* to study traction forces generated by normal and H-ras transformed (PAP2) 3T3 fibroblasts to determine the impact of oncogenic transformation on traction forces [24]. They make some modifications to the system to improve spatial resolution and calculation of results. They report significant differences in the spatial distribution of traction forces between the PAP2 cells and the normal ones, with the latter exhibiting a more scattered unstable distribution. The mean traction forces are also significantly different, with the PAP2 cells showing an order of ten reduction in the magnitude of the forces generated. Butler *et al.* use Fourier transform traction cytometry (FTTC) to compute the traction field produced by human airway smooth muscle cells in a bead-embedded flexible substrate [25]. Using this technique, they report a maximum traction magnitude of about 400 Pa. Though such approaches address the critical flaw in the flexible-sheet technique, they do introduce a few disadvantages. Deconvolution of forces from displacement field maps is both a difficult and computationally intensive process. It is also very difficult to obtain precise measurements of discrete forces generated by different parts of a cell.

### A.2.6 Flexible Sheets with Micropatterned Dots or Grids

An improvement to the Butler *et al.* [25] techniques involves imprinting dots on the flexible sheet and observing the deformation of the grid from the ideal grid. Models of deformation can then be applied to the grid and the cellular forces inferred from the deformations produced. Balaban *et al.* use this tool to measure the traction forces exerted by rat cardiac myocytes and endothelial cells [26]. They compute the forces generated at the focal adhesions using elastic theory based on the semiinfinite space. Unfortunately, they have to make the same assumption as in the case for the embedded beads. They assume that the forces originate from the measured locations and do not propagate across the substrate. They solve the inverse problem of computing the tractions given the displacements using least square minimization techniques. Using this method they report maximum traction forces of 20 nN for rat cardiac fibroblast cells and 70 nN for rat cardiac myocytes.

### A.2.7 Micromachined Cantilever Beam

This technique uses traditional micromachining techniques. A horizontal cantilever beam with an attachment pad at the end and a well beneath is used to measure cell traction forces **Figure 2**. Chicken fibroblast cells are seeded on the substrates. Cells are observed crawling over the cantilevers, which have been calibrated for force using pulled glass micropipettes. A measure of cell traction force is obtained from a product of the cantilever deflection and the stiffness obtained from calibration. Galbraith *et al.* use this micromachined device to estimate the traction forces of chicken embryo fibroblast cells [27]. They report forces as high as 100 nN for the tail region of the fibroblast. This device does not have the problem in which strain propagates across the surface and therefore does not require sophisticated computational algorithms to calculate the cellular forces; however, there are some disadvantages. The cantilever beam can only move in one direction, hence forces generated in directions other than the free axis cannot be measured. Also, there is a spatial resolution limitation, and the fabrication technique is quite challenging.

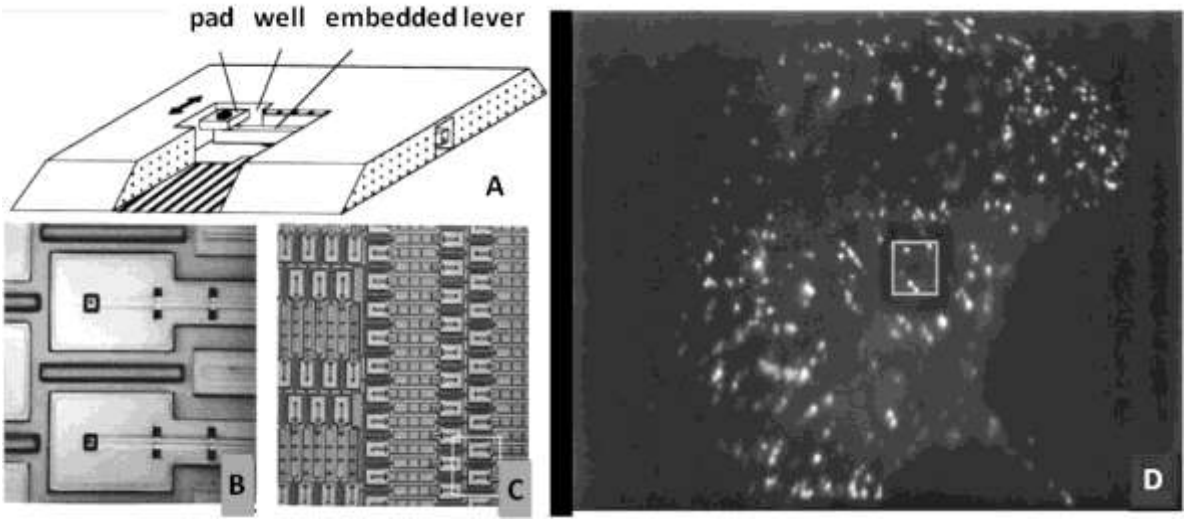


**Figure 2 | Micromachined cantilever beam.** Cantilever beam device and fluorescent image of chicken embryo fibroblasts (CEFs) cell plated on the micromachined substrate [27].

### A.2.8 Array of Vertical Microcantilevers

This technique overcomes the limitations of the horizontal cantilever system by Galbraith *et al.* An array of vertical microcantilevers that have two degrees of freedom is used instead of a single horizontal microcantilever [27]. The individual microcantilevers in the array are usually made of an elastomeric material such as polydimethlysiloxane (PDMS). Tan *et al.* are the first group to report

the use of these arrays to investigate cell traction forces [28]. They use soft lithography techniques to make the microcantilevers of PDMS. The arrays in their device have

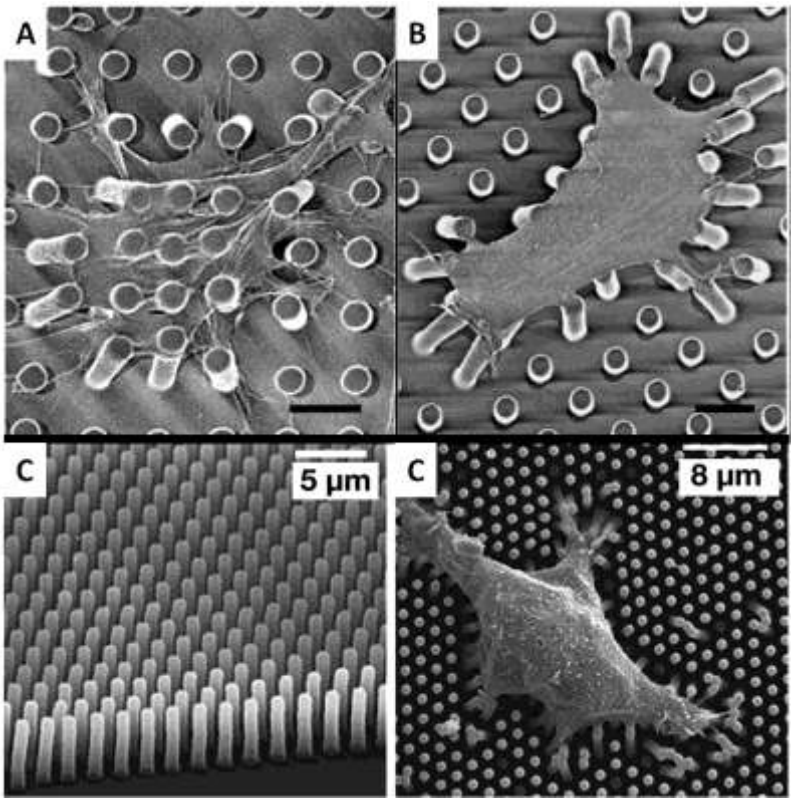


**Figure 3 | Vertical microcantilevers**. **A–B** Scanning electron micrograph (SEM) images of representative smooth muscle cells attached to array of vertical microcantilevers [28]. **C** Scanning electron micrograph of closely spaced array of vertical microcantilevers produced using reactive ion etching techniques, and **D** Individual MDCK cells attached to the array [30].

microcantilevers that are 3 µm in diameter and 11 µm tall and have a center-to center separation of 9 µm. They use this device in combination with micropatterning techniques to investigate the traction forces exerted by spread and unspread bovine pulmonary artery smooth muscle cells (BPASMCs), and show that spread cells exert much greater forces on the microcantilevers than unspread cells. For the spread cells, a maximum force of about 90 nN is recorded. A variation of this technique has been developed by du Roure *et al.*

**Figure 3C-D** [29-30]. They employ photolithographic methods in combination with Deep Reactive Ion Beam Etching (DRIE) to produce master molds in silicon that have much better spatial resolutions and smaller sizes than those produced by Tan *et al.* They also use PDMS as the flexible cantilever material. The improvement in scale and resolution is impressive, but this is a considerably more expensive process than that used by Tan *et al.* Endothelial cells are cultured on the device and allowed to grow to confluence, forming monolayers. They report a maximum traction force of 40

nN exerted by the monolayer at its edge. Individual cells observed on the device generate maximum forces of about 4 nN. Both devices provide a powerful tool, which is used to study microforces of expanding monolayers and single cells as well as investigate the relationship between cell shape, focal adhesion area, and traction forces generated. Petronis *et al.* have also developed cantilever arrays for investigation of mechanical cell-substrate interactions [31]. They fabricate their force-sensitive arrays directly from silicon—a major difference from the two previous methods. They also include attachment pads on their arrays. They employ intermediate lithography steps (masking techniques) to pattern areas with different cantilever heights, thereby generating areas with inherently different mechanical properties. Using a modified design with microcantilevers having a stiffness of 116 nN/µm embedded between rigid ridges, they measure the traction forces exerted by primary human saphenous vein endothelial cells (HSVEC). A range of forces between 7 nN and 40 nN is reported. The main drawback with their technique is that it is not suited to rapid mass-production of the devices through replica casting. Since the arrays and ridges are formed directly in the silicon wafer, any damage to it would require reproduction of the entire device. Our laboratory has focused on using techniques developed by Tan *et al.* and du Roure *et al.* to investigate cellular biomechanics and microforces in vitro. We have been able to produce devices similar to that produced by Tan *et al.* Due to limitations of the contact lithography step for making the original master molds, we were unable to make molds with microcantilever diameters less than 3 µm and spacing less than 8 µm. We improved the lithography technique using contrast enhancement methods and have been able to make microcantilevers with diameters of 2 µm, 7 µm tall, and with spacing of 5 µm, which is close to the theoretical limits for the process [32]. This reduction in feature size is not as impressive as the molds produced using the technique reported by du Roure *et al.* However, unless process parameters are carefully optimized, it appears that DRIE can produce scalloping on the side walls of the silicon master mold, making separation of the PDMS mold very difficult, if not impossible. Based upon our experience, a cryogenic DRIE process may be better suited for fabrication of these devices. Also of concern to us was the difficulty in tracking accurately the displacements of the individual microcantilevers in real time during experiments. The technique of microcontact printing fluorescent proteins that had been reported by Tan *et al.* worked only to a certain degree due to rapid photobleaching and cell interaction with the proteins. We have introduced a technique that improves this by using fluorescent quantum dots instead, which has allowed us to obtain cell force data for both live cells and fixed cells [33]. It has yet to be determined whether these quantum-dot

labels can survive the processing steps of immunohistochemistry, or whether the cells adhere differently to the ends of the labeled microcantilevers. There are still some issues related to the vertical cantilever method that we have yet to address. Neither our study nor those before it address the possibility that the differences between the indices of refraction of the cell, the microcantilevers, and the fluid media will produce refractive artifacts that distort the image and the apparent position of a microcantilever relative to cellular structures. With inverted microscopy, the cells are imaged through the PDMS posts, which when bent might act as tilted cylindrical lenses. With upright microscopy, the posts are viewed through the cell, which may have a curved surface that could act as either a convex or concave lens that might shift the apparent position or size of objects beneath it. It must be noted that other techniques have been used to produce arrays of vertical microcantilevers though not all have been for applications in cellular biomechanics in vitro. McKnight *et al.* have developed a technique where they grow carbon nanofibers, which they use for applications such as DNA delivery to cells as well as for biochemical manipulation [33-34]. These vertical nanofiber arrays could potentially be used to study cellular biomechanics and have the added advantage that they can be used for biochemical manipulation through functionalization of the surfaces [35]. Kim *et al.* also use silicon nanowires as an interface for mammalian cells, though their application has no direct relation to cellular biomechanics [36].

## A.3 Active Measurement Methods

Unlike the passive measurement approaches, the active microrheology estimation methods incorporate some type of force application typically localized at the site of the interrogation. A summary of prominent techniques for active rheology measurement follows.

### A.3.1 Glass Needles

The glass needle method was designed originally for experimentation with neuronal extension and uses a thin glass needle to apply nanonewton or smaller forces. The thin glass rod or needle has been calibrated by a series of precalibrated thin rods, each slightly larger than the previous one. One larger rod is originally calibrated using a known weight, and this rod is used to calibrate a rod slightly smaller than itself. Each rod is then used to calibrate the rod smaller than itself sequentially until the thin glass rod is calibrated [37].

### A.3.2 Cell Poker

The cell poker is a device designed to indent the cell using an oscillating glass needle tip. The cell is suspended from a coverslip on top of the glass needle. The glass needle is attached to a wire needle fastened to a piezoelectric actuator. As the actuator oscillates the glass needle vertically, and the glass needle makes indentations on the cell, the applied force is measured by the difference in displacement between the wire needle and the glass needle. This difference results from the bending of the glass needle, which has been calibrated using a hanging weight, and thus the force resulting in its deformation can be calculated. The cell poker can produce forces less than 10 nN and could also reveal local deformation in different parts of the cell [38-39].

### A.3.3 Atomic Force Microscopy (AFM)

This method involves the use of a sharp tip attached to a flexible cantilever. The tip is used to probe the cell, and the relative deformation of the cell and tip can then be used to estimate the force applied and the stiffness of the cell. Figure 1 shows the setup used by Radmacher *et al.* to investigate the viscoelastic properties of human platelets [40-41]. Weisenhorn *et al.* examine the local deformation of soft surfaces using AFM [42]. Included in the samples examined are metastatic smooth muscle cells from human lungs. They generate force-versus-indentation curves for different cell orientations, with the assumption that the cell is homogenous within all areas tested. They report Young's modulus for the cells between 0.013 and 0.15 MPa. They do report some problems with this technique, however. Deformation of the cell membrane by the tip without any applied force leads to an overestimation of the force-versus indentation curve and subsequently an overestimation of the Young's modulus of the cell. Scanning with too high a force on the tip also leads to cell damage. Hoh *et al.* have employed AFM to investigate the surface morphology and mechanical properties of MDCK cells grown as monolayers [43]. They find that the plasma membrane has an average spring constant of 2 ± 6 mN/m over a deflection range of ~35 nm (2.2 nN). From stiffness curves they report a stiffness of ~35 mN/m at 1 µm depth. Mathur *et al.* use AFM to investigate the viscous and elastic properties of endothelial, cardiac, and skeletal muscle cells. For endothelial cells, they report a variation in elastic modulus across the cell,

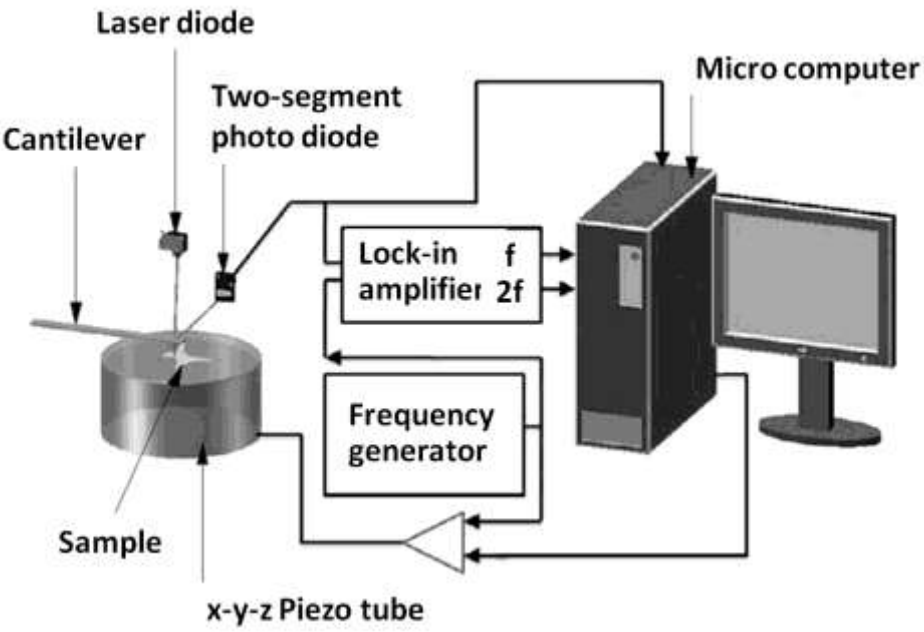


**Figure 4 | Atomic force microscope**. A schematic of an AFM setup, which incorporates optical lever detection and includes electronics for investigating viscoelastic properties of samples [41].

ranging from ~1.4 ± 0.1 kPa near the edge to ~6.8 ± 0.4 kPa over the nucleus. They report no variation in either skeletal or cardiac muscle with an elastic modulus of 100.3 ± 10.7 kPa across cardiac cells and 24.7 ± 3.5 kPa for skeletal muscle. Though AFM has been used to successfully study the mechanical properties of cells, it still has a number of weaknesses. One that is inherent to the technique is the fact that many different tip shapes are used and the shape of the tip determines the nature of the force-deformation curve. This curve is used to deduce the mechanical properties, so any bias introduced by different shapes would be propagated throughout the data analysis steps and might complicate replication of experiments in different laboratories. Also, it is difficult to use commercially available AFMs with scanning electron microscopes (SEMs) to accurately visualize the structural deformation of the cell that occurs when the cell is stretched or indented by the AFM tip, since most SEMs require fixed, desiccated samples, while the AFM can be used on living cells.

### A.3.4 Micropipette Aspiration

In this method, also known as elastimetry, a cell is deformed by applying gentle suction to a micropipette that is placed on the surface of the cell as shown in **Figure 5A**. The geometry of the resulting deformation together with the applied pressure is used to calculate the force applied.

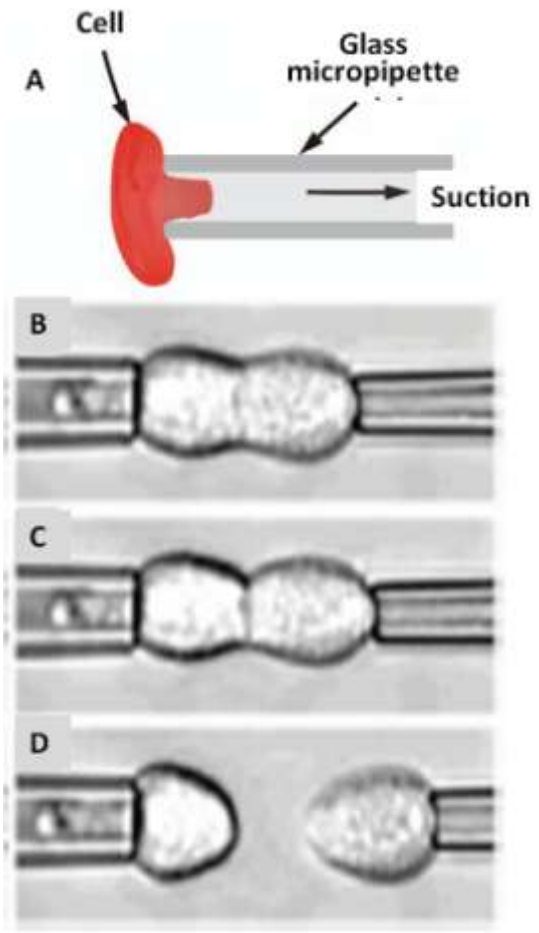


**Figure 5 | Pipettes for measuring cell adhesion forces**. **A** A schematic showing principle of micropipette aspiration. **B–D** Sequence of images showing separation of cells using dual micropipette assay. The change in pressure in the pipetter can be used to infer the force of cell-cell adhesion.

Mechanical properties of cells can then be inferred from this data. Chien *et al.* use this technique to investigate the viscoelastic properties of erythrocyte membranes [44]. They find that deformation occurs in two phases. The initial (rapid) phase exhibits a membrane viscosity in the range of $0.6 \times 10^{-4}$ to $4 \times 10^{-4}$ Pa s. The second (slower) phase shows a high membrane viscosity with a mean value of about $2 \times 10^{-2}$ Pa s. Schmid-Schonbein *et al.* use micropipette aspiration to investigate the mechanical properties of human leukocytes [45]. For rapid motion of the cell into the pipette, they find the shear modulus to be ~506 Pa and for slow motion ~130 Pa. Hiramoto examines the changes in cell surface stiffness during cell cleavage (cytokinesis) in sea urchin eggs [46]. Jones *et al.* examine the alterations of Young's modulus of chondrocytes from normal and osteoarthritic human cartilage [47]. They find no appreciable difference between the Young's modulus of normal chondrocyte cells (0.65 ± 0.63 kPa) and of the osteoarthritic chondrocyte cell (0.67 ± 0.86 kPa). A more recent study was completed by Alexopoulos *et al.* on chondrocyte cells surrounded by a pericellular matrix for both normal and osteoarthritic cartilage [48]. They find that for the normal cells, the Young's modulus is the same for cells isolated from the surface (68.9 ± 18.9 kPa) as that from the middle and deep layers (62 ± 30.5 kPa). However, in osteoarthritic cartilage, the mean Young's modulus significantly decreases from the surface zone (66.5 6 23.3 kPa) to the middle and deep layers (41.3 6 21.1 kPa). They conclude that the pericellular matrix has an important depth-dependent influence on the stress-strain environment of chondrocytes. Chu *et al.* use a dual micropipette assay for a slightly different application—the quantification of the strength of cadherin-dependent cell-cell adhesion **Figure 5B–D** [49]. Doublets of S180 cells stably transfected to express E-cadherin are allowed to adhere to each other with different times of contact. They find that separation force is strongly dependent on the time allowed for contact. A mean force of 20 nN was required to separate cells with a 30 s

contact time and this increased rapidly to ;200 nN after 1 h of contact. They also report a greater separation force (350 versus 200 nN) for preexisting doublets. However, they find that preexisting doublets of S180 cells without E-cadherin have separation forces of only 50 nN.

### A.3.5 Microplate

The microplate method has been developed and used to measure the mechanical properties of surface-adherent cells. In this method, the cell is grown on a rigid microplate coated with fibronectin, and a flexible microplate is placed on top of the cell. The rigid plate is then moved to produce compression, extension, or shear. Measurement of the corresponding deflections in the flexible microplate allows for the accurate measure of the stress imposed on the cell [50]. This method has been used to study fibroblasts and has shown the elastic modulus to be approximately 1 kPa [51-52].

### A.3.6 Shear Flow Methods

Experiments using this method consist of two basic conFiguretions: 1) a cone-and-plate viscometer with a stationary flat plate and a rotating inverted cone which can generate laminar or turbulent flows, or 2) a parallel-plate flow chamber in which cells can be subjected to laminar flow. **Figures 6A**, **6B**, and **6C** show schematics of the two basic conFiguretions. The shear flow chambers can be designed to provide either a constant shear over the entire chamber or a linearly varying shear along the length/width of the chamber. The advantage of the design with linearly varying shear is that it becomes possible to apply different shear stresses between the plates along different sections of the flow chamber without having to change the flow rates or change the dimensions of the chamber. However, in both cases, the shear stress developed on the bottom of the flow chamber is dependent on many factors, including flow rate, viscosity of the fluid, channel width, and channel height. In the case of the linear varying design, two additional variables come into play. First, channel width is a function of the distance from the input port. Also, the total chamber length determines the pressure drop from the entrance to the exit port, hence affecting the amount of shear stress that can be developed. The downstream cells may also be affected by paracrine signals released by upstream cells. Hochmuth *et al.* use a parallel plate flow chamber with a constant shear stress at the surface to estimate the elastic shear modulus of erythrocytes adhered to a glass slide [53]. A least-squares fit to their data gives a shear elastic modulus of 1.31 ± 0.38 Pa. Their other applications of this device involved the investigation of flow effects on cell

metabolism and viability, but were not explicitly used to quantify mechanical response or characteristics. Civelik *et al.* examine rat aortic smooth muscle cell contractility in response to fluid shear stress and look at relationships to the Ca2þ signaling pathway [54]. They use cell area reduction as a metric of contractility. A minimal shear stress of 11 Pa was sufficient to induce contraction. A larger shear stress of 25 Pa caused significant reduction in cell area, due to significant contraction, 3 min after the onset of flow. By 30 min of constant flow, the reduction exceeded 30%. One of their major observations is that this contractile response is Ca2þ-independent. This observation was borne out by the fact that even at 25 Pa of shear stress, there was no activation of Ca2þ signaling pathways, but the cells did mount a normal response when stimulated with Ca2þ-dependent agonists like potassium chloride (KCL) and thapsigarin. Ainslie *et al.* employ the parallel plate shear stress chamber to investigate contractile responses of vascular smooth muscle and the role of glycosaminoglycans (GAGs) on contractility and mechanotransduction [55]. They use a step increase (0 to 25 Pa) in shear, similar to Civelik *et al.*, as well as a ramp increase. The resultant contractility is similar in both cases. Pretreatment with heparinase III or chondroitinase ABC, which remove the GAGs heparin sulfate and chondroitin sulfate, respectively, results in a marked decrease (~20%) in cell contractility under identical shear stress. Other labs have used this shear flow device to investigate cell properties and physiological responses, though not to investigate mechanical properties of cells. Frangos *et al.* use a recirculation-type flow chamber to examine the effects of pulsatile, steady state, and no flow conditions on the production of prostacyclin in cultured human endothelial cells [56]. A minimum shear stress of 10 Pa is enough to elicit a significant increase of prostacyclin. Pulsatile flow, which produces minimum and maximum shear stress of 8 and 12 Pa at a frequency of 1 Hz, results in a 2.2-fold increase in prostacyclin production. One drawback of all the above experiments involving flow chambers is that none have taken into account the inherent curvature of a cell attached to the bottom of the chamber. This means that the shear stress that is actually experienced by the cell will vary from the top of the cell to its attachment on the bottom and cannot be assumed to be the same as the shear stress on the bottom plate of the flow chamber. The shape of the cell, and hence the forces on it, will depend upon the flow rate and the velocity profile of the fluid around the cell. This is evident in the study by Cao *et al.*, who use the setup shown in **Figure 6D** to study cell surface adhesion under flow conditions [57]. Their apparatus is optimized to obtain a side-view of the cell using mirrored side walls and they can visualize the distortion of the cell with

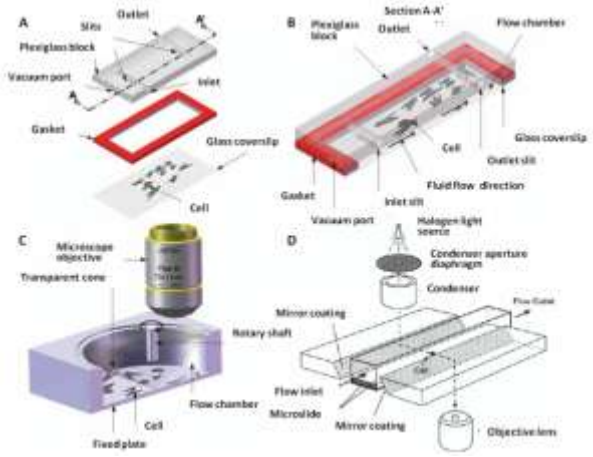

**Figure 6** | **Flow systems for measuring the effect of shear forces on cells. A** Schematic showing exploded view of the parallel plate flow chamber. **B** Schematic showing cut-out view (section A- A') of the parallel plate flow chamber. **C** Schematic showing cut-out view of the cone and-plate flow chamber **D** Schematic of side-view flow chamber used by Cao *et al.* for studying cell-surface adhesion under flow conditions [57].

increased flow rate. One could theoretically use the observed profile of the cell to compute the actual forces delivered to the cell by the flowing stream. An alternative method to reduce the error associated with unknown cell profile in the fluid stream would be to measure the cell thickness profile by using confocal microscopy and deducing the average shear stress experienced by the cell. However, this process would introduce additional sources of error, since confocal microscopy has a vertical resolution that is substantially less than transverse resolution [57-59].

### A.3.7 Optical Trap

A flourishing technique that has recently led to many molecular-scale insights into the cytoskeleton is the optical tweezer or trap **Figure 7**.

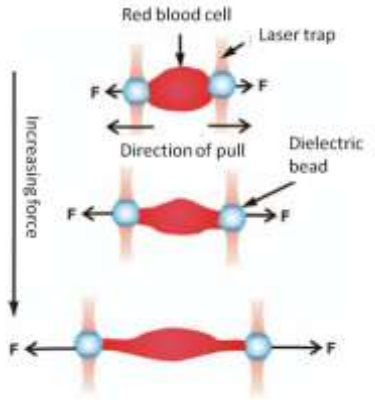


**Figure 7 | Optical trap**. Schematic showing how optical tweezers are used to pull on opposite ends of a cell .

A laser beam passed through a high-aperture objective lens can spatially trap a particle if the scattering force pushing the particle away from the focus point balances the gradient force pulling the particle toward the focus point of the laser [60-62]. To study the microrheology of a cell, one uses a micrometer-sized silica or latex bead as the trapped particle. The trapped particle can be attached to the cell's surface and used to apply local forces on the cell. This method produces forces lower than 100 pN and can be used to measure the cell's linear response [63]. The optical-trap method provides several advantages, including the

ability to measure the mechanical properties of cells not mechanically accessible, the ability to apply forces less than 100 pN, and the detection of strain with time steps as small as 10 ms [64-65]. Newer optical-trap methods have been developed to trap individual cells and thereafter apply stretching forces on them [66-67].Two opposing laser beams trap a cell and then stretch it, recording its strain response. Henon *et al.* use this method to determine the shear modulus of the human erythrocyte membrane inferred from deformations measured as functions of the applied stress and with the assumption that the membrane is incompressible [68]. They find that the membrane shear modulus ranges from 1.7 to 3.3 μN/m with an average value of 2.5 ± 0.4 μN/m. Dao *et al.* also use this tool to examine the mechanics of human erythrocyte deformation, generating forces ten orders of magnitude greater than Henon *et al.* [69]. Using a combination of simulation and experimental methods, they estimate the membrane shear modulus to be 13.3 μN/m. Optical traps were recently used in a clever experimental assay system to measure the rupture force of a complex formed by an ABP (namely, filamin or α-actinin) linking two quasiparallel actin filaments [70]. ABPs regulate the assembly of actin filaments (F-actin) into networks and bundles that provide the structural integrity of the cell. Two ABPs, filamin and α-actinin, have been used extensively to model the mechanical properties of actin networks grown in vitro; however, there is a lack of understanding as to how the molecular interactions between ABPs and F-actin regulate the dynamic properties of the cytoskeleton [70-71].

### A.3.8 Magnetic Tweezers and Magnetic Twisting Cytometry (MTC)

These techniques have been used for many studies on the physical properties of biological tissues. Some of the earliest work was by Crick and Hughes, where they used magnetic particles that had been phagocytosed by chick embryo cells to examine the physical properties of the cell cytoplasm using three experimental modes of movement of the particles: twisting, dragging, and prodding [72]. All of the methods require that beads are first exposed to magnetizing coils, which induce a transient magnetic dipole moment in the beads. A weaker, directional magnetic field or field gradient is then applied to either generate a torque to twist the beads through a specific angle (MTC), or to move the beads linearly as shown in **Figure 8** (magnetic tweezers/magnetic pulling cytometry, Lele *et al.* [73]).

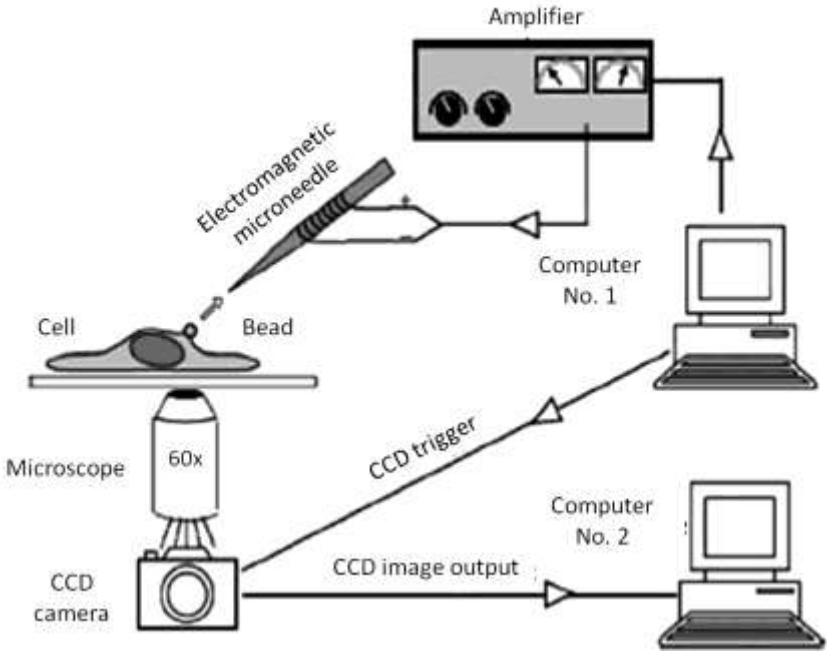


**Figure 8 | Magnetic tweezers**. A schematic of magnetic tweezers setup used by Lele *et al.* to analyze single cell mechanics [73].

In both cases, the torque or force generated is dependent on the strength of the applied magnetic field and/or its gradient as well as on bead properties. Ziemann *et al.* use this technique to measure local viscoelastic moduli of entangled actin networks [74]. Bausch *et al.* use a modification of the Ziemann *et al.* setup to conduct local measurements of viscoelastic parameters of adherent cell surfaces [75]. They are able to bring the magnetic pole piece to within 10–100 µm of the sample and are able to generate forces of 10 nN. Wang *et al.* and Chen *et al.* use another design to investigate cell cytoskeletal mechanics and mechanotransduction [76-77]. The surface of ferromagnetic beads, normally around 0.2 µm in diameter, is coated with specific receptor ligands that promote cell attachment without cell spreading. These beads are then seeded onto the cells where they attach and subsequently a uniform magnetic field in a specific direction is applied to the beads to magnetize them. A twisting coil mounted in tandem with the magnetizing coil is used to generate a weaker magnetic field orthogonal to the initial magnetic field. This induces a twisting moment on the beads, thereby causing portions of the cell to deform. Wang's group uses this to exert controlled shear stresses in the range from 0 to 68 Pa on cell surface receptors. They measure the angular strain as a function of the bead rotation and, for a stress of about 40 Pa, get an angular strain of about 308. There are some disadvantages associated with this system as well. First, it is difficult to control the region of the cell to which the beads bind. If they preferentially

attach at the periphery, or near the nucleus, measurements of the mechanical properties could be biased accordingly. Next, there is no way to ensure complete binding of the beads to the cell surface, which could result in underestimation of cell stiffness. Finally, and perhaps most importantly, the beads lose magnetization with time and must be remagnetized at specific time intervals to maintain the torque applied. Regardless, there is inherent signal degradation over time and, subsequently, experiments lasting longer than one to two hours are not generally feasible with this technique.

### A.3.9 Stretching Devices

Using these methods, cells are cultured on elastic membranes made of flexible silicone sheets whose surfaces can be modified with extracellular matrix (ECM) proteins. The stretching devices can be uniaxial, biaxial, or pressure-controlled. In some of these, the stretch can be applied in a cyclic manner at different frequencies. Wang *et al.* subject endothelial cells to 10% cyclic uniaxial stretch on silicone membranes in the presence or absence of 2,3 butanedione monoxime (BDM), a myosin ATPase inhibitor that is used to block myosin dependent intracellular forces [78]. They show that 40 mM BDM prevents the formation of stress fibers and prevents cells from reorienting themselves in response to the cyclic stretch. Zhuang *et al.* investigate the role of pulsatile stretch on the electrical and mechanical properties of neonatal rat cardiac myocytes [79].

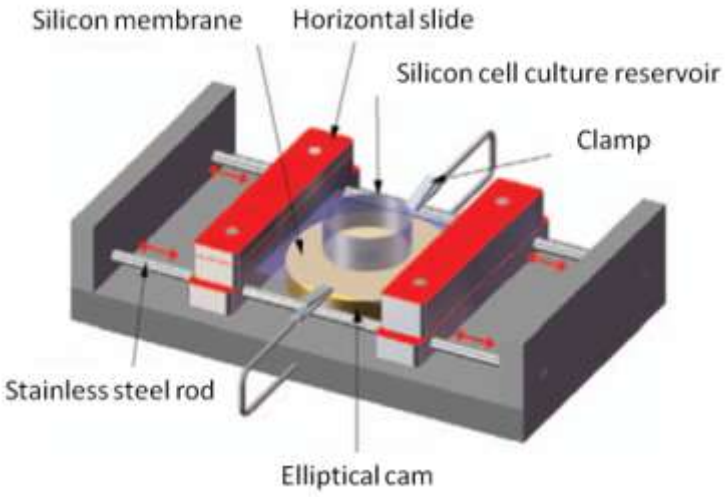


**Figure 9 | Stretching devices**. Schematic of a custom-designed stretching device used by Zhuang *et al.*, which includes a transparent silicone membrane and an elliptical cam whose rotation leads to cyclic stretch of the membrane [79]. The two slide assemblies oscillate horizontally on stainless cylindrical rods (red arrows) and support the transparent silicone membrane, which provides the restoring force to maintain the slides in contact with the cam. The silicone cell reservoir is a segment of silicone tubing glued to the silicone membrane to form the walls of the culture dish. Two clamps produce slight tension along the central axis of the stretch apparatus and thereby reduce transverse shrinking.

**Figure 9** is a schematic of their custom-fabricated stretching apparatus. Included in the device is a silicone membrane which forms part of the culture dish in which the neonatal rat myocytes were seeded and grown. They use the device to examine the effects of pulsatile stretch on some of the characteristics of the transmembrane action potential, as well as its effects on gene expression. They report an increase in N-cadherin expression with increases in the time to which the cells are subjected to pulsatile stretch, but no significant changes in cell area or nuclear size. The methods discussed above all involve the application of active forces either to single cells or a population of cells in culture. One of the main drawbacks with the use of these stretching devices is wrinkling patterns that develop on the sheets and which tend to distort the actual forces that are applied to the sheets. Zhuang *et al.* try to minimize this effect by using clamps on either side of the membrane. Also, as the sheets are continuous, all deformations and displacements are propagated across the entire surface, making calculation of discrete forces and cellular attachment properties very computationally intensive. One point possibly worthy of future investigation is the growth of cells on substrates whose stiffness is more closely matched to that encountered by the cell in vivo, rather than on ones that are so stiff that the cell-generated reaction forces will be vastly smaller than the forces used to stretch the macroscopic, underlying silicone substrate. In a situation with better mechanical matching, it might be possible to observe how a cell remodels itself or proliferates in a manner to reduce or redistribute the externally applied forces. In a stiff system, the cells can remodel, but the external forces may always dominate.

### A.3.10 Carbon Fiber (CF)-based Systems

This method involves the use of carbon fibers, which are normally mounted in glass capillaries and attached to precise position control devices with feedback control mechanisms. The carbon fibers are attached to cells and used as a means to both apply active forces and record forces generated by the cell. The image of the carbon fibers is projected through optics onto a photodiode array which converts this into a usable signal for the feedback control system. The optical system is also connected to an image recording system and can be used to capture and record changes in length of the cell **Figure 10A**. Though this technique could potentially be used for many cell types, it has recently been used to study single cardiac myocytes, which are orders of magnitude shorter than skeletal muscle fibers and correspondingly harder to study. Yasuda *et al.* use this setup to investigate the mechanics of single rat cardiac myocytes under isometric and physiologically loaded conditions [80]. They also investigate the effects of inotropic intervention on myocyte force

generation. They report problems with carbon fiber compliance and indicate that it is quite difficult to produce virtually isometric conditions.

They plot force length relationships and extract workload data. Work output has a maximum value at an intermediate auxotonic load, and falls off above and below this optimal value. Nishimura *et al.* make modifications and improvements to the feedback control system used by Yasuda *et al.* and use it to also investigate rat cardiac myocyte mechanics under isometric, unloaded, and physiologically loaded conditions [81]. Some of the limitations they report include damage to the cells during attachment of the fibers, inaccuracy in measuring sarcomere length due to focus issues, and possible bias introduced into the data by avoiding cells that were too irritable to obtain stable recordings. Iribe *et al.* make further modifications to this setup by introducing the use of bidirectional control [82] instead of the single-sided control used by Yasuda *et al.* and Nishimura *et al.*, which reduced sarcomere blurring [80-81]. They investigate the effects of independently varying preload and after load, as well as modes of contraction on the force length relationships of guinea pig ventricular cardiomyocytes. Some of their reported findings include the fact that the end systolic force-length relation is virtually independent of load at sarcomere lengths of 1.85 to 2.05 µm. It is important to recognize that this approach provides true, closed-loop mechanical control of a single cell, in which the compliance of the measurement system can be controlled independently of its displacement, thereby allowing exploration of cellular mechanics over the full range of forces, displacements, and velocities that are required to fully specify the parameters for an active, viscoelastic model of cellular mechanics.

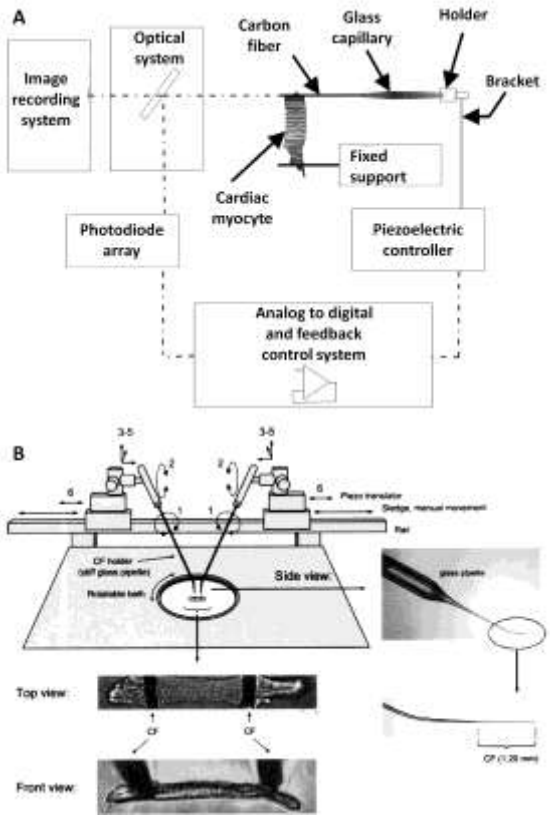


**Figure 10 | Active control of pairs of carbon fibers for studies of cardiomyocyte mechanics**. **A** Schematic showing the general principle of operation of the carbon fiber system used by Yasuda *et al.* [80] **B** Experimental setup and images of carbon fibers attached to individual cardiac myocytes [82].

## References


[1] Addas *et al.* "Microrheology of solutions of semiflexible biopolymer filaments using laser tweezers interferometry". *Phys. Rev. E* 70, 021503 1-16, **2004**.

[2] Lau, A.W.C. *et al.* "Microrheology, stress fluctuations, and active behavior of living cells". *Phys. Rev. Lett*. 91, 198101 1-4, **2003**.

[3] MacKintosh, F.C. and Schimdt, C.F. "Microrheology". *Curr. Opin. Coll. Int. Sci*., 4, 300-307, **1999**.

[4] Mason, T.G. *et al.* "Particle-tracking microrheology of complex fluids". *Phys. Rev. Lett.*, 79, 3282–3285, 1997.

[5] Schmidt, F.G. *et al.* "Viscoelastic properties of semiflexible filamentous bacteriophage fd". *Phys. Rev.* E, 62, 5509–5517, **2000**.

[6] Schnurr, B *et al.* "Determining microscopic viscoelasticity in flexible and semiflexible polymer networks from thermal fluctuations". *Macromolecules* 30, 7781–92, **1997.**

[7] Yap, B. and Kamm, R.D. "Mechanical deformation of neutrophils into narrow channels induces pseudopod projection and changes in biomechanical properties". *J. Appl. Physiol*. 98, 1930–39, **2005**.

[8] Crocker, J.C. and Grier, D.G. "Methods of digital video microscopy for colloidal studies". *J. Colloid Interface Sci*., 179, 298–310, **1996**.

[9] Denk, W. and Webb, W.W. 1990. "Optical measurement of picometer displacements of transparent microscopic objects". *Appl. Opt*. 29, 2382–91, **1990**.

[10] Gittes, F. and Schmidt, C.F. "Interference model for back-focal-plane displacement detection in optical tweezers". *Opt. Lett*. 23, 7–9, **1998**.

[11] Pralle, A. *et al.* "Three-dimensional high-resolution particle tracking for optical tweezers by forward scattered light". *Microsc. Res. Tech*. 44, 378–86, **1999**.

[12] Crocker, J.C. *et al.* "Two-point microrheology of inhomogeneous soft materials". *Phys. Rev. Lett*. 85, 888–91, **2000**.

[13] Levine, A.J. and Lubensky, T.C. "One- and two-particle microrheology". *Phys. Rev. Lett*. 85, 1774–77, **2000**.

[14] Jonas, M. *et al.* "Fast fluorescence laser tracking microrheometry. I: Instrument development". *Biophys. J*. 94:1459–69, **2008**.

[15] Jonas, M. *et al.* "Fast fluorescence laser tracking microrheometry. II: Quantitative studies of cytoskeletal mechanotransduction". *Biophys. J*. 95:895–909, **2008**.

[16] Berne, B.J. and Pecora, R. "Dynamic Light Scattering. Malabar", *FL: Robert E. Krieger*, **1990**.

[17] Hess, S.T. *et al.* "Biological and chemical applications of fluorescence correlation spectroscopy: a review". *Biochemistry* 41, 697–705, **2002**.

[18] Webb, W.W. "Fluorescence correlation spectroscopy: inception, biophysical experimentations, and prospectus". *Appl. Opt*. 40, 3969–83, **2001**.

[19] Harris, A.K. *et al.* "Silicone rubber substrata: a new wrinkle in the study of cell locomotion". *Science* 208, 177–179, **1980**.

[20] Danowski, B.A. "Fibroblast contractility and actin organization are stimulated by microtubule inhibitors". *J. Cell. Sci*. 93, 255–266, **1989**.

[21] Lee J. *et al.* "Traction forces generated by locomoting keratocytes". *J. Cell Biol*. 127, 1957–1964, **1994**.

[22] Pelham, R.J. Jr. and Wang, Y.L. "Cell locomotion and focal adhesions are regulated by substrate flexibility". *Proc Natl Acad Sci* 94, 13661–13665, **1997**.

[23] Dembo, M. and Wang, Y.L. "Stresses at the cell-to-substrate interface during locomotion of fibroblasts". *Biophys. J.* 76, 2307–2316, **1999**.

[24] Munevar S, Wang YL, Dembo M. Traction force microscopy of migrating normal and H-ras transformed 3T3 fibroblasts. *Biophys. J.* 80, 1744–1757, **2001**.

[25] Butler, J.P. *et al.* "Traction fields, moments, and strain energy that cells exert on their surroundings". *Am. J. Physiol. Cell. Physiol.* 282, C595–C605, **2002**.

[26] Balaban N.Q. *et al.* "Force and focal adhesion assembly: a close relationship studied using elastic micropatterned substrates". *Nature Cell Biol*. 3, 466–472, **2001**.

[27] Galbraith, C.G. and Sheetz, M.P. “A micromachined device provides a new bend on fibroblast tractional forces”. *Proc. Natl. Acad. Sci.* 94,9114–9118, **1997**.
[28] Tan, J.L. *et al.* “Cells lying on a bed of microneedles: an approach to isolate mechanical force”. *Proc. Natl. Acad. Sci*. 100, 1484–1489, **2003**.
[29] Roure, O.D. *et al.* “Microfabricated arrays of elastomeric posts to study cellular mechanics”. *Proc SPIE* 5345, 26–34, **2004**.
[30] du Roure, O. *et al.* “Force mapping in epithelial cell migration”. *Proc. Natl. Acad. Sci.* 102, 2390–2395, **2005**.
[31] Petronis, S. *et al.* “Microfabricated force-sensitive elastic substrates for investigation of mechanical cell-substrate interactions”. *J. Micromech. Microeng*. 13, 900–913, **2003**.
[32] Addae-Mensah K,A. *et al.* “A flexible, quantum dot-labeled cantilever post array for studying cellular microforces”. *Sensor Actuat. A-Phys*. 136, 385–397, **2007**.
[33] McKnight, T.E. *et al.* “Intracellular integration of synthetic nanostructures with viable cells for controlled biochemical manipulation”. *Nanotechnology* 14, 551–556, **2003**.
[34] McKnight, T.E. *et al.* “Tracking gene expression after DNA delivery using spatially indexed nanofiber arrays”. *Nano. Lett*. 4, 1213–1219, **2004**.
[35] Fletcher, B.L. *et al.* “Biochemical functionalization of vertically aligned carbon nanofibres”. Nanotech. 17, 2032–2039, **2006**.
[36] Kim W, Ng JK, Kunitake ME, Conklin BR, Yang P. Interfacing silicon nanowires with mammalian cells. J Am Chem Soc 129:7228–7229, **2007**.
[37] Heidemann, S.R. *et al.* “Direct observations of the mechanical behaviors of the cytoskeleton in living fibroblasts”. *J. Cell. Biol*. 145, 109–22, **1999**.
[38] Daily, B. *et al.* “Cell poking: determination of the elastic area compressibility modulus of the erythrocyte membrane”. *Biophys. J*. 45, 671–82, **1984**.
[39] Janmey, P. and Schmidt, C. “Experimental measurements of intracellular mechanics”. See Mofrad & Kamm 2006, pp. 18–49, **2006**.
[40] Radmacher, M. *et al.* “Measuring the viscoelastic properties of human platelets with the atomic force microscope”. *Biophys. J*. 70, 556–567, **1996**.
[41] Radmacher, M. *et al.* “Imaging viscoelasticity by force modulation with the atomic force microscope”. *Biophys. J*. 64, 735–742, **1993**.
[42] Weisenhorn, A.L. *et al.* “Deformation and height anomaly of soft surfaces studied with an AFM”. *Nanotechnology* 4, 106–113, **1993**.
[43] Hoh, J.H. and Schoenenberger, C.A. “Surface morphology and mechanical properties of MDCK monolayers by atomic force microscopy”. *J. Cell. Sci*. 107, 1105–1114, **1994**.
[44] Chien, S. *et al.* “Theoretical and experimental studies on viscoelastic properties of erythrocyte membrane”. *Biophys. J*. 24:463–487, **1978**.
[45] Schmid-Schonbein, G.W. *et al.* “Passive mechanical properties of human leukocytes”. *Biophys. J*. 36, 243–256, **1981**.
[46] Hiramoto Y. “Methods in cell biology”. In: Schroeder TE, Ed. Echinoderm Gametes and Embryos. *New York: Academic Press, Inc*. 435–442, **1986**.
[47] Jones, W.R. *et al.* “Alterations in the Young’s modulus and volumetric properties of chondrocytes isolated from normal and osteoarthritic human cartilage”. *J Biomech*. 32, 119–127, **1999**.
[48] Alexopoulos, L.G. *et al.* “Alterations in the mechanical properties of the human chondrocyte pericellular matrix with osteoarthritis”. *J. Biomech. Eng*. 125, 323–333, **2003**.
[49] Chu Y.S. *et al.* “Force measurements in E-cadherin-mediated cell doublets reveal rapid adhesion strengthened by actin cytoskeleton remodeling through Rac and Cdc42”. *J. Cel.l Biol*. 167, 1183–1194, **2004**.
[50] Thoumine, O. *et al.* “Microplates: a new tool for manipulation and mechanical perturbation of individual cells”. *J. Biochem. Biophys. Methods* 39, 47–62, **1999**.
[51] Caille, N. *et al.* “Contribution of the nucleus to the mechanical properties of endothelial cells”. *J. Biomech.* 35, 177–87, **2002**.
[52] Thoumine , O. *et al.* “Time scale dependent viscoelastic and contractile regimes in fibroblasts probed by microplate manipulation”. *J. Cell. Sci.* 110, 2109–16, **1997**.

[53] Hochmuth, R.M. *et al.* "Measurement of the elastic modulus for red cell membrane using a fluid mechanical technique". *Biophys. J*. 13, 747–762, **1973**.
[54] Civelek, M. *et al.* "Smooth muscle cells contract in response to fluid flow via a Ca2þ-independent signaling mechanism". *J. Appl. Physiol*. 93, 1907–1917, **2002**.
[55] Ainslie, K.M. *et al.* "Vascular smooth muscle cell glycocalyx influences shear stress-mediated contractile response". *J. Appl. Physiol.* 98, 242–249, **2005**.
[56] Frangos J.A. *et al.* "Flow effects on prostacyclin production by cultured human endothelial cells". *Science* 227, 1477–1479, **1985**.
[57] Cao, J. *et al.* "Development of a side-view chamber for studying cell-surface adhesion under flow conditions". *Ann. of Biomed. Eng.* 25, 573–580, **1997**.
[58] Dong, C. *et al.* "Mechanics of leukocyte deformation and adhesion to endothelium in shear flow". *Ann. Biomed. Eng.* 27:298–312, **1999**.
[59] Leyton-Mange, J. *et al.* "Design of a side-view particle imaging velocimetry flow system for cell-substrate adhesion studies". *J. Biomech. Eng.-Trans*. ASME 128, 271–278, **2006**.
[60] Ashkin A. "Optical trapping and manipulation of neutral particles using lasers". *Proc. Natl. Acad. Sci.* USA 94, 4853–60, **1997**.
[61] Lang, M.J. *et al.* "Combined optical trapping and single-molecule fluorescence". *J. Biol*. 2, 6, **2003**.
[62] Svoboda, K. and Block, S.M. "Biological applications of optical forces". *Annu. Rev. Biophys. Biomol. Struct*. 247–85, **1994**.
[63] Peterman, E.J.G. *et al. "*Extending the bandwidth of optical-tweezers interferometry". *Rev. Sci. Instrum.* 74, 3246–49, 2003.
[64] Gittes, F. and Schmidt, C.F. "Interference model for back-focal-plane displacement detection in optical tweezers". *Opt. Lett*. 23, 7–9, **1999**.
[65] Pralle, A. *et al.* "Three-dimensional high-resolution particle tracking for optical tweezers by forward scattered light". *Microsc. Res. Tech*. 44, 378–86, **1999**.
[66] Guck, J. *et al.* "Optical deformability of soft biological dielectrics". *Phys. Rev. Lett*. 84, 5451–54, **2000**.
[67] Guck, J. *et al.* "The optical stretcher: a novel laser tool to micromanipulate cells". *Biophys. J*. 81, 767–84, **2001**.
[68] Henon, S. *et al.* "A new determination of the shear modulus of the human erythrocyte membrane using optical tweezers". *Biophys. J*. 76, 1145–1151, **1999**.
[69] Dao, M. *et al.* "Mechanics of the human red blood cell deformed by optical tweezers". *J. Mech. Phys. Solids* 51, 2259–2280, **2003** and *J. Mech. Phys. Solids* 53, 493–494, **2005**.
[70] Ferrer, J.M. *et al.* "Measuring molecular rupture forces between single actin filaments and actin-binding proteins". *Proc. Natl. Acad. Sci*. USA 105, 9221–26, **2008**.
[71] Kolahi, K.S. and Mofrad, M.R.K. "Molecular mechanics of filamin rod domain". *Biophys. J*. 94, 1075–83, **2008**.
[72] Crick, F.H.C. *et al.* "The physical properties of cytoplasm: a study by means of the magnetic particle method Part I. Experimental". *Exp. Cell. Res*. 1, 37–80, **1950**.
[73] Lele, T.P. *et al.* "Methods in cell biology". In: Wang Y-L, Discher DE, Eds. *Cell Mechanics*. New York: Academic Press, 443–472, **2007**.
[74] Ziemann, F. *et al.* "Local measurements of viscoelastic moduli of entangled actin networks using an oscillating magnetic bead micro-rheometer". *Biophys. J*. 66, 2210–2216, **1994**.
[75] Bausch, A.R. *et al.* "Measurement of local viscoelasticity and forces in living cells by magnetic tweezers". *Biophys. J*. 76, 573–579, **1999**.
[76] Wang, N. *et al.* "Mechanotransduction across the cell surface and through the cytoskeleton". *Science* 260, 1124–1127, **1993**.
[77] Chen, J. *et al.* "Twisting integrin receptors increases endothelin-1 gene expression in endothelial cells". *Am. J. Physiol. Cell Physiol*. 280, C1475–C1484, **2001**.
[78] Wang, J.H.C. *et al.* "Contractility affects stress fiber remodeling and reorientation of endothelial cells subjected to cyclic mechanical stretching". *Ann. Biomed. Eng*. 28, 1165–1171, **2000**.
[79] Zhuang, J.P. *et al.* "Pulsatile stretch remodels cell-to-cell communication in cultured myocytes". *Circ. Res*. 87, 316–322, **2000**.

[80] Yasuda, Si *et al.* "A novel method to study contraction characteristics of a single cardiac myocyte using carbon fibers". *Am. J. Physiol. Heart Circ. Physiol*. 281, H1442–H1446, **2001**.
[81] Nishimura, S. *et al.* "Single cell mechanics of rat cardiomyocytes under isometric, unloaded, and physiologically loaded conditions". *Am. J. Physiol. Heart Circ. Physiol*. 287, H196–H202, **2004**.
[82] Iribe, G. *et al.* "Force-length relations in isolated intact cardiomyocytes subjected to dynamic changes in mechanical load". *Am. J. Physiol. Heart Circ. Physiol*. 292, H1487–H1497, **2007**.

# Appendix B

# Analytical-Computational Models for Cell Mechanics

## B.1 Introduction

In this appendix, we provide an overview of the experimental tools and associated analytical/computational approaches and that are currently used in understanding various aspects of cell and biomolecular mechanics.

## B.2 Mechanical Models for Living Cells

If tissue level continuum mechanics has a consolidate basis [1], it's not valid the same consideration for single cell mechanics, though the mechanical properties of individual cells determine the structural integrity of whole tissues.

They have been developed various computational models, each of which tries to describe the behavior of cells or subcellular components, that utilize material laws depending on the experimental conditions, such as the level and rate of loading, as well as the cell type.

We offer an overview of the mechanical models developed in the last decades by various researchers. Two computational models macro-areas can be identified: (i) the continuum-based models area [2-3] and (ii) the micro/nanostructural models area [3]. The underlying assumption for treating a material as a continuum is that the smallest dimension to be considered is much larger that the space over which structures and properties vary significantly. Continuum-based computational models have been developed in order to interpret the overall mechanical response of individual cells measured through experimental techniques. When the length scale of interest is comparable to the structural features of the system under study, micro-scale approaches such as atomistic and molecular simulation or network theories have to be studied. In particular, micro/nanostructural models intend to define specific molecular pathways for mechanical force transmission and sensation and identify with the cytoskeleton, an organized structural system

consisting of actin filaments, intermediate filaments and microtubules, the mechanical regulatory machine. In effect, it's well known that the mechanical properties of the cytoskeleton (CSK) are a key determinant not only for cell shape, but also for other cellular functions, including spreading, crawling, polarity and cytokinesis. In particular, the CSK has been considered the main component in the control of the mechanical properties and functions of adherent cells. So, in order to quantify cell elasticity and cytoskeletal changes and utilize this information as key element by which detecting the presence and the progression of certain pathologies, such as cancer, detailed data on cytoskeletal composition and architecture are necessary. For suspended cells, the microscopic spectrin-network model was developed to investigate the contribution of the cell membrane and spectrin network to the large deformation of red blood cells.

It would be to be hoped have the availability of a model able to capture the response of living systems , traversing the different length scales involved in biomechanics, from tissues or organs level to molecular level **Figure 1**.

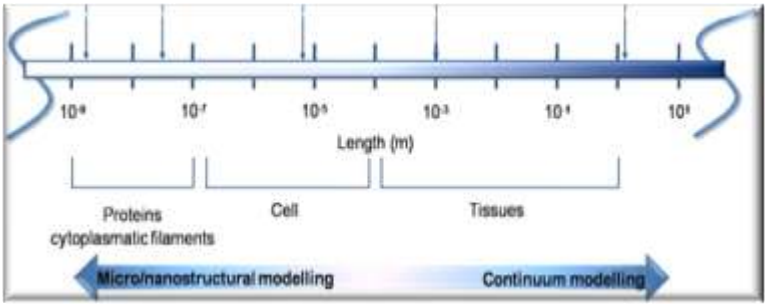


**Figure 1 | Length scales in biomechanics**

Then, so as to investigate the way in which stress and strains induced on the cell are transmitted to the cytoskeletal and subcellular components, multi-scale models have been elaborated. Separate computations at different scales are performed and then coupled to perform a comprehensive characterization **Figure 2** .

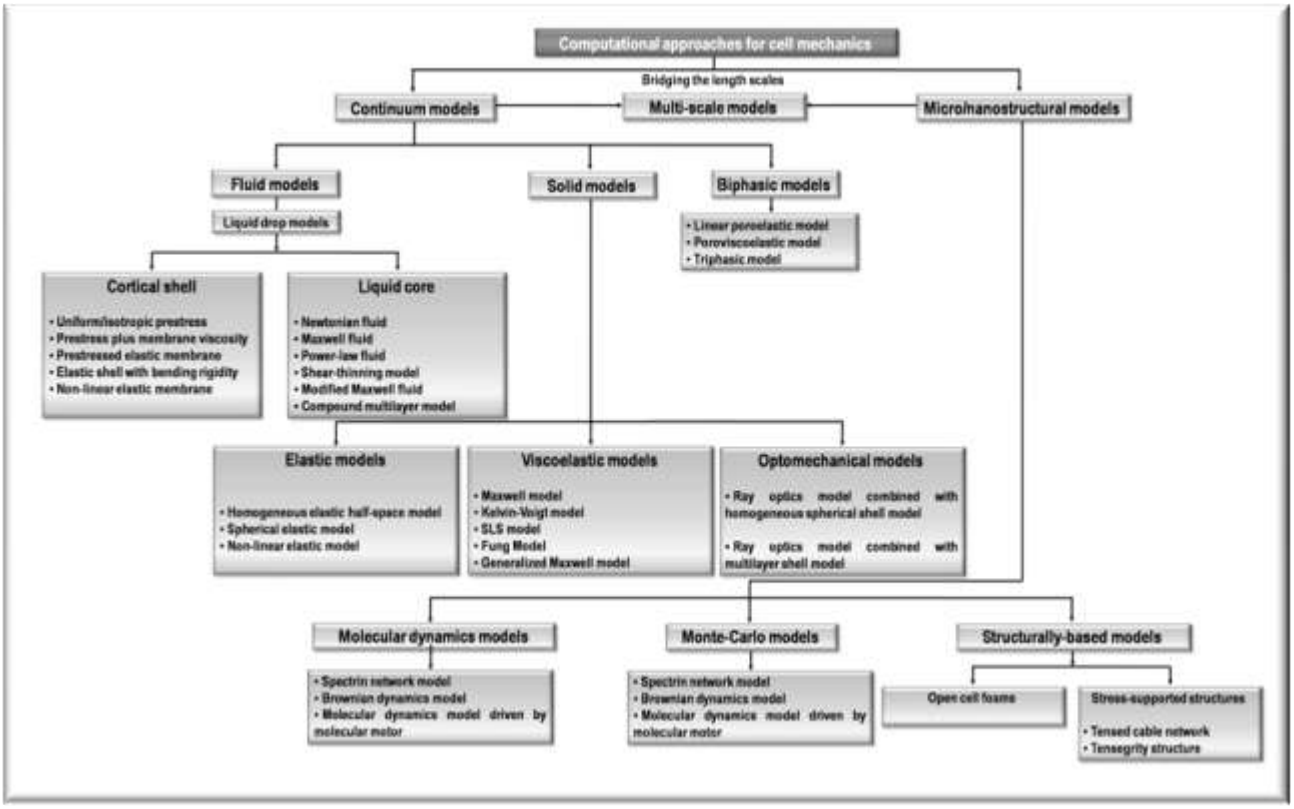


**Figure 2 |Computational approaches for cell mechanics**

### B.3 Continuum Mechanical Models

In the area of continuum-based models, it's necessary to distinguish between three main modeling approaches, depending on the physical behavior of the individual cell: fluid models, in which the foremost component is a viscous or viscoelastic fluid surrounded by the cell membrane, that sustains a cortical tension (liquid drop models); solid models, that consider the cell as an elastic or viscoelastic homogeneous solid continuum; and biphasic models, whose aim is to describe accurately the deformation behavior of chondrocytes in cartilage.

#### B.3.1 Fluid Models

Fluid models are able to exemplify the deformability of cells of the circulatory system, essential to explain blood flow. Mostly, liquid drop models have been utilized to describe liquid-like response of many nonadherent cells when aspirated into small micropipettes. The pioneers of a method to study the passive flow of liquid-like cells into micropipettes were Young and Evans, that modeled the cell plainly as a spherical uniform Newtonian liquid core, with an average viscosity,

surrounded by an anisotropic viscous cortical shell with a persistent lateral tension [4]. Tsai *et al.* tried that the neutrophil cytoplasm exhibits a non-Newtonian behavior, with a decreasing viscosity while the mean shear rate increases. This behavior has been characterized as that of a power-law fluid, returning results in excellent agreement with the measurements obtained by magnetic probes inside the living cells [5]. Considering the naught of Newtonian liquid drop models in accounting for the effects of pressure exercised on neutrophils by aspiration and pipette size on the aspiration rate, and the fading memory of the elastic response, different other model have been proposed: in such cases the cytoplasm has been modeled has a Maxwell fluid and the cortex as an elastic membrane with a non-linear stress-strain response. Instead, Drury and Micah for the first time incorporated in their model both shear thinning of the cytoplasm and surface viscosity, finding a surface viscosity and an interior viscosity that decrease in a similar fashion when the shear rate increases [6]. However, in all these model it's been assumed that the cell interior can be modeled as a uniform liquid, but the elastic recoil followed by slow recovery upon expulsion of leukocyte deformation suggested a dual-time response, that can be explained considering the multilayer internal structure of the leukocyte: the outermost elastic cortex, that determines the elastic response, the intermediate cytoplasm, to which the rapid recovery can be attributed and the innermost stiff nucleus, that determines the slower recovery phase. Kan *et al.* studied the rheological behavior of leukocytes and lymphocyte, using a three-layer incompressible Newtonian fluid system and investigated the effects of nucleus size and eccentricity [7]. Marella and Udaykumar tried to analyze the recovery and deformation response of leukocyte, considering the predominant structural component in a three-layer compound model: the cortical membrane has been modeled as a nonlinear elastic membrane; a compound cell model has been used to consider the stiff nucleus and a shear-thinning model has been assumed for the cytoplasmic viscosity [8]. More recently, basing on the Newtonian and viscoelastic drop model, Zhou *et al.* have explored the deformation and transit of neutrophils form a larger vessel into a narrow capillary, finding results fitting the experimental observations: the entrance time decreases with the pressure drop, increases with the cell viscosity and decreases with the relaxation time of the viscoelastic cytoplasm [9].

### B.3.2 Solid Models

Solid models characterize the mechanical properties of chondrocytes, bone cells, fibroblasts and endothelial cells. Theret *et al.* developed an infinite homogeneous half-space model, that assumes the cell as a homogenous, incompressible elastic half space. The main results are the effective Young's modulus for the endothelial cells, extrapolated by micropipette experiments and depending on the applied pressure difference, a function that defines the boundary condition between the cell and the micropipette [10]. Even if this model neglects the dependence on the loading rate and loading history and represents a rough approximation to the mechanical behavior of a substrate–attached cell, that is finite, nonhomogeneous and with a complicated morphology, it has been utilized both as a basis for viscoelastic models, and to investigate the factors that can modify the cell mechanical properties, such as the effect of cellular cholesterol on the increase of membrane stiffness of bovine aortic endothelial cells [11]. Haider and Guilak have modeled the cell as an incompressible elastic continuum, homogeneous and isotropic and spherical at its initial state. Unlike the halfspace model, the spherical cell model includes effect of nonlinearity in the cell response, due to the finite cell dimension, curvature of the cell boundary, evolution of the cell-micropipette contact region and curvature of the edges of the micropipette, employing a direct boundary integral equation method. The numerical computation has posed the basis for more complex modeling descriptions of the cell (more complex geometries, nonlinear constitutive behavior, inhomogeneities in cellular properties) [12]. As early said, the mechanics of cells in inadequately described by a linear elastic model, but is necessary to account for the viscoelastic behavior. Schmid-Schönbein *et al.* analyzed for the first time the time-dependent deformation of the neutrophil for small strains, considering this cell to be a solid homogeneous viscoelastic body and using a standard linear solid (SLS) model [13]. This rheological model is known to offer a realistic behavior of materials over the whole frequency range from creep and stress relaxation to dynamic modulus, dynamic loss factor, rate effects and impact loading, in contrast to the simpler Kelvin and Maxwell models. The linear half-space model and SLS model have been also used by Koey *et al.* to understand the mechanical behavior of anchorage-dependent cells, such as human articular chondrocytes, and mechanotransductional pathways [14]. Baush *et al.*, pondering the importance of viscoelasticity in the regulation of the cell shape of resting and moving cells, have designed a magnetic bead microrheometer and applied tangential force pulses on the magnetic beads fixed to the integrin receptors of the cell membrane, extrapolating creep response and relaxation curves. A three-phasic response has been observed and analyzed in terms of a generalized

Maxwell model, constituted by a series arrangement of a dashpot and a Voigt body. The viscoelastic behavior of the adhering cell surface has been characterized by three parameters: an effective elastic constant, a relaxation time and a viscosity [15-16]. The same mechanical equivalent circuit has been adopted to probe the association of distinct families of membrane receptors, such as the integrins, functionalizing the magnetic beads with macromolecules of extracellular matrix [17]. Among the other proposed viscoelastic models, the Fung model, composed by a combination of two ideal spring and two dashpot in parallel, has been used to give a description of viscoelastic parameters of the cytoplasm (shear elastic modulus, the effective viscosities and the strain relaxation time), when mechanical stress are generated by rotation of magnetic chains under the influence of rotating external magnetic fields [18]. Peeters *et al.* for the first time have quantified the global viscoelastic properties of adherent cells over a wide range of axial strains (~10-40%), performing a series of dynamic experiments over two frequency decades (0.1-10 Hz). They have utilized a non linear viscoelastic model to fit the experimentally obtained force-deformation curves, reflecting the viscoelastic behavior of cells, such as would be in vivo [19]. Although more realistic models have been derived via the basic Maxwell and Kelvin-Voigt elements, in a more recent work a simple viscoelastic Maxwell model has been utilized for simulating and predicting the development and remodeling of biological systems. The authors have performed a numerical analysis, in which cytoskeleton and membrane/actin cortex are modeled as an incompressible, homogeneous isotropic viscoelastic body, while blood is treated as a Newtonian fluid. The finite element model includes also contact elements with a Neo-Hookean behavior, representing the regions of focal adhesion matrix ligands and integrin receptors bonds, whose dynamics is described by the Kramers reaction-rate theory [20].

In the context of continuous models, opto-mechanical models have been performed to fit experimental measurements obtained by optical tweezers, a laser device used to deform living cells. Guck *et al.* have developed an hybrid model, that considers the net optical force transferred to the surface of cell. The interaction of light with cells is described by Ray Optics (RO), that decomposes the incident laser beam into individual rays with appropriate intensity, momentum and direction, that propagate in a straight line in uniform, nondispersive media. In this work, the only component of erythrocytes is a thin composite shell, made of the plasma membrane, the 2-dimensional cytoskeleton and the glycocalix: an hypothesis of homogeneous spherical shell is made and membrane theory, in which only stretching energy is considered, while bending energy is neglected, is used [21]. More recently, Xu *et al.* have proposed a rigorous solution, Generalized

Lorenz-Mie theory (GLMT), and a simplified theory, based on geometrical considerations (Geometric Optics), to describe the real stress distribution on a homogeneous sphere. It's to be hoped that GLMT theory is transferred in cell elasticity measurements [22]. Ekpenyong *et al.* have extended the RO theory to consider the effects of multiple internal reflections, using a cosine-squared approximate function. This model has been utilized instead of RO theory, basing on either major- or minor-axis deformation measurements, providing Red blood cells consistent with literature values [23].

### B.3.3 Biphasic Models

As well known, cartilage supports primarily load imposed on it by hydrostatic pressure of the fluid in the composite material, rather than by elastic recoil of the solid matrix material. Cartilage mechanics has been extensively explained by biphasic and triphasic models. In the first case, the solid matrix is considered, whereas the interstitial fluid is treated as incompressible and inviscid. Triphasic model identifies three main components in cartilage: (1) a solid phase of collagen and proteoglycan extracellular matrix; (2) the interstitial water; and (3) the Na+ and Cl- ions of NaCl and utilizes the general equations of mass transport in a structure consisting of a solid immobile matrix and a fluid mixture phase presented in terms of chemical potential [1]. Even so, little is known about the mechanisms of mechanotransduction in chondrocytes. Several attempts have been made to clarify the role of chondrocytes in cartilage and the extension of biphasic theory from cartilaginous tissue scale to microscopic cell level has been considered the best way to describe the deformation behavior of chondrocytes. Shin and Athanasiou have conducted displacement controlled indentation tests on individual MG63 cells and utilized a linear biphasic theory based on the assumption that the viscoelastic behavior of cells was caused by the interaction of a linear elastic solid phase and an inviscid fluid. They applied a finite element method to fit the material properties (aggregate modulus, Poisson's ratio, and permeability) of cells [24]. The experimental data about mechanical behavior of articular cartilage and chondrocytes have been utilized to conduct a multi-scale study, taking into account the contribution of the cells to the overall mechanical behavior of cartilage. Wu *et al.* have used homogenization theory, describing the cartilage as a macroscopic body, whose properties depend on the material properties of the cells, matrix and volumetric fractions of the cells [25]. Instead, Guilak and Mow have included the presence of a pericellular matrix, whose material properties differ profoundly from that of chondrocytes and extracellular matrix, influencing the stress and strain distribution

within the chondrocytes [26]. The integration of principles that regulate chondrocyte mechanics and mechanism that govern mechanotransduction in articular cartilage poses the basis to develop strategies for cartilage engineering incorporating mechanical stimulation [27].

### B.4 Micro/nanostructural Mechanical Models

Cells are active biological materials, able to move, deform, interact and elaborate mechanical stimuli. Their internal dynamic structures are highly organized and are decisive in control of cell shape and in creating movements. Both the mechanics and dynamics of these structures are defined by their material properties (elasticity and viscosity). In order to understand totally the physical behavior of cells and develop mechanistic models of cell movements, it's fundamental to study the mechanics of the systems of molecules that drive cellular organization, shape changes and movement. The purpose of developed models at the micro-scale level is not only identifying the molecular components entangled in cell structure, but also determining how they integrate in the overall body and contribute with their biochemical, mechanical properties to regulate cell movements and shape changes. An in-depth study about the nonstationary time dependent behavior of heterogeneously and hierarchically organized systems, such as living cells, can be useful to understand the wide set of mechanical responses that they exhibit, depending not only on the material properties, frequency, but also on the place where stimulus is applied. Several recent works focus their attention on the cell dynamic behavior, that require an interplay among different length scales, force scales and timescales [29]. Micro/nanostructural models describe the properties of assemblies of molecules in terms of their structure and the microscopic interactions between them. In this framework, computer simulations represent a complement to a conventional experiments and act as a bridge between the microscopic length and time scales and the macroscopic world, letting to obtain predictions of bulk properties. Two main families of simulation technique can be identified: the first refers to theoretical methods for studying molecular systems ranging from small molecular systems to large biological molecules and material assemblies. These methods are known as molecular dynamics (MD) algorithms and utilize classical/Newtonian mechanics to characterize the behavior of system with propagation of time. The second class consists of stochastic models, known as Monte Carlo (MC) molecular modeling that, unlike MD approach, doesn't reproduce the dynamics of a system, but generates states

according to appropriate Boltzmann probabilities. Additionally, there is a whole range of hybrid techniques which combines features of both. In the context of micro/nanostructural models, structurally-based models have to be taken into account: they recognize the cytoskeleton (CSK) as the main cell component to govern cell shape and cellular functions and identifies the presence of a pre-existing mechanical tension (pre-stress) in the CSK, which is generated actively (ATP-mediated processes) and passively by interactions established between cell and ECM. The rearrangement of CSK filamentous network guarantees the ability of cell to withstand external loads.

### B.4.1 Simulation Techniques: Molecular Dynamics and Monte Carlo Approaches

In the framework of micromechanical models, molecular dynamics-based approaches have to be retained. Molecular dynamics (MD) models have been utilized to study the microscopic mechanics of molecules, in order to understand the way by which mechanical forces or deformation are sensed and transduced into biological signals, that start fundamental processes, such as cell growth, differentiation and movement. MD starts with a previously specified set of initial coordinates and velocities for all the particles in the system and considers a force field to describe the interactions among the different atoms. The molecular dynamics approach requires the solution of Newton's equations of motion for all particles in the system. In biology, MD simulations have added important information about the principal types of protein filaments of the cellular cytoskeleton, allowing the investigation of the mechanical properties of the microtubules and related motor proteins [29]; the correspondence between actin monomer conformation and the filament structure[30]; the discover of the existence of strain hardening and viscoelasticity of vimentin coiled-coil alpha-helical dimers, the building blocks of intermediate filaments [31]. A variant of MD is Brownian Molecular dynamics (BMD), which considers additional frictional forces to account for dissipation. BMD has been used to investigate the influence of various parameters (pore size, fiber diameter, degree of isotropy) on the growth and morphology of the network resulting by interactions between actin filaments [32]; to simulate the motion of a microtubule guided by protein motors [33]; or to demonstrate the importance of the interaction between the actin protein network and the lipid bilayer of membrane [34].

Monte-Carlo (MC) methods are a class of stochastic computational algorithms, often used to simulate physical systems, characterized by a large number of freedom degree. Dynamic MC method is used to investigate non-equilibrium systems such as a reaction, diffusion and so-forth.

Also MC simulations have been used to study biomolecules, offering the advantage to sample the conFiguretion spaces of these systems more rapidly than Molecular dynamics. A wide number of MC simulation approaches has been proposed for studying the protein folding mechanism [35], to predict the growth processes of rigid biopolymers [36], such as actin filaments, intermediate filaments and microtubules, investigating the driving role of dinein motors [37]. Stochastic MC models have been also adopted to simulate biochemistry in the cell, particularly cytoskeleton self-organization [38], and to develop mechanistic models of voltage-gated ion channels, whose switching controls the transmembrane voltage [39].

As just said, to describe the complex mechanochemical machine of living cell, it's necessary to explore processes that involve different length and time scales. A combination of computational methods must be used, adopting a multiscale computational strategy. Coarse grain (CG) approach represents the bridge between MD, used at the most microscopic scale, and continuum or semi-continuum (microstructured) models, by which the molecular degrees of freedom are progressively reduced, due to a lower interest for fine interaction details [40].

MD simulations and CG analysis have been used to model the connection between actin monomer conformation and elastic properties of the cytoskeleton [30], but more extensively to simulate lipid bilayers. Multiscale simulation methods are based on the transfer of material properties or transport coefficients from detailed molecular models in constitutive relationship valid at longer spatial and temporal scales. The mesoscale simulations have allowed to explore the thermal fluctuations of RBC membrane, modeled as a bidimensional network, composed by particles arranged in a regular triangulation; to simulate RBCs motion under shear flow and test the sensitivity of coarse-graining procedure, performing a set of stretching experiments at different levels of coarse graining [41]; but also to determine its modulus in high and low surface tension conditions [42].

In other cases, probabilistic Monte Carlo approach has allowed to explain how macromolecular assembly systems properties can emerge from low-level physical interactions. CG Monte Carlo simulations have been used to study the cell motility by considering the mechanism of actin filaments polymerization through a lattice network model [43], and to explore the whole-cell equilibrium and large-scale deformations of RBCs, through a preliminary reduction of degrees of freedom to a range computationally tractable of the triangulated cytoskeleton model [44-45].

To guarantee a correct link between different length scales, it's necessary to impose constraints on the system, in terms of stress conditions (such as self-stress state and prestress), or geometric factors, such as fixed surface area and/or enclosed volume.

In the perspective of whole cell study, network models based MD and MC simulations have been used to describe primarily cytoskeletal dynamics of human erythrocyte. The erythrocyte's remarkable mechanical properties originate from the unique architecture of its cell wall, which is the main load bearing component as there are no stress fibers inside the cell. The cell wall is composed by a spectrin tetramer network tethered to a phospholipid bilayer. Three-dimensional spectrin random network models have been extensively utilized to investigate the full-cell equilibrium shape evolution, such as folding of cell wall during large deformation in human red blood cells (RBC) [46-47], and combined with a coarse-grained cytoskeletal model to simulate solid-to-fluid transition and demonstrate the decreasing of solid network's shear modulus and the loss of structural stability, when deformation exceed a critical value [48]. Models able to describe active remodeling of the RBC cytoskeleton have been proposed. The strain softening behavior of the static network of cytoskeletal flexible polymers, described by the wormlike chains theory, has been simulated by a field of independent "curvature motors", that, through the consumption of ATP, controls the stiffness of this network. An excessive deformation of the RBC cytoskeleton causes an increasing of the time to rebind the diassociated spectrin [49]. Recently, Levine and MacKintosh have developed a two-fluid model of a semiflexible network driven by molecular motor. The presence of motor forces in the cytskeleton invalidates the hypothesis of thermal equilibrium, that generally is assumed. The consideration of molecular motors explains the low-frequency fluctuation enhancement and the nonequilibrium stiffening of the network [50].

The cytoskeletal filamentous network plays a central role in determining the viscoelastic properties of cells and their dynamic changes, accomplished by modulating the keratin network, are necessary for the migration of cancer cells. For this reason, it's fundamental to widen the knowledge of processes that determine the morphology of keratin network. Among statistical methods, random tessellation is a model based on geometric characteristics of the foam structure, which are estimate from reconstructed tomographic images of the materials. It has been used to model keratin filaments networks and its remodeling in pancreatic cells [51].

### B.4.2 Structurally-based Models

It has been widely discussed about the primary role of cell cytoskeleton in determining cell shape and cell deformability. The CSK has a regulatory function in the mechanotransduction, the mechanism by which mechanical stimuli are recognized by cells and converted into chemical activities, that mediate growth and critical functions of living cells [52]. The CSK has been modeled as a filamentous network and different models have been proposed to explain what mechanisms and which molecular structures determines mechanical properties of adherent cells. In particular, two structurally based models of CSK have been examined: open cell foam network and stress-supported structures, that include tensed cable networks and tensegrity structures. Here, a brief overview about these models is presented, with a particular attention given to tensegrity models. A close examination is offered in [53-54].

Open cell foams are structures containing pores that are connected to each other and form an interconnected network which is relatively soft. Satcher and Dewey for the first time have used the theory of foams to estimate the bulk elastic shear and compressive/tension moduli. They have adopted a simple model geometry and considered the deformations consequent to the stretching or bending of single constituents. The model proposed have quantified the mechanical properties in functions of density and moment of inertia, that can be determined by constituent filament properties and empirical constants [55].

Stress-supported structures are networks that are stabilized introducing prestress to stiffen mechanisms. The difference between the various types of those structures in the way utilized to balance the pre-existing tension. In such cases, the balance is guaranteed by internal elements, in others by attachment to the externally objects, but sometimes the stability is reached by contribution both of internal and external elements. Tensed cable networks and tensegrity structures belong to this category.

Tensed cable structures are networks composed by cables, that bear initial tension, giving stability to the system. The preexisting tension is provided actively by the actomyosin contractile apparatus and passively by the osmotic pressure of cytoplasm and cell distension on the substrate. Prestressed cable networks have been extensively used to model the deformability of different cells. For example, spectrin red blood cells cytoskeleton has been modeled considering that all the spectrin is organized in a tetrameric network topology and that an average of six tetramers are joined at each actin junctions, where there is freedom of rotating [56]. Instead, Coughlin and Stamenović have used two planar different model to represent adherent cells cytoskeletons: in

the first the cables are organized into a planar lattice of regular hexagons and in the second into a planar lattice of equilateral triangles, founding that the tension of actin network is the structure that provides stability and resistance to the cell [57]. Cable networks have been used also to demonstrate the strict correlation existing between active cellular contractility and cell and tissue shape and how the developmental processes can be guided in a similar manner by mechanical factors at cellular and tissue level [58].

Tensegrity structures are a particular subclass of tensed cable structures, in which the prestress is completely balanced by internal elements. The model of the cell based on tensegrity architecture has allowed to relate mechanics to molecular chemistry and to create a mathematical framework to explain the behavior of living cells. The tensegrity model describes the cytoskeleton as a discrete mechanical network that transmits mechanical loads through the cytoplasm; so, the response of cell to stress depends on molecular connectivity between the internal CSK lattice and the cell surface, and on interactions between actin filaments, intermediate filaments and microtubules, the three cytoskeletal filament systems. The key feature of the tensegrity model is in the critical role of prestress for cell shape. A symmetrical cell model, in which the tensed filaments are represented by 24 cables and the microtubules by six struts, has been used to demonstrate the increasing of stiffness when prestress is enhanced, and, for a fixed prestress, the linearly stiffening behavior showed by cultured cells in experimental observations [59]. Ingber has considered that, although the regular spherical structural model generates results in agreement with quantitative measurements, the living cell has a more complex structural organization and uses a multimodular tensegrity arrangement. In this way, the collapse of a single module doesn't compromise the full stability, but the multimodularity guarantees the repair or substitution of disrupted subsystems [60]. Cañadas *et al.* have investigated the viscoelastic properties of cytoskeleton, modeling the cell with the same six-struts tensegrity structure utilized in the linear elastic analyses. The authors have used a Voigt model for the 24 pre-stretched cables to understand the measure in which the cytoskeleton determines the viscoelastic properties of adherent cells. They have found a faster cellular mechanical response than that of single element, so that the cytoskeletal topological arrangement has an orienting function in solidification process [61]. Sultan *et al.* have also used the same spherical model to predict the dynamic behavior exhibited by cells during oscillatory loadings, finding for the first time the observed dependence of loss modulus on prestress [62-63]. Ulterior complications have been introduced in the spherical model: stability analyses have been performed, allowing to the struts to buckle, and conditions of simple

and compound bifurcation have been explored [64-65]. In the works discussed above, the prestress is considered totally balanced by cytoskeletal microtubules. However, for the tissue cells it's necessary the adherence to substrate for their survival and the anchorage to the ECM contributes to partly balance the preexisting tensile stress sustained by the cytoskeleton. Stamenović has explored the measure in which disruption of microtubules affects cell deformability, observing hardening or softening behaviors, depending on the extent of cell spreading [66]. If the contribution of microtubules to the cell deformability cannot be ignored, the stabilization effect of cell structure on ECM provided by actin stress fibers (SFs) is essential. Tensegrity models have been used to describe the molecular architecture of SFs [67] and investigate the way in which they influence the elasticity of the CSK and, therefore, guide cell migration and mechanosensing [68].

### B.5 Multi-scale Modeling Approach

Understanding the principles that rule the design of biological systems means to define the correlation existing between structure and function and explain in which way the processes on the molecular scale are transferred on the cellular and then tissue level. In fact, it's well known that the mechanical behavior of biological structures is governed by phenomena occurring on different scales of observation. Multi-scale approaches might bridge the gap between molecules, cells and tissues, developing separate computations at different length scales and combining the results to obtain a complete description. From a computational point of view, an appropriate incorporation of micromechanical effects into macroscopic constitutive equations is necessary.

An important characteristic of living organisms is the process of self-organization, that has been explained by the use of a hierarchy of tensegrity networks. This solution optimizes structural efficiencies, that is maximization of strength per mass, and realizes the mechanical coupling of the parts with the whole: mechanical stresses applied at the macro-scale result in structural rearrangement at the cell and molecular level [60,69-70]. But structural detailed information is needed to determine whether the forces withstood by cells generated from within, from outside, from external pressure or shear. For this scope, it's clarifying the role of molecular biomechanics, that tries to elucidate the interconnection between mechanical properties and spatial arrangement of the cytoskeletal molecules and the mechanics of whole cells. Different models have been proposed to describe the complex rheological behavior of living cells. Prestress and

contractility generation in tensegrity networks can be explained by soft glassy models that consider the arrangement of stress fibers at the meso-scale, but also non-equilibrium interactions of myosin and actin filaments within the stress fibers at the micro-scale [71-72].

Multi-scale models are essential also to describe the dynamic nature of living structures and then the dependence of their mechanical properties on the time-scale of the measurement. Interestingly, multi-scale approach has been used to model invasion and metastasis of cancer, ranging from molecular processes to production of forces necessary for directed movement at the cell and tissue-level [73].

## References


[1] Fung Y.C."Biomechanics: Mechanical Properties of Living Tissues", **1993.**

[2] Lim C. T. *et al.* "Mechanical models for living cells – a review". J. Biomech. 39, 195-216, **2006**.

[3] Vaziri A. and Garvind A. "Cell and biomolecular mechanics in *silico*". Nature Mat. 7, 15-23, **2008**.

[4] Yeung A. and Evans E. "Cortical shell-liquid core for passive flow of liquid-like spherical cells into micropipets". Biophys. J. 56, 139-149, **1989**.

[5] Tsai M. *et al.* "Passive mechanical behavior of human neutrophils: Power-law Fluid". Biophys. J. 65, 2078-2088, **1993**.

[6] Drury J. L. and Dembo M. "Aspiration of human neutrophils: effects of shear thinning and cortical dissipation". Biophys. J. 81, 3166-3177, **2001**.

[7] Kan H.C. *et al.* "Effects of nucleus on leukocyte recovery". Ann. Biomed. Eng. 27, 648-655, **1999**.

[8] Marella S. V. and Udaykumar H. S. "Computational analysis of the deformability of leukocytes modeled with viscous and elastic structural components". Phys. Fluids 16 (2), 244-264, **2004**.

[9] Zhou C. *et al.* "Simulation of neutrophil deformation and transport in capillaries using Newtonian and viscoelastic drop models". Ann. Biomed. Eng. 35 (5), 766-78, **2007**.

[10] Theret D. P. *et al.* "The application of a homogeneous half-space model in the analysis of endothelial cell micropipette measurements". J. Biomed. Eng. 110 (3), 190-199, **1988**.

[11] **Byfield F. J. *et al.* "**Cholesterol Depletion Increases Membrane Stiffness of Aortic Endothelial Cells". 87 (5), 3336-3343, **2004**.

[12] Haider M. A. and Guilak F. "An axisymmetric boundary integral model for assessing elastic cell properties in the micropipette aspiration contact model". J. Biomed. Eng. 124, 586-595, **2002**.

[13] Schmid-Schönbein *et al.* "Passive mechanical properties of human leukocytes". Biophys. J. 36, 243-256, **1981**.

[14] Koay E. J. *et al.* "Creep indentation of single cells". J. Biomed. Eng. 125, 334-, **2003.**

[15] Koay E. J. *et al.* "Creep indentation of single cells". Journal J. Biomed. Eng. 125, 334-, **2003.**

[16] Bausch A. R. *et al.* "Measurements of local viscoelasticity and forces in living cells by magnetic tweezers" Biophy. J. 76, 573-579, **1999**.

[17] Bausch A. R. *et al.* "Rapid stiffening of receptor-actin linkages in endothelial cells stimulated with thrombin: a magnetic bead microrheology study" Biophys. J. 80, 2649-2657, **2001**.

[18] Lunov O. *et al.* "A model for magnetic bead microrheometry" J. Magn. Magn. Mat. 311, 162-165, **2006**.

[19] Peeters E.A.G. *et al.* "Viscoelastic properties of single attached cells under compression" J. Biomech. Eng. 127, 237-243, **2005**.

[20] Kopzac A. M. *et al.* "Simulation and prediction of endothelial cell adhesion modulated by molecular engineering" Comp. Meth. Appl. Mech. Eng. 197, 2340-2352, **2008**.

[21] Guck J. *et al.* "The optical stretcher: a new laser tool to micromanipulate cells" Biophys. J. 81, 767-784, **2001**.

[22] Xu F. *et al.* "Optical stress on the surface of a particle: Homogeneous sphere" Phy. Rev. A 79 (5), 53808-533822, **2009**.

[23] Ekpenyong A. E. *et al.* "Determination of cell elasticity through hybrid ray optics and continuum mechanics modeling of cell deformation in the optical stretcher" Appl. Opt. 48 (32), 6344-6354, **2009**.

[24] Shin D. and Athanasiou. "Cytoindentation for obtaining cell biomechanical properties" J. Orth. Res. 17 (6), 3085-3095, **1999**.

[25] Wu J. Z. *et al.* "Modelling of location- and time-dependent of chondrocytes during cartilage loading" J. Biomech. 32 (6), 139-149, **1999**.

[26] Guilak F. and Mow V.C. "The mechanical environment of the chondrocytes: a biphasic elements model of cell-matrix interactions in articular cartilage" J. Biomech. 33 (12), 1663-1673, **2000**.

[27] Shieh A.C. and Athanasiou K. A. "Principles of cell mechanics for cartilage tissue engineering". Ann. Biomed. Eng. 31, 1-11, **2002**.

[28] Fletcher D. A. and Geissler P. L. "Active biological materials". Annu. Rev. Phys. Chem. 60, 469-486, **2009**.

[29] Wells D. B. and Aksimentiev A "Mechanical properties of a complete microtubule from all-atom Molecular Dynamics simulation" Biophys. J. 96(3) Supplement 1, 506a, **2006**.
[30] Chu J.W. and Voth G.A. "Allostery of actin filaments: Molecular dynamics simulations and coarse-grained analysis" PNAS One 102 (37), 13111-13116, **2005**.
[31] Ackbarow T. and Buehler M. J. "Superelasticity, energy dissipation and strain hardening of vimentin coiled-coil intermediate filaments: atomistic and continuum studies" J. Mat. Sci. 42, 8771-8787, **2007**.
[32] Kim T. *et al.* "Computational analysis of a cross-linked actin-like network" Exp. Mech. 49, 91-104, **2007**.
[33] Quen C. *et al.* "The coordination of protein motors and the kinetic behavior of microtubule – A computational study" Biophy. Chem. 129, 60-69, **2007**.
[34] Zhu Q. *et al.* "A hybrid model for erythrocyte membrane: a single unit of protein network coupled with lipid bilayer". Biophys. J. 93, 386-400, **2007**.
[35] Hansmann U. and Okamoto Y. "New Monte Carlo algorithms for protein folding" Curr. Opin. Struct. Biol. 9, 177-183, **1999**.
[36] Son J. *et al.* "Monte Carlo simulations of rigid biopolymers growth processes" J. Chem. Phys. 123, 1-7 (124902), **2005**.
[37] Hen Q. *et al.* "Phenomenological simulation of self-organization driven by dynein c". 130, 1-8 (214107), **2009**.
[38] LeDuc P. and Schwartz R. "Computational models of molecular self-organization in cellular environments" Cell Biochem. Biophys. 48, 16-31, **2007**.
[39] Boey S. K. *et al.* "Simulations of the erythrocyte cytoskeleton at large deformation. I. Microscopic models" Biophys. J. 75, 1573-1583, **1998**.
[40] Discher D. E. *et al.* "Simulations of the erythrocyte cytoskeleton at large deformation. I. Micropipette aspiration" Biophys. J. 75, 1584-1597, **1998**.
[41] Pivkin I. V. and Karniadakis G. E. "Accurate coarse-grained modeling of red blood cells" Phys. Rev. Lett. 101, 1-4 (118105), **2008**.
[42] Ayton G. and Voth G. A. "Bridging microscopic and mesoscopic simulations of lipid bilayers" Biophys. J. 83, 33578-3370, **2002**.
[43] Puskar K. *et al.* "Evaluating spatial constraints in cellular assembly processes using a Monte Carlo approach" Cell Biochem. Biophy. 45, 195-201, **2006**.
[44] Erdem R. and Aydimer E. "Monte carlo simulation for statistical mechanics model of ion-channel cooperativity in cell membranes" Phys. Rev. 79, 1- 7 (031919), **2009**.
[45] Hale J. P. *et al.* "Red blood cell thermal fluctuations: comparison between experiment and molecular dynamics simulations" Soft Matter 5, 3603-3606, **2009**.
[46] Li J. *et al.* "Spectrin-level modeling of the cytoskeleton and optical tweezers stretching of the erythrocyte". Biophys. J. 88, 3707-3719, **2005**.
[47] Dao M. *et al.* "Molecularly based analysis of deformation of spectrin network and human erythrocyte". Mat. Sci. Eng. 26, 1232-1244, **2006**.
[48] Li J. *et al.* "Cytoskeletal dynamics of human erythrocyte". PNAS 104 (12), 4937-4942, **2007**.
[49] Gov N. S. "Active elastic network: cytoskeleton of the red blood cell" Phys. Rev. 75, 1-6 (11921), **2007**.
[50] Levine A. J. and MacKintosh F. C. "The mechanics and fluctuation spectrum of active gels" J. Phys. Chem. 113, 3820-3830, **2009**.
[51] Beil M. *et al.* "Fitting of random tessellation models to keratin filament network" J. Theor. Biol. 241, 62-72, **2006**.
[52] Wang N. *et al.* "Mechanotransduction across the cell surface and through the cytoskeleton" Science 260, 1124-1127, **1993**.
[53] Stamenović D. and Coughlin M. F. "The role of prestress and architecture of the cytoskeleton and deformability of cytoskeletal filaments in mechanics of adherent cells: a quantitative analysis" J. Theor. Biol. 201, 63-74, **1999**.
[54] Stamenović D. and Ingber D. E. "Models of cytoskeletal mechanics of adherent cells" Biomech. Model. Mechanobiol. 1, 95-108, **2002**.
[55] Satcher R. L. and Dewey C. F. "Theoretical estimates of mechanical properties of the endothelial cell cytoskeleton" Biophys. J. 71, 109-118, **1996**.

[56] Hansen J. C. *et al.* "An elastic network model based on the structure of the red blood cell membrane skeleton" Biophys. J. 70, 146-166, **1996**.
[57] Coughlin M. F. and Stamenović D. "A prestressed cable network model of the adherent cell cytoskeleton" Biophys. J. 84, 1328-1336, **2003**.
[58] Bischofs I. B. *et al.* "Filamentous network mechanics and active contractility determine cell and tissue shape" Biophys. J. 95, 3488-3496, **2008**.
[59] Wang N. *et al.* "Mechanical behavior in living cells consistent with the tensegrity model" PNAS 98 (14), 7765-7770, **2001**.
[60] Ingber D. E. "Tensegrity I. Cell structure and hierarchical systems biology" J. Cell Sci. 116, 1157-1173, **2003**.
[61] Cañadas P. *et al.* "A cellular tensegrity model to analyse the structural viscoelasticity of the cytoskeleton" J. Theor. Biol. 218, 155-173, **2002**.
[62] Sultan C. *et al.* "A computational tensegrity model predicts dynamics rheological behaviors of living cells" J. Biomed. Eng. 32 (4), 520-530, **2003**.
[63] Stamenović D. "Effects of cytoskeletal prestress on cell rheological behavior" Acta Biomaterialia 1, 255-262, **2005**.
[64] Lazopoulos K.A. "Stability of an elastic cytoskeletal tensegrity model" Int. J. Solids Struct. 42, 3459-3469, **2005**.
[65] Lazopoulos K.A. and Lazopoulou N.K. "On the elastic solution of a tensegrity structure: application to cell mechanics" Acta Mechanica 182, 253-263, **2006**.
[66] Stamenović D. "Microtubules may harden or soften cells, depending on the extent of cell distension" J. Biomech. 38, 1728-1732, **2005**.
[67] Luo Y. *et al.* "A multi-modular tensegrity model of an actin stress fiber" J. Biomech. 41, 2379-2387, **2008**.
[68] Lazopoulos K.A. and Stamenović D. "Durotaxis as an elastic stability phenomenon" J. Biomech. 41, 1289-1294, **2008**..
[69] Ingber D. E. "Tensegrity and mechanotransduction" J. Bodywork Mov. Ther. 12, 198-200, **2008**.
[70] Stamenović D. S. and Ingber D. E. "Tensegrity-guided self assembly: form molecules to living cells" Soft Matter 5, 1137-1145, **2008**.
[71] Shen T. and Wolynes P.G. "Nonequilibrium statistical mechanical models for cytoskeletal assembly: towards understanding tensegrity in cells" Phys. Rev. E 72 (4), 1-11 (041927), **2005**.
[72] Kollmannsberger P. and Fabry B. "Active soft glassy rheology of adherent cells" Soft Matter 5, 1771-1774, **2009**.
[73] Stolarska M. A. *et al.* "Multi-scale models of cell and tissue dynamics" Phil. Trans. of the Royal Society A 367, 3525-2553, **2009**.